Artificial Intelligence Review (2024) 57:59
https://doi.org/10.1007/s10462-023-10653-7

A novel metaheuristic inspired by horned lizard defense tactics

Hernán Peraza-Vázquez[1] · Adrián Peña-Delgado[2] · Marco Merino-Treviño[1,3] · Ana Beatriz Morales-Cepeda[3] · Neha Sinha[4]

Accepted: 19 December 2023 / Published online: 16 February 2024

Abstract
This paper introduces HLOA, a novel metaheuristic optimization algorithm that mathematically mimics crypsis, skin darkening or lightening, blood-squirting, and move-to-escape defense methods. In crypsis behavior, the lizard changes its color by becoming translucent to avoid detection by its predators. The horned lizard can lighten or darken its skin, depending on whether or not it needs to decrease or increase its solar thermal gain. The skin darkening or lightening strategy is modeled by including the stimulating hormone melanophore rate(α-MHS) that influences these skin color changes. Further, the move-to-evasion strategy is also mathematically described. The horned lizard's shooting blood defense mechanism, described as a projectile motion, is also modeled. These strategies balance exploitation and exploration mechanisms for local and global search over the solution space. HLOA performance is benchmarked with sixty-three optimization problems from the literature, testbench problems provided in IEEE CEC- 2017 "Constrained Real-Parameter Optimization", analyzed for dimensions 10, 30, 50, and 100, as well as testbench functions from IEEE CEC-06 2019 "100-Digit Challenge". Moreover, three real-world constraint optimization applications from IEEE CEC2020 and two engineering problems, the multiple gravity assist optimization and the optimal power flow problem, are also studied. Wilcoxon and Friedman statistics tests compare the HLOA algorithm results against ten recent bio-inspired algorithms. Wilcoxon shows that HLOA provides the optimal solution for most testbench functions more effectively than competing algorithms. At the same time, the Friedman statistics test ranks the HLOA first, and the n-dimensional analysis shows that it performs better on the constrained optimization problems for dimensions 50 and 100. The source code is free and available from https://www.mathworks.com/matlabcentral/fileexchange/159658-horned-lizard-optimization-algorithm-hloa.

Keywords Optimization · Bio-inspired algorithm · Metaheuristics · Horned Lizard · Crypsis

Extended author information available on the last page of the article

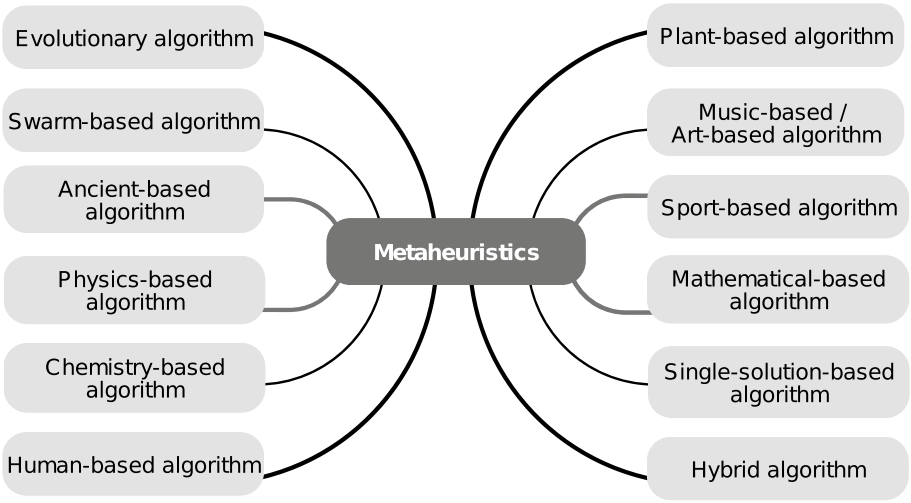

Fig. 1 Metaheuristics classification

1 Introduction

Optimization determines the optimal values of a problem's variables to minimize (or maximize) an objective function. It can be represented in the following way:

Given a function f to minimize, where $f : \mathbb{R}^D \rightarrow \mathbb{R}$, with D as the dimension of the problem (number of variables), sought a vector $x_o \in \mathbb{R}^D$ such that $f(x_o) \leqslant f(x)\ \forall x \in \mathbb{R}^D$, while x_o satisfying inequality and equality constraints, $g_p(x_0) \leqslant 0$ and, $h_q(x_0) = 0$, with $p = 1, 2, .., P$ and, $q = 1, 2, .., Q$, where P and Q, are number of inequality and equality constraints, respectively. Additionally, it must be met that $x_i^l \leqslant x_i \leqslant x_i^u$, where $i = 1, 2, .., D$ and i-th variable varies in the interval $[x_i^l, x_i^u]$.

Optimization problem-solving strategies are classified as Deterministic or Stochastic. Deterministic methods are grouped as gradient-based or not gradient-based, where both classifications show good performance for linear, convex, and simple optimization tasks. Nevertheless, these methods don't work in certain cases that involve complex problems, objective functions that can't be differentiated, search spaces that aren't linear, problems that aren't convex, and NP-hard problems. Given that many real-world optimization problems are NP-hard, the scientific community frequently uses stochastic methodologies such as metaheuristics instead of deterministic methods.

Some of the metaheuristics and their classification are depicted in Fig. 1 and described as follows:

- *Evolutionary algorithm*: Genetic Algorithm (GA) (Holland 2006), Differential Evolution (DE) (Ahmad et al. 2022), Cultural Algorithm (Maheri et al. 2021)(CA), Memetic Algorithm (MA) (Ahrari and Essam 2022), Evolutionary Strategy (ES) (Beyer et al. 2002), and Gradient Evolution Algorithm (GEA) (Kim and Lee 2023).
- *Swarm-based algorithm*: Particle Swarm Optimization(PSO) (Kennedy and Eberhart 1995), Dingo Optimization Algorithm (DOA) (Peraza-Vázquez et al. 2021), Black

Widow Optimization Algorithm (BWOA) (Peña-Delgado et al. 2020), Jumping Spider optimization Algorithm (JSOA) (Peraza-Vázquez et al. 2021), Fennec Fox Algorithm (FFA) (Trojovska et al. 2022), Artificial Rabbits Optimization (ARO) (Wang et al. 2022), Tunicate Swarm Algorithm (TSA) (Kaur et al. 2020), and Mountain Gazelle Optimizer (Abdollahzadeh et al. 2022).

- *Ancient-based algorithm*: Giza Pyramids Construction (GPC) (Harifi et al. 2021) and Al-Biruni Earth Radius (BER) Metaheuristic Search Optimization Algorithm (El-Kenawy et al. 2022).
- *Physics-based algorithm*: Simulated Annealing (SA) (Duan and Hou 2021), Thermal Exchange Optimization (TEO) (Kaveh and Dadras 2017), Gravitational Search Algorithm (GSA) (Mittal et al. 2021), Momentum Search Algorithm (MSA) (Dehghani and Samet 2020), Water Cycle Algorithm (WCA) (Sadollah et al. 2016), Electro-Magnetism Optimization (EMO) (Abedinpourshotorban et al. 2016), Kepler optimization algorithm (KOA) (Abdel-Basset et al. 2023), and Cyclical Parthenogenesis Algorithm (CPA) (Kaveh and Bakhshpoori 2019)
- *Chemistry-based algorithm*: Chemical Reaction Optimization (CRO) (Lam and Li 2012), Crystal Structure Algorithm (CryStAl) (Talatahari et al. 2021), and Artificial Chemical Process (ACP) (Irizarry 2004).
- *Human-based algorithm*: Sewing Training-Based Optimization (STBO) (Dehghani et al. 2022), Society Civilization Algorithm (SCA) (Ray and Liew 2003), Anarchic Society Optimization (ASO) (Ahmadi-Javid 2011), Teamwork Optimization Algorithm (TOA) (Dehghani and Trojovský 2021), Imperialist Competitive Algorithm (ICA) (Atashpaz-Gargari and Lucas 2007), and Coronavirus Mask Protection Algorithm (CMPA) (Yuan et al. 2023).
- *Plant-based algorithm*: Invasive Weed Optimization(IWO) (Xing and Gao 2014), Artificial Plant Optimization (APO) (Zhao et al. 2011), Artificial Root Foraging Algorithm (ARFA) (Liu et al. 2017), Rooted Tree Optimization (RTO) (Labbi et al. 2016), Artificial Algae Algorithm (AAA) (Uymaz et al. 2015), Willow Catkin Optimization Algorithm (WCO) (Pan et al. 2023), Strawberry Algorithm (SBA) (Khan 2018), and Waterwheel Plant Algorithm (Abdelhamid et al. 2023).
- *Music-based / Art-based algorithm*: Harmony Search Algorithm (HSA) (Kim 2016), Chaotic harmony search algorithm (CJSA) (Alatas 2010), Musical Composition Algorithm (MMC) (Mora-Gutiérrez et al. 2014), Melody Search Algorithm (MSA) (Ashrafi and Dariane 2011,) and Stochastic Paint Optimizer (Kaveh et al. 2022).
- *Sport-based algorithm*: Volleyball Premier League (VPL) (Moghdani and Salimifard 2018), Puzzle Optimization Algorithm (POA) (Patil et al. 2022), Running City game optimizer (RCGO) (Ma et al. 2023), Football Game-Based Optimization (FGBO) (Fadakar and Ebrahimi 2016), and Alpine Skiing Optimization (ASO) (Yuan et al. 2022, 2023a, b).
- *Mathematical-based algorithm*: Stochastic Fractal Search (SFS) (Salimi 2015), Hyper-Spherical Search (HSS) (Karami et al. 2014), Arithmetic Optimization Algorithm (AOA) (Abualigah et al. 2021), and Sine-Cosine Algorithm (SCA) (Mirjalili 2016).
- *Single-solution-based algorithm*: Large Neighbourhood Search (LNBS) (Pisinger and Ropke 2010), Tabu Search (TS) (Yu et al. 2023), and Variable Neighbourhood Search (VNBS) (Hansen and Mladenovići 2018).
- *Hybrid algorithm*: Cuckoo optimization algorithm and SailFish optimizer (COA-SFO) (Ikram et al. 2023), Hybrid Mutualism Mechanism-inspired Butterfly and Flower Pollination Optimization Algorithm (HMMB-FPOA) (Pratha et al. 2023), Butterfly Optimization Algorithm Combined with Black Widow Optimization (BFA-BWOA) (Xu et al.

2022), Equilibrium Whale Optimization Algorithm (EWOA) (Tan and Mohamad-Saleh 2023), Improved Dingo Optimization Algorithm (IDOA) (Almazán-Covarrubias et al. 2022), Cuckoo Search and Stochastic Paint Optimizer (CSSPO) (Ismail et al. 2023), Elite opposition-based learning, Chaotic k-best gravitational search strategy, and Grey wolf optimizer (EOCSGWO) (Yuan et al. 2022), Adaptive resistance and Stamina strategy-based Dragonfly algorithm (ARSSDA) (Yuan et al. 2020), and Coulomb force search strategy-based dragonfly algorithm (CFSSDA) (Yuan et al. 2020).

Since no algorithm can effectively and efficiently solve any optimization or instances of the same problem (Joyce and Herrmann 2017), the scientific community keeps developing new algorithms to solve challenging optimization problems that outperform or vie with those already described in the literature.

A generic metaheuristic framework consists of four phases described below and depicted in Fig. 2.

Phase 1: A set of initial population vectors are randomly generated. This population will evolve with each iteration. Each vector represents the search agent, where the population size can affect the algorithm's performance.

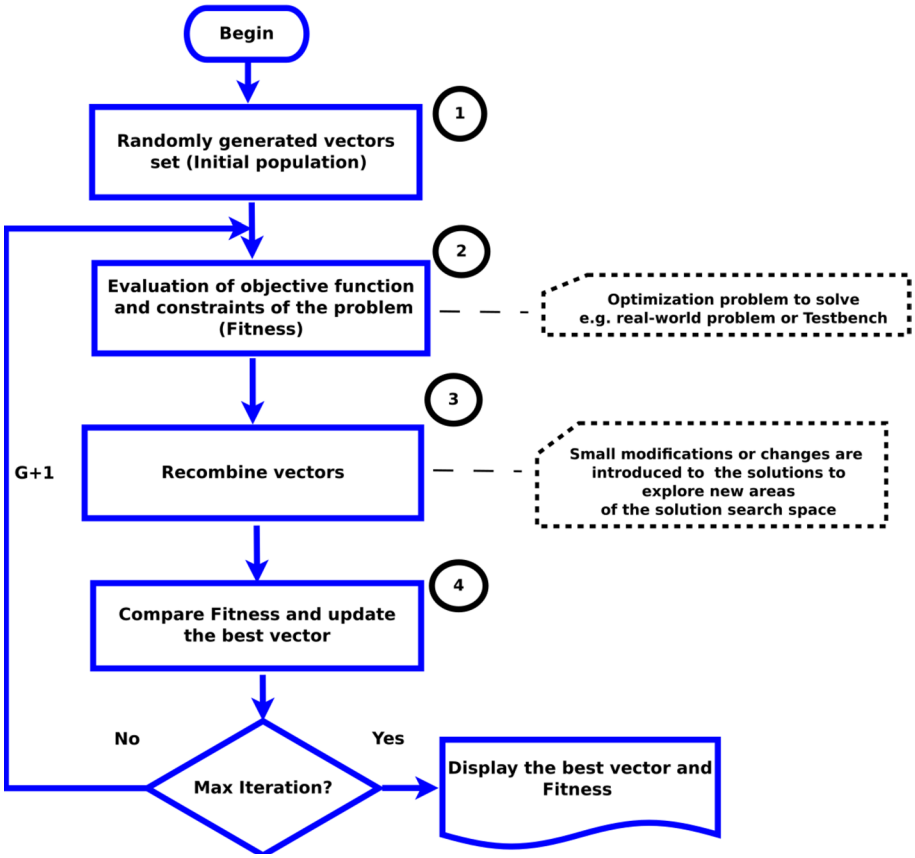

Fig. 2 The generic framework of a Metaheuristic Algorithm

Phase 2: Fitness is the result of evaluating the entire population of the objective function of each vector. When minimizing, the population's lowest fitness vector is best.

Phase 3: Here, it is required to incorporate mathematical functions recombining the vectors. These functions can model the behavior of living beings or physical/chemical phenomena as bio-inspired functions.

Phase 4: The vector with the best fitness is then compared to the fitness of the previously recombined vectors in each iteration. If the number of iterations has not been met, stop condition, it returns to phase 2. Otherwise, the best fitness value reached is reported. The number of iterations, known as generations, is a value defined before starting the algorithm that influences the algorithm's performance in this evolutionary process.

Finally, every metaheuristic should have a good balance between the ability to explore (diversify) and exploit (intensify) the search solution space. In other words, it should have global and local search strategies to improve its performance.

This paper proposes a Horned Lizard Optimization Algorithm (HLOA) as a novel swarm-based algorithm. This algorithm was inspired by how the horned lizard reptile conceals and defends itself from predators. The contributions of this work can be briefed as follows:

- A novel bio-inspired optimization algorithm that encompasses all aspects of the Horned Lizard's behavior to defend himself from their predators. Four defense strategies include crypsis behavior, skin darkening or lightening blood-Squirting, and move-to-escape. Also, the alpha-melanophore stimulating hormone rate, which influences their skin color change, is considered. These strategies could inspire other researchers to explore new directions and applications in the bio-inspired algorithms field, leading to a proliferation of related research.
- HLOA performance is evaluated in the following set of functions: IEEE CEC 2017 "Constrained Real-Parameter Optimization" for 10-dimensional, 30-dimensional, 50-dimensional, and 100-dimensional benchmark problems, IEEE CEC06-2019 "100-Digit Challenge" test functions, and sixty-three testbench functions from the literature. Furthermore, three real-world constraint optimization applications from CEC2020 and two engineering problems, multiple gravity assist optimization and the optimal power flow problem, were also tested.
- When comparing the HLOA algorithm to other approaches, it allows the scientific community to understand the relative strengths and weaknesses of different techniques evaluated with the same test instances.
- The algorithm is validated with Friedman tests, Wilcoxon tests, and convergence analyses. The results are compared to those of ten recently developed bio-inspired metaheuristic algorithms.
- The scientific community can access the HLOA's Matlab source code to support this study's findings.

The remaining sections of this paper are structured as follows: The second section illustrates the HLOA bio-inspiration, a detailed mathematical formulation, the time complexity, and the pseudo-code. Then, the performance of the proposed approach is benchmarked with several testbench functions, and their comparison with ten recent bio-inspired algorithms is presented in the third section. In the fourth section, the algorithm's results and discussion are presented. The fifth section describes the application of HLOA to real-world optimization problems and the constraint-handling technique employed. Finally, the paper summarizes the conclusions and future work.

2 Horned lizard optimization algorithm (HLOA)

2.1 Biological fundamentals

The horned lizard is scientifically known as Phrynosoma. It is an endemic reptile from south-central regions of the US to northeastern Mexico. They are adapted to arid or semi-arid extreme temperature areas. Horned lizards feed on various species, including grasshoppers, crickets, beetles, spiders, ticks, butterflies, and moths (Leaché and McGuire 2006). Their primary passive method of defense is crypsis (Stevens and Merilaita 2011; Ruxton et al. 2004). This method consists of the capacity to blend in with its surroundings through color, pattern, and shape. For example, the color pattern of the Horned Lizards changes geographically to match the terrain, and their spines cover their body outlines, making them hard to spot (Ruxton et al. 2004). Another passive defensive strategy is move-to-escape. Moreover, when threatened, this lizard employs aggressive tactics such as expelling a short stream of blood that travels more than a meter away (Cooper and Sherbrooke 2010; Middendorf 2001). It should be noted that all reptiles, horned lizards included, resort to thermoregulation since they cannot produce their body heat, depending on the surrounding temperature, to maintain their warmth (Lara-Reséndiz et al. 2015; Grigg and Buckley 2013). In addition, the horned lizard can lighten or darken its skin, depending on whether or not it needs to decrease or increase its solar thermal gain. Thus, at high temperatures (25° - 40° C), they acquire lighting color, whereas at low temperatures (16° - 17° C), they acquire darkened skin. Dark skin does not reflect any color; on the contrary, it absorbs all wavelengths of light, turning them into heat. The rapid color change of the skin of the horned lizard is due to the effects of temperature on their alpha-melanophore stimulating hormone (α-MSH) (Sherbrooke 1997) (Fig. 3).

2.2 Mathematical model and optimization algorithm

As previously described, the lizard can defend itself by changing its colors to match its surroundings. Additionally, it can lighten or darken its skin, depending on whether it needs to increase or decrease its solar thermal gain. The rate of the lizard's alpha-melanophore-stimulating hormone (α-MSH) is a factor in this rapid color change. Moreover, it can also shoot a short stream of blood to defend against its prey. In this work, each of these lizards'

Fig. 3 Horned Lizard Phrynosoma. Photograph by Brdavids (published under a CC BY 2.0 license)

defense behaviors, described before, are mathematically modeled as part of the optimization algorithm.

2.2.1 Strategy 1: Crypsis behavior

Crypsis is the process through which an organism can blend in with its surroundings by imitating characteristics of the environment, such as color and texture, or even by becoming translucent, making it difficult for predators or prey to detect or recognize them, see Fig. 5. It is an adaptive behavior that helps organisms avoid detection, thus increasing their chances of survival in the wild world (Ruxton et al. 2004). As the scope of this work is based on the horned lizard, it is to be noted that its crypsis method is mathematically represented through color theory (Westland et al. 2012; Niall 2017).

On the other hand, The International Commission on Illumination (CIE) (Niall 2017) standardized light sources by the amount of emitted energy, throughout the visible spectrum (400 to 700 nm), at each wavelength. In addition, the organization defined a color evaluation system, e.g., L*a*b system for Cartesian coordinates and L*C*h system for polar coordinates, to compute a color in a color space.

In the L*a*b system, L* indicates the luminosity, and a* and b* are the chromatic coordinates, as shown below.

$$\begin{aligned} a^* &= \begin{cases} +a, & indicates\ Red \\ -a, & indicates\ Green \end{cases} \\ b^* &= \begin{cases} +b, & indicates\ Yellow \\ -b, & indicates\ Blue \end{cases} \end{aligned} \tag{1}$$

In the L*C*h system, L* defines lightness, C* specifies color intensity, and h* indicates hue angle (an angular measurement). Hue moves in a circle around the "equator" to describe the color family (red, yellow, green, and blue) and all the colors in between. i.e., The numbers on the hue circle range from 0 to 360, starting with red at 0 degrees, then moving counterclockwise through yellow, green, blue, then back to red. The L axis describes the luminous intensity of the color. Comparing the value makes it possible to classify colors as light or dark. Both color system representations are shown in Figs. 4 and 5.

The transformation of rectangular coordinates to polar coordinates can be seen in Eq. 2.

$$\begin{aligned} c^* &= \sqrt{a^{*2} + b^{*2}} \\ h &= arcTg\left(\frac{b^*}{a^*}\right) \end{aligned} \tag{2}$$

c* and h values correspond to chroma (or saturation) and hue, respectively. The value of h is the hue angle and is expressed in degrees ranging from 0° to 360°. The inverse formulas are as follows:

$$\begin{aligned} a^* &= c^* \cos(h) \\ b^* &= c^* sin(h) \end{aligned} \tag{3}$$

Without loss of generality, let the ordered pair (a_p^*, b_q^*) and (a_r^*, b_s^*) be any two colors, with $p \neq q \neq r \neq s$. So, any two new colors, e.g., $colorVar_1$ and $colorVar_2$, can be obtained with the following arithmetic operations shown in Eq. 4

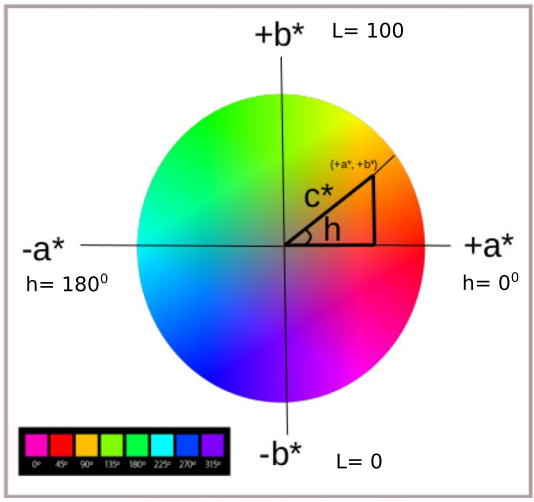

Fig. 4 Representation of the color space for the CIE L*a*b and L*C*h systems

Fig. 5 Horned Lizard Crypsis. Photograph by Paul Asman and Jill Lenoble (published under a CC BY 2.0 license)

$$\begin{aligned} colorVar_1 &= b_p^* - a_q^* - a_r^* + b_s^* \\ colorVar_2 &= b_p^* - a_q^* + a_r^* - b_s^* \end{aligned} \tag{4}$$

These colors can be represented in a single equation, as shown below.

$$colorVar = b_p^* - a_q^* \pm \left[a_r^* - b_s^*\right] \tag{5}$$

Eq. 5 can be represented in the inverse form as follows:

$$colorVar = c_1 \sin(h_p) - c_1 \cos(h_q) \pm \left[c_2 \cos(h_r) - c_2 \sin(h_s)\right] \tag{6}$$

where the angles (hue) meets $h_p \neq h_q \neq h_r \neq h_s$, and chroma $c_1 \neq c_2$. Finally, c_1 and c_2 are factorized as shown in Eq. 7.

$$colorVar = c_1 \left[\sin(h_p) - \cos(h_q)\right] \pm c_2 \left[\cos(h_r) - \sin(h_s)\right] \tag{7}$$

An equation that contains the arithmetic operation of chromatic coordinates represented in Eq. 7, can be seen below.

$$\begin{aligned} \vec{x}_i(t+1) = \vec{x}_{best}(t) + \left(\partial - \frac{\partial \cdot t}{Max\_iter}\right) \\ \left[c_1\left(\sin(\vec{x}_{r_1}(t)) - \cos(\vec{x}_{r_2}(t))\right) - (-1)^{\sigma} c_2\left(\cos(\vec{x}_{r_3}(t)) - \sin(\vec{x}_{r_4}(t))\right)\right] \end{aligned} \tag{8}$$

Where $\vec{x}_i(t+1)$ is the new search agent position (horned lizard) in the solution search space for the generation $t+1$, $\vec{x}_{best}(t)$ is the best search agent for the generation t; r_1, r_2, r_3 and, r_4 are integer random numbers generated between 1 and the utmost number of search agents, with $r_1 \neq r_2 \neq r_3 \neq r_4$; $\vec{x}_{r_1}(t)$, $\vec{x}_{r_2}(t)$, $\vec{x}_{r_3}(t)$ and, $\vec{x}_{r_4}(t)$ are the r_1, r_2, r_3, r_4-th search agent selected; *Max_iter* represents the utmost number of iterations (generations), σ is a binary value obtained by Algorithm 1, ∂ is set to 2, and, c_1, c_2, with $c_1 \neq c_2$, are random numbers taken from Table 29 containing the normalized color palette.

Algorithm 1 σ procedure

```
Begin procedure
if rand() ≤ 0.5 then
    return 0
else
    return 1
end if
End procedure
```

2.2.2 Strategy 2: Skin darkening or lightening

The horned lizard can lighten or darken its skin, depending on whether or not it needs to decrease or increase its solar thermal gain (Sherbrooke and Sherbrooke 1988). Thermal energy obeys the same conservation laws as light energy (Burtt 1981). Therefore, it is the key to the relationship between color and temperature. Thus, colors that reflect lighter repel more heat. In this way, dark colors absorb more heat because they absorb more light energy (Burtt 1981). The color changes in the skin of the horned lizard are represented by Eqs. 9 and 10. Equation 9 represents the lightning-skin strategy. Whereas, Eq. 10 represents the darkening-skin strategy.

Table 1 The color palette used for lightening or darkening the skin

Name	Color	Hexadecimal	Decimal	Normalized
$Lightening_1$		E8E8E8	15263976	0.0
$Lightening_2$		9398BF	9672895	0.4046661
$Darkening_1$		763660	7747080	0.5440510
$Darkening_2$		161617	1447447	1

$$\vec{x}_{worst}(t) = \vec{x}_{best}(t) + \frac{1}{2}Light_1 \sin\left(\vec{x}_{r_1}(t) - \vec{x}_{r_2}(t)\right) - (-1)^{\sigma}\frac{1}{2}Light_2 \sin\left(\vec{x}_{r_3}(t) - \vec{x}_{r_4}(t)\right) \tag{9}$$

$$\vec{x}_{worst}(t) = \vec{x}_{best}(t) + \frac{1}{2}Dark_1 \sin\left(\vec{x}_{r_1}(t) - \vec{x}_{r_2}(t)\right) - (-1)^{\sigma}\frac{1}{2}Dark_2 \sin\left(\vec{x}_{r_3}(t) - \vec{x}_{r_4}(t)\right) \tag{10}$$

Where $Light_1$ and $Light_2$ are random numbers generated between $Lightening_1$ (0 value) and $Lighthening_2$ (0.4046661 value), using these normalized values taken from Table 1. Analogously, $Dark_1$ and $Dark_2$ are random numbers generated between $Darkening_1$ (0.5440510 value) and $Darkening_2$(1 value), also using the normalized values from Table 1.

In addition, for both Eqs., 9 and 10, $\vec{x}_{worst}(t)$ and $\vec{x}_{best}(t)$ are the worst and the best search agent found, respectively. r_1, r_2, r_3 and, r_4 are integer random numbers generated between 1 and the utmost number of search agents, with $r_1 \neq r_2 \neq r_3 \neq r_4$; $\vec{x}_{r_1}(t)$, $\vec{x}_{r_2}(t)$, $\vec{x}_{r_3}(t)$ and, $\vec{x}_{r_4}(t)$ are the r_1, r_2, r_3, r_4-th search agent selected. Finally, σ is a binary value obtained by algorithm 1. The skin color change strategy is shown in Algorithm 2.

Algorithm 2 Darkening or lightening of skin procedure

Algorithm 2 Darkening or lightening of skin procedure

1: Generate $Light_1$ and $Light_2$ randomly from Table 1
2: Generate $Dark_1$ and $Dark_2$ randomly from Table 1
3: Generate r_1, r_2, r_3 and r_4 integer value randomly between [1, size Maximum Search Agents], where $r_1 \neq r_2 \neq r_3 \neq r_4$
4: **if** σ **then**
5: Apply lightening skin. Compute equation 9
6: **else**
7: Apply darkening skin. Compute equation 10
8: **end if**
9: End procedure

Notice that the worst search agent in the t iteration is replaced by the new one obtained by the skin-darkening or skin-lightening strategy.

2.2.3 Strategy 3: blood-squirting

The Horned lizard fends off enemies by shooting blood from its eyes (Middendorf 2001). The shooting blood defense mechanism can be represented as a projectile motion, depicted in Fig. 6. To obtain the equations of motion, we separate the projectile motion into its two components, X-axis (horizontal) and Y-axis (vertical):

In the horizontal direction, the shot of blood describes a uniform line movement, so its equation of motion will be given by:

$$\vec{v} = \vec{v_0} + \int_0^t \vec{g}\,dt = \vec{v_0} + \vec{g}\,t \tag{11}$$

In the vertical direction, the shot of blood describes a uniformly accelerated rectilinear motion, it is as follows:

$$\vec{r} = \vec{r_0} + \int_0^t \left(\vec{v_o} + \vec{g}\,t\right) dt = \vec{r_0} + \vec{v_o}\,t + \frac{1}{2}\,\vec{g}\,t^2 \tag{12}$$

$$\vec{r}_0 = \vec{0} \tag{13}$$

The vector equations, position, and velocity, are represented by Eqs. 14 and 15, respectively.

$$\vec{v_0} = v_0 \cos(\alpha) t\,\vec{j} + \left((v_0 \sin(\alpha))t - \frac{1}{2} g t^2\right)\vec{k} \tag{14}$$

$$\vec{v} = \vec{r} = \left(v_0 \cos(\alpha)\right)\vec{j} + \left(v_0 \sin(\alpha) - gt\right)\vec{k} \tag{15}$$

Finally, the trajectory can be expressed as follows:

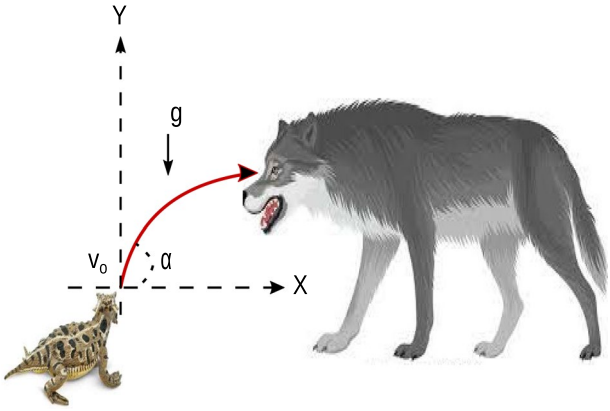

Fig. 6 Horned lizard shooting blood

$$\vec{x}_i(t+1) = \left[v_o \cos\left(\alpha \frac{t}{Max\_iter}\right) + \varepsilon\right] \vec{x}_{best}(t) + \left[v_o \sin\left(\alpha - \frac{\alpha t}{Max\_iter}\right) - g + \varepsilon\right] \vec{x}_i(t) \tag{16}$$

Where $\vec{x}_i(t+1)$ is the new search agent position (horned lizard) in the solution search space for the generation $t+1$, $\vec{x}_{best}(t)$ is the best search agent found, the current search agent is $\vec{x}_i(t)$, *Max_iter* represents the utmost number of iterations (generations), t is the current iteration, v_0 is set to 1 seg, α is set to $\frac{\pi}{2}$, ϵ is set to $1E$-6 and, g is the gravity of the earth, 0.009807 km/s^2

2.2.4 Strategy 4: move-to-escape

In this strategy, the horned lizard performs a random fast move around the environment to escape predators. Ruxton et al. (2004). A function that includes a local and global movement is proposed for the mathematical modeling of this evasion strategy; it is described in Eq. 17 and depicted in Fig. 7. In this equation $walk\left(\frac{1}{2} - \varepsilon\right)\vec{x}_i(t)$ is a local motion around $\vec{x}_i(t)$, and adding $\vec{x}_{best}(t)$ generates a displacement through the solution search space (the global movement).

$$\vec{x}_i(t+1) = \vec{x}_{best}(t) + walk\left(\frac{1}{2} - \varepsilon\right)\vec{x}_i(t) \tag{17}$$

Where $\vec{x}_i(t+1)$ is the new search agent position (horned lizard) in the solution search space for the generation $t+1$, $\vec{x}_{best}(t)$ is the best search agent for the generation t, *walk* is a random number generated between -1 and 1, ϵ is a random number generated from a standard Cauchy distribution with the mean and σ set to 0 and 1, respectively. $\vec{x}_i(t)$ is the current i-th search agent in the t generation.

2.2.5 Strategy 5: α-melanophore stimulating hormone (α-MSH) rate

The horned lizard can lighten or darken its skin, depending on whether or not it needs to decrease or increase its solar thermal gain. The rapid alteration in coloration observed on the skin of horned lizards can be attributed to the influence of temperature on the α-melanophore stimulating hormone (α-MSH). Additional information regarding the study on hormone levels in horned lizards can be seen in Sherbrooke (1997). In this research, the horned lizards' α-melanophore rate value is defined in the following equation:

$$melanophore(i) = \frac{Fitness_{\max} - Fitness(i)}{Fitness_{\max} - Fitness_{\min}} \tag{18}$$

Where $Fitness_{min}$ and $Fitness_{max}$ are the best and the worst fitness value in the current t generation, respectively, whereas fitness(i) is the current fitness value of the i-th search agent.

The $melanophore(i)$ value vector obtained by computing Eq. 18 is normalized in the interval of [0, 1]. A low α-MSH rate, less than 0.3, replaces search agents in Eq. 19, as described in Algorithm 3.

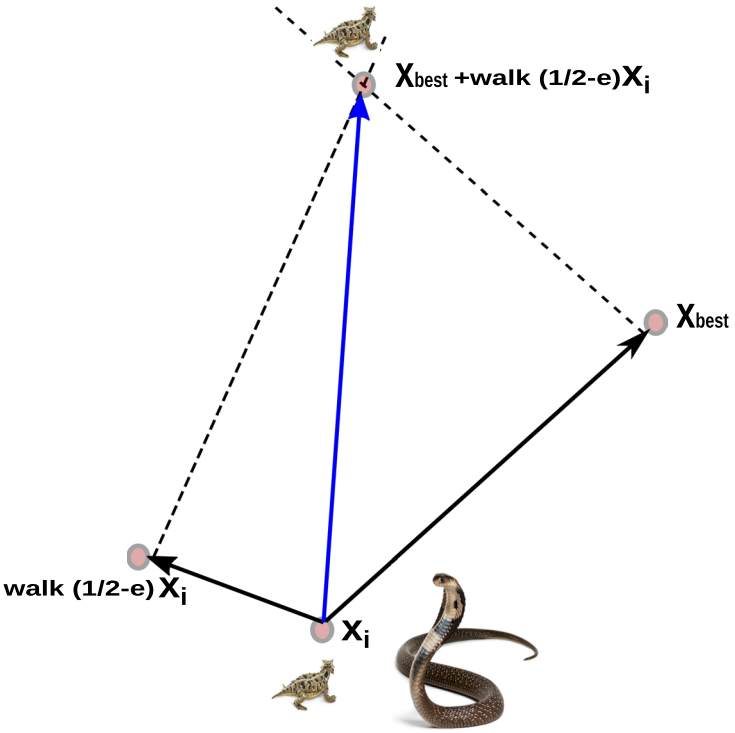

Fig. 7 Horned lizard escaping from predators

$$\vec{x}_i(t) = \vec{x}_{best}(t) + \frac{1}{2}[\vec{x}_{r_1}(t) - (-1)^{\sigma}\vec{x}_{r_2}(t)] \tag{19}$$

Where $\vec{x}_i(t)$ is the current search agent, $\vec{x}_{best}(t)$ is the best search agent found, r_1 and r_2 are integer random numbers generated between 1 and the utmost number of search agents, with $r_1 \neq r_2$, $\vec{x}_{r_1}(t)$ and, $\vec{x}_{r_2}(t)$, are the r_1, r_2-th search agent selected and, σ is a binary value obtained by Algorithm 1

Algorithm 3 α-melanophore procedure

```
Begin procedure
for i = 1 to sizePopulation do
    if melanophore(i) ≤ 0.3 then
        Strategy 5: x⃗_i search agent replaced in Equation 19.
    end if
end for
End procedure
```

2.2.6 The HLOA's time complexity

The HLOA's time complexity analysis includes the analysis of the initialization of the population, fitness evaluation, and updating search agents (lizards). The initialization of the HLOA population is O(PopSize x D), where popSize is the number of search agents (Lizards), and D is the dimension of the optimization problem (design variables number). O(T) represents the time complexity of computing the fitness value, i.e. objective function value. Thus, The amount of time required for the initial evaluation of fitness is bounded by O(PopSize × O (T)). Therefore, the HLOA main loop's computational complexity is O(MaxIteration x PopSize x (D+ O(T))), as summarized in Algorithm 4 (Fig. 8).

2.2.7 Pseudo code for HLOA

In Algorithm 4, the pseudo-code of the HLOA algorithm is described.

Algorithm 4 Horned Lizard Optimizer Algorithm

procedure HLOA
Initialization of parameters. Specify the number of search agents, Population size, and Maximum number of iterations.
Generate the initial population randomly.
while iteration $<$ Max Number of Iterations **do**
    if *Crypsis?* **then**
        Strategy 1: Crypsis. Compute Eq. 8
    else
        if Flee? **then**
            Strategy 4: Move-to-escape. Compute Eq.17
        else
            Strategy 3: Bloodstream shoot Strategy. Compute Eq.16
        end if
    end if
    Replace the worst search agent by skin darkening (Compute Eq.10) or lightening (Compute Eq.9) Strategy 2. They are selected randomly.
    if *Low α-melanophore rate?* **then**
        Strategy 5. Replace search agents with low α-melanophore rate by applying Eq. 19, Algorithm 3.
    end if
    Calculate x_{new}, the fitness value of the new search agents
    if $x_{new} < x_*$ **then**
        $x_* = x_{new}$
    end if
    $iteration = iteration + 1$
end while
Display x_*, the best optimal solution
end procedure

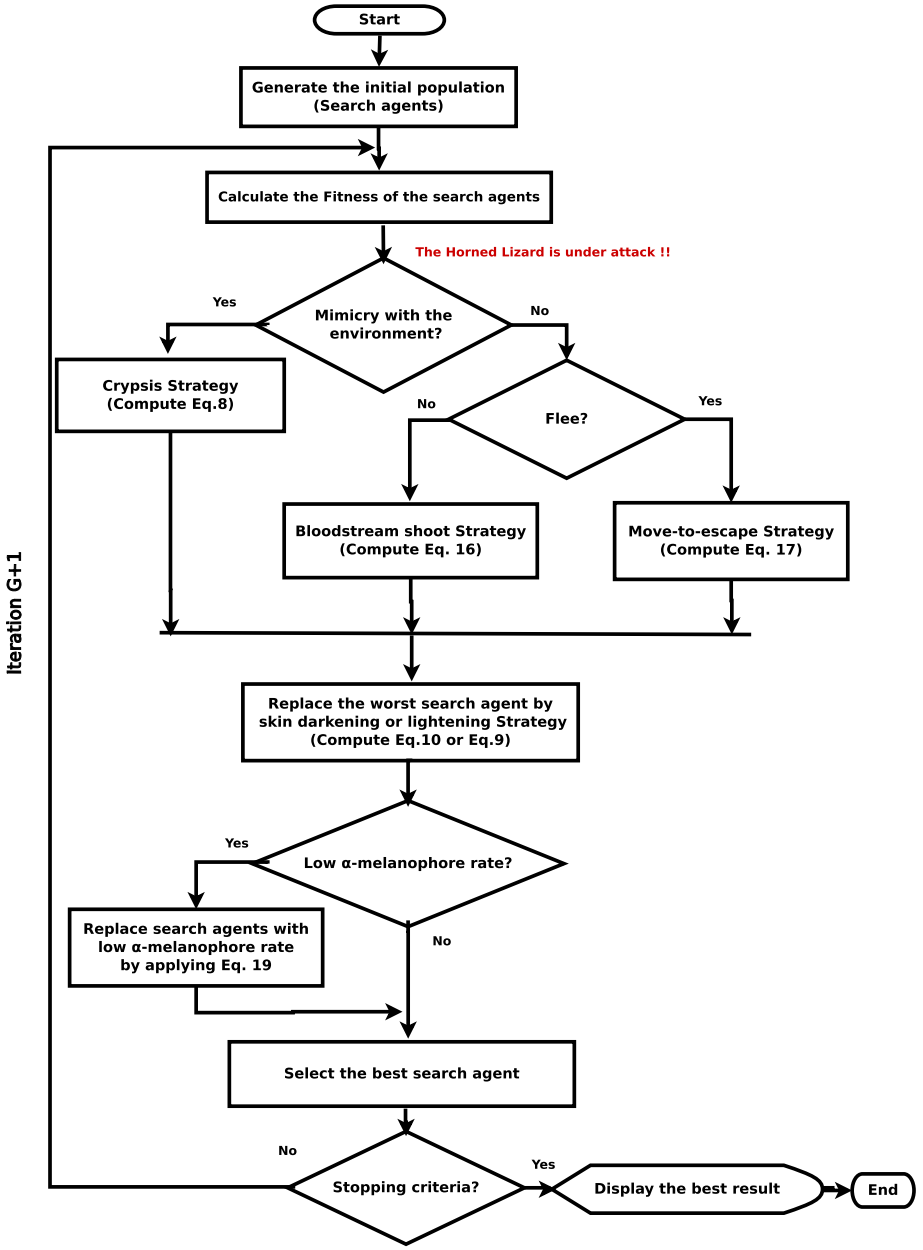

Fig. 8 HLOA flowchart

3 Experimental setup

The numerical efficiency and stability of the HLOA algorithm were evaluated by solving 63 classical benchmark optimization functions reported in the literature. Each of these functions is described in Appendix A, Tables 30, 31, and 32, where Dim represents the function's dimension, Interval is the boundary of the search space for the function and, the optimum value is f_{min}. The HLOA algorithm was compared with ten recent bio-inspired algorithms as described below:

- *Jumping Spider Optimization Algorithm (JSOA)*: The algorithm mimics the behavior of the Arachnida Salticidade spiders in nature and mathematically models its hunting strategies: search, persecution, and jumping skills to get the prey (Peraza-Vázquez et al. 2021).
- *Black Widow Optimization Algorithm (BWOA)*: It is based on modeling different spiders' movement strategies for courtship-mating and the pheromone rate associated with cannibalistic behavior in female spiders (Peña-Delgado et al. 2020).
- *Coot Bird Algorithm (COOT)*: The Coot algorithm imitates two different modes of movement of birds on the water surface (Naruei and Keynia 2021).
- *Crystal Structure Algorithm (CSA)*: The algorithm is based on the principles underpinning the natural occurrence of crystal structures forming from the addition of the basis to the lattice points, which may be observed in the symmetrical arrangement of constituents in crystalline minerals (Talatahari et al. 2021).
- *Dingo Optimization Algorithm (DOA)*: The algorithm mimics the social behavior of the Australian dingo dog. Its inspiration comes from the hunting strategies of dingoes attacking by persecution, grouping tactics, and scavenging behavior (Peraza-Vázquez et al. 2021).
- *Enhanced Jaya Algorithm (EJAYA)*: The classic version of the Jaya algorithm has the defect of easily getting trapped in local optima. This updated version uses the population information more efficiently to improve its performance (Zhang et al. 2021).
- *Rat Swarm Optimizer (RSO)*: The inspiration of this optimizer is the attacking and chasing behaviors of rats in nature (Dhiman et al. 2021).
- *Smell Agent Optimization (SAO)*: The algorithm is based on the relationships between a smelling agent and an object evaporating a smell molecule (Salawudeen et al. 2021).
- *Tunicate Swarm Algorithm (TSA)*: The algorithm imitates jet propulsion and swarm behaviors of tunicates during the navigation and foraging process (Kaur et al. 2020).
- *Wild Horse Optimizer (WHO)*: The algorithm is based on the social behavior of wild horses, such as grazing, chasing, dominating, leading, and mating. The mathematical model includes the representation of mares, foals, and stallions living in groups (Naruei and Keynia 2021).

Each algorithm's benchmark function was executed 30 times, with the population size and number of iterations set to 30 and 200, respectively. Furthermore, the Wilcoxon signed-rank test was used to compare their performance, and the ranking of each algorithm was obtained by the Friedman test. It is to be noted that the three best-ranked algorithms determined by this selection are then evaluated on IEEE CEC 2017 and CEC 2019, as described below.

Table 2 Initial values for the controlling parameters of algorithms

Algorithm	Parameters	Value
For all algorithms	Population size for all problems	30
	Maximum iterations for Testbench Functions and Real-World Problems	200
	Number of replications for Testbench Functions	30
HLOA	Does not use additional parameters	–
JSOA	Does not use additional parameters	–
BWOA	Does not use additional parameters	–
DOA	Hunting probability (P)	0.5
	Scavenger probability (Q)	0.7
COOT	R_1, R_2, R_3, R_4	[0,1]
	R	[− 1,1]
CSA	r_1, r_2, r_3, r_4	[0,1]
EJAYA	Does not use additional parameters	–
RSO	R	[1,5]
	C	[0,2]
SAO	r_0, r_1, r_2, r_3	(0,1]
	olfaction capacity (Olf)	0.75
	Step (SL)	0.9
TSA	c_1,c_2,c_3, r_{and}	[0,1]
	P_{min}	1
	P_{max}	4
WHO	R	[− 2,2]
	R_1, R_2, R_3	[0,1]
	PC	0.13
	PS	0.2

Table 3 IEEE CEC-C06 2019 Benchmarks "The 100-Digit Challenge:"

No	Function	Dim	Interval	f_{min}
CEC-1	Storn's Chebyshev polynomial fitting problem	9	[− 8192, 8192]	1
CEC-2	Inverse Hilbert matrix problem	16	[− 16284,16284]	1
CEC-3	Lennard–Jones minimum energy cluster	18	[− 4, 4]	1
CEC-4	Rastrigin's function	10	[− 100,100]	1
CEC-5	Griewangk's function	10	[− 100,100]	1
CEC-6	Weierstrass function	10	[− 100,100]	1
CEC-7	Modified Schwefel's function	10	[− 100,100]	1
CEC-8	Expanded Schaffer's F6 function	10	[− 100,100]	1
CEC-9	Happy Cat function	10	[− 100,100]	1
CEC-10	Ackley function	10	[− 100,100]	1

IEEE CEC 2017 Testbech Functions: Experimental studies are performed on 28 10-dimensional, 30-dimensional, 50-dimensional, and 100-dimensional benchmark problems from the IEEE CEC 2017 "Constrained Real-Parameter Optimization", as outlined in Table 33.

Table 4 Comparison of optimization results obtained for 63 benchmark functions

Algorithms	HLOA			JSOA			BWOA		
	Best	Ave	Std	Best	Ave.	Std.	Best	Ave.	Std.
F1	− 8.88E-16	− 8.88E-16	0.00E+00	− 8.88E-16	− 8.88E-16	0.00E+00	− 8.88E-16	− 8.88E-16	0.00E+00
F2	− 2.00E+02	− 2.00E+02	0.00E+00	− 2.00E+02	− 2.00E+02	0.00E+00	− 2.00E+02	− 2.00E+02	0.00E+00
F3	− 1.86E+02	− 1.86E+02	8.54E-14	− 1.86E+02	− 1.86E+02	8.67E-14	− 1.86E+02	− 1.86E+02	4.84E-04
F4	− 4.59E+00	− 4.27E+00	4.32E-01	− 4.59E+00	− 4.56E+00	1.61E-01	− 4.59E+00	− 4.35E+00	5.98E-01
F5	− 1.08E+00	− 1.08E+00	2.70E-16	− 1.08E+00	− 1.08E+00	1.80E-16	− 1.08E+00	− 1.07E+00	1.50E-02
F6	0.00E+00	0.00E+00	0.00E+00	0.00E+00	0.00E+00	0.00E+00	0.00E+00	0.00E+00	0.00E+00
F7	− 2.83E+13	− 2.28E+13	8.97E+12	− 2.83E+13	− 2.33E+13	9.94E+12	− 2.83E+13	− 1.96E+13	1.21E+13
F8	1.00E+00	1.00E+00	0.00E+00	1.00E+00	1.00E+00	0.00E+00	1.00E+00	1.00E+00	0.00E+00
F9	4.47E-21	1.27E-01	2.89E-01	1.73E-21	1.02E-01	2.63E-01	3.72E-17	1.02E-01	2.63E-01
F10	− 1.07E+02	− 9.96E+01	1.30E+01	− 1.07E+02	− 1.03E+02	7.91E+00	− 1.07E+02	− 9.96E+01	1.30E+01
F11	0.00E+00	0.00E+00	0.00E+00	0.00E+00	0.00E+00	0.00E+00	0.00E+00	0.00E+00	0.00E+00
F12	0.00E+00	0.00E+00	0.00E+00	0.00E+00	0.00E+00	0.00E+00	0.00E+00	0.00E+00	0.00E+00
F13	6.36E-23	8.57E-18	2.54E-17	4.96E-22	3.76E-16	1.62E-15	2.55E-14	5.33E-11	2.69E-10
F14	1.85E-23	3.83E-15	1.91E-14	2.75E-20	1.17E-12	6.43E-12	1.75E-14	3.49E-08	1.83E-07
F15	2.59E-109	8.05E-91	4.37E-90	3.90E-75	1.98E-67	9.22E-67	1.69E-253	1.23E-194	0.00E+00
F16	2.71E-03	3.61E-02	1.64E-02	1.48E-02	4.64E-02	8.58E-03	5.65E-03	4.52E-02	1.00E-02
F17	− 2.06E+00	− 2.06E+00	1.63E-15	− 2.06E+00	− 2.06E+00	9.76E-16	− 2.06E+00	− 2.06E+00	1.03E-13
F18	− 2.48E+04	− 2.48E+04	3.24E-12	− 2.48E+04	− 2.48E+04	8.46E-12	− 2.48E+04	− 1.90E+04	1.07E+04
F19	− 1.00E+00	− 1.00E+00	0.00E+00	− 1.00E+00	− 1.00E+00	0.00E+00	− 1.00E+00	− 1.00E+00	0.00E+00
F20	− 1.00E+00	− 1.00E+00	2.93E-13	− 1.00E+00	− 1.00E+00	2.06E-17	− 1.00E+00	− 1.00E+00	3.46E-12
F21	8.63E-128	8.90E-102	4.85E-101	3.38E-77	1.83E-69	8.81E-69	2.80E-264	2.72E-193	0.00E+00
F22	− 1.00E+00	− 1.00E+00	0.00E+00	− 1.00E+00	− 1.00E+00	0.00E+00	− 1.00E+00	− 1.00E+00	0.00E+00
F23	3.00E+00	7.50E+00	1.60E+01	3.00E+00	3.00E+00	9.91E-15	3.00E+00	9.30E+00	2.09E+01
F24	− 2.87E+00	− 2.87E+00	3.95E-16	− 2.87E+00	− 2.87E+00	3.87E-16	− 2.87E+00	− 2.87E+00	1.86E-15
F25	0.00E+00	0.00E+00	0.00E+00	0.00E+00	0.00E+00	0.00E+00	0.00E+00	0.00E+00	0.00E+00
F26	8.65E-02	2.59E-01	1.91E-01	6.47E-02	4.13E-01	1.78E-01	1.61E-01	4.91E-01	2.10E-01
F27	4.33E-21	6.00E-17	1.65E-16	1.83E-19	4.77E-16	1.96E-15	7.69E-14	8.87E-11	2.39E-10

Table 4 (continued)

Algorithms	HLOA			JSOA			BWOA		
	Best	Ave	Std	Best	Ave.	Std.	Best	Ave.	Std.
F28	− 1.51E+01	− 1.51E+01	5.42E-15	− 1.51E+01	− 1.51E+01	5.42E-15	− 1.51E+01	− 1.51E+01	5.42E-15
F29	− 6.74E-01	− 6.74E-01	1.32E-16	− 6.74E-01	− 6.74E-01	3.57E-17	− 6.74E-01	− 6.74E-01	1.16E-09
F30	3.81E-20	5.28E-02	1.54E-01	4.99E-18	6.92E-03	3.79E-02	9.02E-12	7.52E-01	3.70E-01
F31	2.02E+02	2.02E+02	0.00E+00	2.02E+02	2.02E+02	0.00E+00	2.02E+02	2.02E+02	0.00E+00
F32	1.00E+02	1.00E+02	0.00E+00	1.00E+02	1.00E+02	0.00E+00	1.00E+02	1.00E+02	0.00E+00
F33	3.22E+01	3.46E+01	1.80E+00	3.20E+01	3.20E+01	1.08E-14	3.20E+01	3.20E+01	1.08E-14
F34	9.00E-01	9.00E-01	4.52E-16	9.00E-01	9.00E-01	4.52E-16	9.00E-01	9.00E-01	4.52E-16
F35	0.00E+00	0.00E+00	0.00E+00	0.00E+00	0.00E+00	0.00E+00	0.00E+00	0.00E+00	0.00E+00
F36	6.98E+02	1.29E+03	3.35E+02	1.66E+03	2.14E+03	1.48E+02	2.94E+03	4.35E+03	6.48E+02
F37	2.36E-05	8.12E-04	8.88E-04	1.08E-05	2.95E-04	3.31E-04	2.16E-05	4.44E-04	3.99E-04
F38	0.00E+00	0.00E+00	0.00E+00	0.00E+00	0.00E+00	0.00E+00	0.00E+00	0.00E+00	0.00E+00
F39	− 5.00E+00	− 1.95E+00	2.43E+00	0.00E+00	1.82E-38	6.19E-38	− 5.00E+00	− 1.67E-01	9.13E-01
F40	2.24E-02	2.68E+01	7.13E+00	1.07E-16	4.08E-01	1.11E+00	2.89E+01	2.90E+01	2.93E-02
F41	2.77E-53	1.43E-45	7.41E-45	0.00E+00	1.10E-37	5.37E-37	1.95E-117	4.36E-78	2.39E-77
F42	0.00E+00	0.00E+00	0.00E+00	0.00E+00	0.00E+00	0.00E+00	0.00E+00	0.00E+00	0.00E+00
F43	0.00E+00	0.00E+00	0.00E+00	0.00E+00	0.00E+00	0.00E+00	0.00E+00	0.00E+00	0.00E+00
F44	1.57E-03	1.57E-03	1.10E-06	1.57E-03	1.57E-03	6.92E-07	1.57E-03	1.57E-03	1.24E-06
F45	2.93E-01	2.93E-01	5.50E-10	2.93E-01	2.93E-01	3.93E-06	2.93E-01	2.93E-01	6.01E-06
F46	2.31E-51	5.23E-47	2.16E-46	0.00E+00	2.70E-39	4.38E-39	2.60E-136	4.26E-97	2.30E-96
F47	7.73E-57	2.02E-48	3.97E-48	0.00E+00	7.56E-40	2.61E-39	8.32E-125	9.58E-95	5.23E-94
F48	2.00E-58	2.80E-46	1.38E-45	0.00E+00	2.89E-39	1.11E-38	6.01E-126	2.20E-91	1.20E-90
F49	0.00E+00	0.00E+00	0.00E+00	0.00E+00	7.48E-297	0.00E+00	0.00E+00	0.00E+00	0.00E+00
F50	3.90E+03	5.84E+03	1.02E+03	3.82E-04	3.04E+03	1.48E+03	7.10E+03	8.41E+03	5.64E+02
F51	− 4.45E+02	− 3.30E+02	1.07E+02	− 4.45E+02	− 4.41E+02	9.00E+00	− 1.96E+02	− 1.46E+02	9.58E+00
F52	− 3.86E+02	− 3.21E+02	4.09E+01	− 3.86E+02	− 3.66E+02	4.27E+01	− 2.22E+02	− 1.57E+02	1.81E+01
F53	− 3.19E+32	− 1.85E+31	6.25E+31	− 8.75E+33	− 4.23E+32	1.68E+33	− 5.94E+25	− 3.05E+24	1.10E+25

Table 4 (continued)

Algorithms	HLOA			JSOA			BWOA		
	Best	Ave	Std	Best	Ave.	Std.	Best	Ave.	Std.
F54	5.61E-104	1.97E-89	1.03E-88	0.00E+00	1.67E-67	4.30E-67	1.59E-242	2.98E-199	0.00E+00
F55	− 1.03E+03	− 9.87E+02	1.94E+01	− 1.17E+03	− 8.23E+02	2.37E+02	− 7.46E+02	− 6.42E+02	5.21E+01
F56	1.55E-101	3.73E-88	2.04E-87	0.00E+00	2.23E-65	1.19E-64	4.78E-258	8.80E-197	0.00E+00
F57	4.20E-119	6.21E-106	3.37E-105	0.00E+00	4.17E-70	2.19E-69	4.29E-257	9.11E-192	0.00E+00
F58	0.00E+00	0.00E+00	0.00E+00	0.00E+00	0.00E+00	0.00E+00	0.00E+00	0.00E+00	0.00E+00
F59	4.29E-43	3.70E-07	1.88E-06	2.18E-34	9.39E-30	1.84E-29	5.39E-82	3.13E-18	1.72E-17
F60	3.51E-12	5.52E-12	3.61E-12	0.00E+00	3.51E-13	1.07E-12	3.51E-12	6.67E-08	2.38E-07
F61	− 1.00E+00	− 1.00E+00	0.00E+00	− 1.00E+00	− 1.00E+00	0.00E+00	− 1.00E+00	− 1.00E+00	0.00E+00
F62	− 1.00E+00	− 1.00E+00	0.00E+00	− 1.00E+00	− 1.00E+00	0.00E+00	− 1.00E+00	− 1.00E+00	0.00E+00
F63	9.30E-106	4.87E-90	2.66E-89	3.29E-72	1.26E-63	4.29E-63	7.42E-263	6.29E-194	0.00E+00
Algorithms									
	DOA			COOT			CSA		
	Best	Ave.	Std.	Best	Ave.	Std.	Best	Ave.	Std.
F1	− 8.88E-16	− 8.88E-16	0.00E+00	6.16E-10	3.08E-06	8.60E-06	3.37E-08	2.55E-04	4.37E-04
F2	− 2.00E+02	− 2.00E+02	0.00E+00	− 2.00E+02	− 2.00E+02	4.57E− 10	− 2.00E+02	− 2.00E+02	3.08E-11
F3	− 1.86E+02	− 1.86E+02	1.78E-06	− 1.86E+02	− 1.86E+02	2.37E-07	− 1.86E+02	− 1.86E+02	4.30E-08
F4	− 4.59E+00	− 4.59E+00	2.02E-12	− 4.59E+00	− 4.59E+00	1.07E-05	− 4.59E+00	− 4.59E+00	1.55E-04
F5	− 1.08E+00	− 1.08E+00	2.06E-16	− 1.08E+00	− 1.08E+00	2.18E-16	− 1.08E+00	− 1.08E+00	3.10E-09
F6	0.00E+00	0.00E+00	0.00E+00	0.00E+00	0.00E+00	0.00E+00	0.00E+00	0.00E+00	0.00E+00
F7	− 2.83E+13	− 1.20E+13	1.33E+13	− 2.43E+11	− 6.88E+10	6.87E+10	− 2.83E+13	− 2.76E+13	9.37E+11
F8	1.00E+00	1.00E+00	0.00E+00	1.00E+00	1.00E+00	4.39E-11	1.00E+00	1.00E+00	3.84E-14
F9	0.00E+00	2.54E-02	1.39E-01	9.34E-17	2.13E-09	5.94E-09	3.77E-07	2.04E-05	2.14E-05
F10	− 1.07E+02	− 1.06E+02	3.55E+00	− 1.07E+02	− 1.07E+02	1.81E-02	− 1.07E+02	− 1.07E+02	6.07E-03
F11	0.00E+00	0.00E+00	0.00E+00	0.00E+00	7.25E-16	2.69E-15	0.00E+00	0.00E+00	0.00E+00

Table 4 (continued)

Algorithms									
	DOA			COOT			CSA		
	Best	Ave.	Std.	Best	Ave.	Std.	Best	Ave.	Std.
F12	0.00E+00	0.00E+00	0.00E+00	0.00E+00	9.95E-14	5.17E-13	0.00E+00	0.00E+00	0.00E+00
F13	0.00E+00	2.50E-10	1.36E-09	2.29E-19	1.71E-08	8.51E-08	1.41E-06	1.98E-04	1.74E-04
F14	1.38E-87	1.57E-04	8.61E-04	4.17E-17	7.37E-12	2.40E-11	2.19E-05	5.39E-04	3.98E-04
F15	1.94E-174	3.79E-30	2.07E-29	2.78E-25	6.11E-09	3.32E-08	8.10E-18	1.20E-09	2.28E-09
F16	1.70E-03	9.71E-02	3.25E-01	1.13E-02	2.69E-01	6.96E-01	1.56E-01	4.35E-01	2.17E-01
F17	− 2.06E+00	− 2.06E+00	1.06E-08	− 2.06E+00	− 2.06E+00	4.74E-07	− 2.06E+00	− 2.06E+00	8.34E-07
F18	− 2.48E+04	− 2.48E+04	7.28E-03	− 2.48E+04	− 2.48E+04	1.49E-05	− 2.48E+04	− 2.48E+04	7.55E-01
F19	− 1.00E+00	− 1.00E+00	0.00E+00	− 1.00E+00	− 9.98E-01	1.16E-02	− 1.00E+00	− 1.00E+00	1.02E-12
F20	− 1.00E+00	− 1.00E+00	1.36E-08	− 1.00E+00	− 1.00E+00	8.48E-09	− 1.00E+00	− 1.00E+00	2.19E-04
F21	0.00E+00	1.44E-42	7.86E-42	1.69E-36	4.14E-23	2.18E-22	7.59E-25	2.51E-20	5.38E-20
F22	− 1.00E+00	− 1.00E+00	0.00E+00	− 1.00E+00	− 1.00E+00	2.31E-12	− 1.00E+00	− 1.00E+00	3.20E-10
F23	3.00E+00	3.00E+00	1.76E-07	3.00E+00	3.00E+00	6.38E-09	3.00E+00	3.00E+00	8.27E-04
F24	− 2.87E+00	− 2.87E+00	6.85E-16	− 2.87E+00	− 2.87E+00	3.67E-12	− 2.87E+00	− 2.87E+00	3.66E-07
F25	0.00E+00	0.00E+00	0.00E+00	0.00E+00	3.29E-08	1.61E-07	0.00E+00	2.26E-06	1.13E-05
F26	7.67E-02	4.20E-01	2.11E-01	5.57E-02	1.68E-01	7.15E-02	6.80E-02	1.50E-01	4.57E-02
F27	0.00E+00	6.39E-08	3.50E-07	4.22E-15	4.08E-05	1.85E-04	6.40E-05	1.55E-03	1.51E-03
F28	− 1.51E+01	− 1.51E+01	5.42E-15	− 1.51E+01	− 1.51E+01	5.42E-15	− 1.51E+01	− 1.51E+01	5.42E-15
F29	− 6.74E-01	− 6.74E-01	1.62E-06	− 6.74E-01	− 6.74E-01	3.29E-11	− 6.74E-01	− 6.74E-01	7.67E-08
F30	0.00E+00	2.47E-01	2.56E-01	2.47E-11	7.54E-03	3.88E-02	1.72E-05	3.30E-04	3.14E-04
F31	2.02E+02	2.02E+02	0.00E+00	2.02E+02	2.02E+02	0.00E+00	2.02E+02	2.02E+02	0.00E+00
F32	1.00E+02	1.00E+02	0.00E+00	1.00E+02	1.00E+02	0.00E+00	1.00E+02	1.00E+02	0.00E+00
F33	3.20E+01	3.20E+01	1.08E-14	3.25E+01	3.57E+01	1.62E+00	3.20E+01	3.20E+01	1.08E-14
F34	9.00E-01	9.00E-01	4.61E-16	9.00E-01	1.41E+00	1.16E+00	9.00E-01	9.00E-01	5.45E-06
F35	0.00E+00	0.00E+00	0.00E+00	0.00E+00	0.00E+00	0.00E+00	0.00E+00	0.00E+00	0.00E+00

Table 4 (continued)

Algorithms	DOA			COOT			CSA		
	Best	Ave.	Std.	Best	Ave.	Std.	Best	Ave.	Std.
F36	2.00E+03	2.98E+03	6.44E+02	3.93E+02	1.63E+03	5.49E+02	1.48E+03	2.20E+03	3.49E+02
F37	1.09E-04	6.61E-04	6.20E-04	8.20E-04	8.89E-03	6.02E-03	2.61E-06	2.62E-03	1.63E-03
F38	0.00E+00	0.00E+00	0.00E+00	0.00E+00	1.78E-02	9.74E-02	1.25E-12	6.34E-06	1.86E-05
F39	− 5.00E+00	− 7.97E-01	1.82E+00	− 4.69E+00	− 4.52E+00	1.06E-01	− 2.26E+00	− 7.24E-01	6.54E-01
F40	2.88E+01	2.89E+01	3.79E-02	2.83E+01	3.32E+01	1.03E+01	2.88E+01	2.88E+01	3.02E-02
F41	0.00E+00	3.33E-03	1.82E-02	4.12E-11	1.12E-01	1.14E-01	2.83E-06	3.50E-02	4.68E-02
F42	0.00E+00	0.00E+00	0.00E+00	0.00E+00	2.22E-17	8.94E-17	0.00E+00	0.00E+00	0.00E+00
F43	0.00E+00	0.00E+00	0.00E+00	0.00E+00	2.09E-14	1.14E-13	0.00E+00	0.00E+00	0.00E+00
F44	1.57E-03	1.59E-03	5.54E-05	1.57E-03	1.78E-03	5.08E-04	1.57E-03	1.57E-03	2.49E-06
F45	2.93E-01	2.93E-01	1.62E-05	2.93E-01	2.93E-01	2.17E-05	2.93E-01	2.93E-01	1.88E-06
F46	2.02E-93	1.07E-15	5.84E-15	1.90E-10	9.38E-05	2.13E-04	3.24E-07	4.24E-03	1.33E-02
F47	2.59E-126	1.18E-14	6.04E-14	2.05E-10	3.10E-05	8.85E-05	3.75E-08	2.45E-04	4.04E-04
F48	8.96E-86	1.13E-18	6.19E-18	1.63E-10	4.54E+20	2.48E+21	3.44E-07	2.83E-03	4.76E-03
F49	0.00E+00	1.86E-57	1.02E-56	2.55E-116	7.01E-64	2.67E-63	1.82E-110	1.53E-38	8.18E-38
F50	5.81E+03	7.78E+03	8.56E+02	4.25E+03	6.10E+03	9.03E+02	6.40E+03	7.71E+03	3.87E+02
F51	− 1.46E+02	− 1.15E+02	2.40E+01	− 2.49E+02	− 1.54E+02	3.78E+01	− 1.81E+02	− 1.48E+02	1.22E+01
F52	− 2.42E+02	− 1.60E+02	3.85E+01	− 1.93E+02	− 1.40E+02	2.12E+01	− 2.19E+02	− 1.65E+02	1.86E+01
F53	− 2.74E+26	− 9.29E+24	4.99E+25	− 3.45E+24	− 1.76E+23	6.41E+23	− 1.33E+25	− 6.57E+23	2.44E+24
F54	3.86E-153	4.26E-19	2.33E-18	5.89E-22	1.70E-11	8.58E-11	5.17E-17	9.36E-09	3.08E-08
F55	− 7.88E+02	− 7.22E+02	5.16E+01	− 1.07E+03	− 9.89E+02	5.48E+01	− 8.57E+02	− 8.10E+02	2.57E+01
F56	5.94E-226	1.83E-24	1.00E-23	5.36E-20	1.90E-09	6.99E-09	9.94E-13	2.99E-07	1.15E-06
F57	1.95E-272	4.08E-48	1.96E-47	3.86E-40	2.91E-23	1.24E-22	4.01E-28	3.52E-23	1.32E-22
F58	0.00E+00	0.00E+00	0.00E+00	0.00E+00	0.00E+00	0.00E+00	0.00E+00	0.00E+00	0.00E+00
F59	1.67E-107	1.63E-11	7.33E-11	5.31E-13	5.21E-05	1.53E-04	9.80E-11	1.30E-07	3.84E-07

Table 4 (continued)

Algorithms	DOA			COOT			CSA		
	Best	Ave.	Std.	Best	Ave.	Std.	Best	Ave.	Std.
F60	0.00E+00	8.27E-09	2.44E-08	3.51E-12	7.50E-12	5.83E-12	3.51E-12	3.63E-12	2.23E-13
F61	− 1.00E+00	− 8.00E-01	6.09E-01	− 1.00E+00	− 3.05E-01	9.49E-01	− 1.00E+00	− 1.00E+00	1.13E-09
F62	− 1.00E+00	− 1.00E+00	5.96E-08	− 1.00E+00	− 6.43E-01	4.33E-01	− 1.00E+00	− 9.79E-01	5.12E-02
F63	1.58E-219	1.02E-23	5.57E-23	1.01E-26	4.42E-04	2.42E-03	5.58E-14	8.93E-09	2.43E-08

Algorithms	EJAYA			RSO			SAO			TSA			WHO		
	Best	Ave	Std	Best	Ave.	Std.	Best	Ave.	Std.	Best	Ave.	Std.	Best	Ave.	Std.
F1	3.46E+00	6.33E+00	1.73E+00	− 8.88E-16	− 8.88E-16	0.00E+00	4.34E-02	5.97E-01	1.33E+00	7.59E-05	2.13E+00	1.60E+00	8.18E-11	1.19E-08	2.21E-08
F2	− 2.00E+02	− 2.00E+02	1.09E-10	− 2.00E+02	− 2.00E+02	0.00E+00	− 2.00E+02	− 1.98E+02	3.26E+00	− 2.00E+02	− 2.00E+02	2.99E-14	− 2.00E+02	− 2.00E+02	0.00E+00
F3	− 1.86E+02	− 1.86E+02	8.67E-14	− 1.86E+02	− 1.86E+02	7.88E-09	− 1.86E+02	− 1.75E+02	2.76E+01	− 1.86E+02	− 1.86E+02	4.79E-04	− 1.86E+02	− 1.86E+02	8.67E-14
F4	− 4.59E+00	− 4.59E+00	2.86E-08	− 4.59E+00	− 4.59E+00	5.39E-04	− 4.59E+00	− 3.16E+00	1.45E+00	− 4.59E+00	− 4.27E+00	4.32E-01	− 4.59E+00	− 4.56E+00	1.61E-01
F5	− 1.08E+00	− 1.08E+00	4.12E-17	− 1.08E+00	− 1.08E+00	9.61E-05	− 1.08E+00	− 1.04E+00	3.75E-02	− 1.08E+00	− 1.08E+00	2.68E-10	− 1.08E+00	− 1.08E+00	0.00E+00
F6	0.00E+00	7.47E+00	4.83E+00	0.00E+00	0.00E+00	0.00E+00	0.00E+00	1.08E+00	7.77E-01	1.28E+01	3.06E+01	7.49E+00	0.00E+00	0.00E+00	0.00E+00
F7	− 4.70E+09	− 9.99E+08	1.30E+09	− 1.13E+05	− 1.01E+04	2.37E+04	− 2.83E+13	− 1.40E+13	1.13E+13	− 1.35E+10	− 5.93E+08	2.46E+09	− 4.53E+11	− 6.24E+10	9.25E+10
F8	1.00E+00	1.00E+00	1.06E-12	1.00E+00	1.00E+00	0.00E+00	1.01E+00	5.54E+02	1.40E+03	1.00E+00	1.00E+00	0.00E+00	1.00E+00	1.00E+00	0.00E+00
F9	1.07E-20	1.86E-14	3.60E-14	1.65E-03	6.75E-02	1.90E-01	1.61E-06	4.09E-03	5.01E-03	1.98E-09	1.49E-01	3.03E-01	0.00E+00	2.54E-02	1.39E-01
F10	− 1.07E+02	− 1.07E+02	5.59E-06	− 1.07E+02	− 1.07E+02	5.46E-01	− 1.07E+02	− 1.06E+02	2.23E+00	− 1.07E+02	− 1.04E+02	7.37E+00	− 1.07E+02	− 1.07E+02	4.71E-14
F11	0.00E+00	2.96E-16	1.26E-15	0.00E+00	0.00E+00	0.00E+00	1.04E-03	1.62E+01	4.48E+01	0.00E+00	1.71E-04	9.39E-04	0.00E+00	0.00E+00	0.00E+00
F12	0.00E+00	4.63E-17	1.84E-16	0.00E+00	0.00E+00	0.00E+00	1.56E-03	3.05E+00	7.98E+00	0.00E+00	9.46E-02	1.10E-01	0.00E+00	0.00E+00	0.00E+00
F13	1.10E-23	6.45E-21	1.50E-20	1.13E-03	2.96E-02	2.69E-02	2.47E-06	8.70E-02	4.74E-01	2.37E-06	6.00E-01	2.96E+00	0.00E+00	2.10E-31	1.15E-30
F14	5.07E-25	5.37E-22	1.68E-21	4.44E-07	1.20E-03	1.46E-03	9.88E-06	1.13E-02	3.08E-02	1.74E-05	2.70E-04	2.72E-04	1.38E-87	1.05E-31	5.76E-31
F15	3.78E-01	1.66E+00	1.17E+00	0.00E+00	5.99E-115	1.11E-114	2.68E-04	1.21E-02	1.09E-02	1.97E-10	1.00E-08	1.90E-08	1.18E-21	2.20E-18	3.56E-18
F16	2.15E-02	9.85E-02	6.33E-02	2.08E-01	1.52E+00	7.87E-01	1.60E-01	1.24E+00	7.71E-01	5.42E-02	4.60E-01	2.21E-01	1.54E-04	1.24E-02	9.51E-03
F17	− 2.06E+00	− 2.06E+00	1.15E-08	− 2.06E+00	− 2.06E+00	4.97E-05	− 2.06E+00	− 2.06E+00	8.61E-04	− 2.06E+00	− 2.06E+00	6.07E-07	− 2.06E+00	− 2.06E+00	1.63E-14

Table 4 (continued)

Algorithms															
	EJAYA			RSO			SAO			TSA			WHO		
	Best	Ave	Std	Best	Ave.	Std.	Best	Ave.	Std.	Best	Ave.	Std.	Best	Ave.	Std.
F18	− 2.48E+04	− 2.48E+04	6.43E-05	− 2.48E+04	− 2.48E+04	1.12E+00	− 2.48E+04	− 2.33E+04	2.24E+03	− 2.48E+04	− 2.31E+04	6.29E+03	− 2.48E+04	− 2.48E+04	9.38E-05
F19	− 1.00E+00	− 9.99E-01	2.79E-03	− 1.00E+00	− 1.00E+00	0.00E+00	− 9.98E-01	− 9.48E-01	3.99E-02	− 1.00E+00	− 9.43E-01	1.95E-02	− 1.00E+00	− 9.98E-01	1.16E-02
F20	− 1.00E+00	− 1.00E+00	7.55E-08	− 9.98E-01	− 9.23E-01	1.01E-01	− 1.00E+00	− 5.27E-01	4.93E-01	− 1.00E+00	− 6.00E-01	4.98E-01	− 1.00E+00	− 1.00E+00	0.00E+00
F21	4.95E-23	6.33E-15	3.21E-14	0.00E+00	1.42E-112	7.75E-112	5.65E-04	1.61E-01	2.23E-01	4.30E-57	2.86E-21	1.57E-20	1.68E-80	8.27E-67	2.50E-66
F22	− 1.00E+00	− 9.95E-01	4.29E-03	− 1.00E+00	− 1.00E+00	0.00E+00	− 1.00E+00	− 9.96E-01	4.30E-03	− 1.00E+00	− 1.00E+00	4.26E-10	− 1.00E+00	− 1.00E+00	0.00E+00
F23	3.00E+00	3.00E+00	5.45E-15	3.00E+00	3.00E+00	1.14E-03	3.00E+00	3.79E+00	1.68E+00	3.00E+00	1.11E+01	1.76E+01	3.00E+00	3.00E+00	2.30E-15
F24	− 2.87E+00	− 2.87E+00	5.89E-16	− 2.87E+00	− 2.87E+00	2.02E-04	− 2.87E+00	− 2.87E+00	3.61E-05	− 2.87E+00	− 2.84E+00	2.12E-01	− 2.87E+00	− 2.87E+00	4.74E-16
F25	1.24E+00	1.92E+00	5.09E-01	0.00E+00	0.00E+00	0.00E+00	7.07E-05	2.81E+00	5.39E+00	5.65E-07	1.91E-02	2.07E-02	0.00E+00	9.88E-14	2.76E-13
F26	8.42E-02	1.69E-01	6.14E-02	1.31E-01	2.99E-01	5.73E-02	1.25E-02	7.30E-02	4.34E-02	1.50E-01	3.44E-01	8.40E-02	3.87E-02	9.96E-02	5.56E-02
F27	9.93E-12	2.67E-06	7.05E-06	1.18E-04	9.37E-02	1.39E-01	6.90E-07	1.69E-02	3.03E-02	3.55E-05	9.06E-04	8.31E-04	0.00E+00	8.95E-15	2.92E-14
F28	− 1.51E+01	− 1.51E+01	5.42E-15	− 1.51E+01	− 1.51E+01	5.42E-15	− 1.51E+01	− 1.51E+01	5.42E-15	− 1.51E+01	− 1.51E+01	5.42E-15	− 1.51E+01	− 1.51E+01	5.42E-15
F29	− 6.74E-01	− 6.74E-01	1.65E-14	− 6.74E-01	− 5.76E-01	1.46E-01	− 6.74E-01	− 5.99E-01	1.45E-01	− 6.74E-01	− 6.74E-01	3.40E-06	− 6.74E-01	− 6.74E-01	8.50E-17
F30	2.84E-15	3.80E-10	8.43E-10	3.30E-01	8.77E-01	1.92E-01	8.38E-07	9.56E-02	1.61E-01	2.65E-06	6.31E-05	6.95E-05	3.65E-30	1.13E-01	2.29E-01
F31	2.02E+02	2.02E+02	0.00E+00	2.02E+02	2.02E+02	0.00E+00	2.02E+02	2.02E+02	0.00E+00	2.02E+02	2.02E+02	0.00E+00	2.02E+02	2.02E+02	0.00E+00
F32	1.00E+02	1.00E+02	0.00E+00	1.00E+02	1.00E+02	0.00E+00	1.00E+02	1.00E+02	0.00E+00	1.00E+02	1.00E+02	0.00E+00	1.00E+02	1.00E+02	0.00E+00
F33	3.22E+01	3.49E+01	1.48E+00	4.41E+01	4.41E+01	7.23E-15	3.20E+01	3.20E+01	1.08E-14	3.20E+01	3.20E+01	1.08E-14	3.21E+01	3.43E+01	1.59E+00
F34	1.38E+00	2.66E+00	5.77E-01	9.00E-01	2.69E+00	1.68E+00	1.05E+00	6.05E+00	3.02E+00	3.74E+00	4.78E+00	7.23E-01	9.00E-01	1.61E+00	6.48E-01
F35	5.78E-22	1.19E-07	4.00E-07	0.00E+00	0.00E+00	0.00E+00	0.00E+00	1.82E-06	4.45E-06	1.74E-40	6.78E-29	2.31E-28	0.00E+00	0.00E+00	0.00E+00
F36	1.72E+05	3.47E+06	3.64E+06	3.03E+03	4.86E+03	8.15E+02	1.56E+03	3.29E+07	1.08E+08	2.76E+02	9.70E+02	3.83E+02	2.61E+02	9.15E+02	4.46E+02
F37	5.63E-02	1.78E-01	7.91E-02	7.75E-07	1.19E-03	1.50E-03	3.89E-03	5.64E-02	5.54E-02	5.58E-03	3.47E-02	2.15E-02	1.55E-04	3.30E-03	2.85E-03
F38	1.13E+02	1.55E+02	2.01E+01	0.00E+00	0.00E+00	0.00E+00	1.40E-01	7.88E+01	8.70E+01	1.53E+02	2.08E+02	3.49E+01	0.00E+00	1.65E-03	5.07E-03
F39	− 4.58E+00	− 4.24E+00	2.21E-01	− 5.00E+00	− 4.83E+00	9.12E-01	9.73E-03	1.12E-01	1.57E-01	− 5.00E+00	− 5.00E+00	2.64E-04	− 4.86E+00	− 4.52E+00	3.46E-01
F40	4.03E+01	9.37E+01	3.94E+01	2.88E+01	2.89E+01	8.82E-02	1.10E-01	5.76E+00	9.96E+00	2.71E+01	2.85E+01	6.19E-01	2.64E+01	6.06E+01	5.75E+01
F41	2.38E+00	3.43E+00	6.93E-01	0.00E+00	3.66E-02	4.90E-02	9.99E-02	1.44E+00	1.60E+00	3.00E-01	5.30E-01	1.18E-01	4.72E-05	1.02E-01	6.70E-02
F42	4.66E-15	1.69E-09	8.94E-09	0.00E+00	0.00E+00	0.00E+00	4.88E-07	3.79E-02	5.30E-02	0.00E+00	7.07E-04	8.81E-04	0.00E+00	0.00E+00	0.00E+00
F43	8.26E-14	1.05E-09	3.19E-09	0.00E+00	0.00E+00	0.00E+00	2.04E-07	4.80E-02	5.64E-02	0.00E+00	1.04E-04	5.72E-04	0.00E+00	0.00E+00	0.00E+00

Table 4 (continued)

Algorithms															
	EJAYA			RSO			SAO			TSA			WHO		
	Best	Ave	Std	Best	Ave.	Std.	Best	Ave.	Std.	Best	Ave.	Std.	Best	Ave.	Std.
F44	1.57E-03	1.64E-03	1.41E-04	1.57E-03	1.57E-03	5.58E-06	1.58E-03	2.53E-02	3.67E-02	1.57E-03	1.57E-03	4.19E-06	1.57E-03	1.57E-03	4.33E-06
F45	2.93E-01	2.93E-01	3.37E-05	2.93E-01	2.93E-01	1.30E-05	2.93E-01	3.07E-01	2.21E-02	2.93E-01	2.93E-01	3.39E-06	2.93E-01	2.93E-01	6.15E-10
F46	1.98E+01	4.26E+01	1.56E+01	0.00E+00	9.23E-51	3.70E-50	2.87E-01	3.73E+01	7.69E+01	1.42E-04	1.03E-03	8.30E-04	1.16E-10	2.24E-08	2.79E-08
F47	9.69E+00	1.27E+01	1.96E+00	0.00E+00	4.82E-09	2.64E-08	1.80E-02	1.29E+00	3.04E+00	1.10E+00	6.49E+00	3.42E+00	1.35E-08	4.24E-06	7.24E-06
F48	2.11E+02	1.16E+15	6.32E+15	0.00E+00	1.20E-53	4.71E-53	4.20E-01	9.72E+18	3.41E+19	1.53E-04	1.17E-03	1.28E-03	4.46E-08	2.09E+02	2.96E+02
F49	7.83E-04	6.24E+00	1.73E+01	0.00E+00	0.00E+00	0.00E+00	6.16E-21	9.53E-11	3.49E-10	2.13E-28	3.36E-19	1.20E-18	4.37E-91	4.05E-62	2.22E-61
F50	6.75E+03	7.77E+03	4.93E+02	5.06E+03	7.34E+03	1.50E+03	2.04E+02	7.55E+03	3.21E+03	5.78E+03	6.85E+03	6.30E+02	2.87E+03	4.47E+03	6.56E+02
F51	− 1.49E+02	− 1.18E+02	1.27E+01	− 2.12E+02	− 1.63E+02	2.08E+01	− 4.45E+02	− 1.56E+02	8.59E+01	− 1.58E+02	− 1.33E+02	1.45E+01	− 3.09E+02	− 2.27E+02	2.59E+01
F52	− 1.55E+02	− 1.23E+02	1.50E+01	− 2.15E+02	− 1.72E+02	3.43E+01	− 3.81E+02	− 1.51E+02	7.23E+01	− 1.74E+02	− 1.38E+02	1.91E+01	− 2.31E+02	− 2.06E+02	1.73E+01
F53	− 4.55E+23	− 1.93E+22	8.32E+22	− 7.51E+27	− 6.48E+26	1.56E+27	− 2.36E+30	− 1.99E+29	5.72E+29	− 7.53E+24	− 7.21E+23	1.99E+24	− 1.23E+28	− 5.64E+26	2.27E+27
F54	5.31E-02	3.16E-01	3.43E-01	0.00E+00	4.27E-101	2.28E-100	1.25E-04	1.89E-02	3.05E-02	6.92E-11	9.60E-09	1.35E-08	6.56E-23	1.56E-17	7.72E-17
F55	− 1.05E+03	− 8.80E+02	9.92E+01	− 8.75E+02	− 6.58E+02	8.45E+01	− 1.17E+03	− 1.17E+03	5.52E-01	− 9.66E+02	− 8.51E+02	6.99E+01	− 1.08E+03	− 1.02E+03	3.34E+01
F56	3.42E+00	1.39E+01	7.97E+00	0.00E+00	1.95E-98	8.44E-98	1.35E-02	5.33E-01	5.58E-01	1.77E-08	5.70E-07	9.45E-07	4.29E-20	1.77E-16	4.32E-16
F57	7.83E-25	1.58E-21	3.32E-21	0.00E+00	6.44E-116	2.94E-115	1.04E-04	9.31E-03	1.85E-02	2.84E-55	5.97E-02	1.22E-01	1.74E-80	6.23E-67	3.00E-66
F58	0.00E+00	0.00E+00	0.00E+00	0.00E+00	0.00E+00	0.00E+00	0.00E+00	8.08E-02	1.51E-01	0.00E+00	4.62E-22	1.92E-21	0.00E+00	0.00E+00	0.00E+00
F59	1.21E-03	3.54E-01	9.14E-01	0.00E+00	6.38E-18	2.85E-17	6.49E-05	7.06E-03	1.24E-02	8.12E-03	2.11E+02	9.93E+02	4.91E-21	1.02E-11	5.03E-11
F60	7.39E-12	1.06E-11	1.66E-12	0.00E+00	1.93E-10	4.12E-10	3.55E-12	4.30E-08	1.25E-07	6.47E-09	2.74E-07	6.78E-07	1.48E-11	2.18E-11	3.32E-12
F61	9.95E-01	9.95E-01	3.39E-16	− 1.00E+00	4.63E-01	8.97E-01	9.95E-01	9.96E-01	4.76E-04	9.97E-01	9.98E-01	2.33E-04	− 1.00E+00	− 8.67E-01	5.06E-01
F62	5.62E-13	3.27E-12	2.48E-12	− 1.00E+00	− 2.00E-01	4.07E-01	1.43E-16	2.15E-14	5.00E-14	4.30E-13	8.97E-13	6.89E-13	− 9.97E-01	− 4.19E-01	3.99E-01
F63	3.53E+01	8.73E+01	3.98E+01	0.00E+00	1.18E-100	6.46E-100	1.02E+00	6.25E+01	7.92E+01	1.02E-03	2.10E-02	3.43E-02	1.73E-11	1.38E-06	3.46E-06

IEEE CEC-06 2019 Testbech Functions: The "100-Digit Challenge" testbench functions from IEEE CEC-06 2019 are described in Table 3.

The entire parameter settings for each algorithm are shown in Table 2. All experiments were conducted on a standard desktop computer with the following specifications: Intel core i7-10750 H CPU, 2.60 GHz, 32 GB RAM, Linux Kubuntu 20.04 LTS operating system, and implemented in MATLAB R2021b.

4 Results and discussion

This section presents the computational results of HLOA on benchmark optimization problems. The comparison results are shown in Table 4, displaying the best, mean, and standard deviation values. Moreover, Figs. 9, 10, and 11 summarize the convergence graphs of all functions versus all algorithms chosen for this investigation. To analyze the significant differences between the results of the proposed HLOA and the other algorithms, a non-parametric Wilcoxon Signed-rank test with a significance level of %5 was conducted. This trial determines the significance level of two algorithms. An algorithm is statistically significant if the calculated p-value is less than 0.05. Table 5 summarizes the result of this test. Furthermore, the eleven algorithms were ranked by computing the Friedman test for 63 benchmark functions. Friedman test ranks the algorithms according to their average performance and generates a ranking score, where a lower value indicates a better performance. The results are shown in Table 6. According to the statistical data presented in Table 4, the Horned Lizard Optimization Algorithm (HLOA) can achieve exceptional outcomes. Among the 63 benchmark functions, there are unimodal and multimodal functions to test the algorithm's capabilities related to the exploitation and exploration in the solution space. A more reliable way to compare the performance of algorithms when solving benchmark functions is through statistical tests. The results of the Wilcoxon rank-sum test, in Table 5, indicate that HLOA outperformed the following algorithms: Black

Table 5 Statistical results of Wilcoxon signed-rank test for HLOA versus other algorithms for 63 functions, with a significance level of %5

HLOA vs JSOA		**HLOA vs BWOA**	
(+/=/-)	*p*-value	(+/=/-)	*p*-value
22/26/15	7.92E-01	28/19/16	**3.40E-04**
HLOA vs DOA		**HLOA vs COOT**	
(+/=/-)	p-value	(+/=/-)	p-value
36/16/11	**6.54E-03**	48/5/10	**1.99E-04**
HLOA vs CSA		**HLOA vs EJAYA**	
(+/=/-)	p-value	(+/=/-)	p-value
43/9/11	**5.79E-03**	47/3/13	**1.40E-05**
HLOA vs RSO		**HLOA vs SAO**	
(+/=/-)	p-value	(+/=/-)	p-value
30/16/17	**1.67E-03**	54/2/7	**7.60E-07**
HLOA vs TSA		**HLOA vs WHO**	
(+/=/-)	p-value	(+/=/-)	p-value
52/4/7	**2.00E-06**	31/13/19	4.31E-01

The bold numbers in the table indicate a significant difference between the two related Algorithms where HLOA was outstanding

Table 6 Friedman test of all compared algorithms for 63 functions

	HLOA	JSOA	BWOA	DOA	COOT	CSA	EJAYA	RSO	SAO	TSA	WHO
Sum of ranks	248.22	250.11	313.74	340.2	411.39	381.78	475.65	364.14	560.07	529.2	291.06
Mean of ranks	3.94	3.97	4.98	5.4	6.53	6.06	7.55	5.78	8.89	8.4	4.62
Overall ranks	**1**	**2**	**4**	**5**	**8**	**7**	**9**	**6**	**11**	**10**	**3**

The bold number in a table indicates the order of the ranked algorithms by the Freidman test

Table 7 IEEE CEC 2017 Benchmarks "Constrained Real-Parameter Optimization" results for Dimension 10, from the best ranked algorithms

Function	HLOA			JSOA			BWOA			WHO		
	Best	Ave	Std	Best	Ave	Std	Best	Ave	Std	Best	Ave	Std
C01	7.72e+0	9.46e+1	9.06e+1	1.20e+3	3.73e+3	2.27e+3	7.11e+2	3.28e+3	1.94e+3	9.05e−2	6.15e+0	6.87e+0
C02	9.38e+0	9.02e+1	7.10e+1	1.04e+3	4.49e+3	2.89e+3	1.04e+3	3.88e+3	3.02e+3	1.26e−2	5.28e+0	8.46e+0
C03	1.91e+3	1.11e+4	7.00e+3	2.02e+3	7.21e+3	3.00e+3	1.36e+3	8.91e+3	4.68e+3	6.06e+2	4.44e+3	2.35e+3
C04	6.49e+1	9.24e+1	2.15e+1	7.71e+1	1.12e+2	1.78e+1	8.69e+1	1.19e+2	2.04e+1	1.90e+1	4.32e+1	1.14e+1
C05	1.65e+1	9.47e+4	2.45e+5	9.70e+2	6.52e+6	2.04e+7	7.08e+2	8.07e+6	3.23e+7	5.56e−1	9.79e+0	1.26e+1
C06	2.86e+2	1.01e+4	1.32e+4	1.06e+3	4.56e+4	4.41e+4	7.28e+2	3.05e+4	3.47e+4	1.22e+2	1.82e+3	1.52e+3
C07	-8.01e+1	2.36e+6	6.34e+6	-6.63e+1	9.84e+7	8.12e+7	-1.45e+2	5.70e+7	5.96e+7	-1.62e+2	-4.72e+1	4.71e+1
C08	1.55e+3	7.87e+5	1.16e+6	1.66e+6	1.90e+7	1.22e+7	3.98e+6	4.09e+7	3.26e+7	7.51e−2	1.88e+3	5.76e+3
C09	1.30e+0	4.92e+2	1.23e+3	4.09e+0	1.31e+6	2.96e+6	1.28e+1	6.08e+5	1.62e+6	-1.82e−2	7.54e+1	3.36e+2
C10	2.91e+3	1.52e+6	4.25e+6	1.82e+10	1.33e+11	1.08e+11	4.62e+9	1.84e+11	1.87e+11	9.63e−4	5.44e+0	2.52e+1
C11	4.92e+2	9.56e+5	2.09e+6	1.09e+7	7.54e+7	3.81e+7	1.98e+6	4.91e+7	3.37e+7	2.96e+1	2.81e+6	1.08e+7
C12	8.24e+0	3.38e+1	2.03e+1	1.34e+9	6.64e+9	5.11e+9	4.68e+8	4.47e+9	4.35e+9	3.99e+0	5.24e+0	4.68e+0
C13	9.80e+3	2.46e+7	4.79e+7	1.18e+8	8.49e+9	5.87e+9	2.03e+8	4.32e+9	3.01e+9	3.89e−3	5.60e+1	1.25e+2
C14	3.32e+0	2.67e+3	7.22e+3	3.81e+8	1.10e+10	8.91e+9	1.49e+8	7.78e+9	8.73e+9	2.38e+0	2.90e+0	3.02e−1
C15	1.18e+1	1.70e+1	3.12e+0	3.27e+8	3.71e+9	3.49e+9	1.49e+1	2.26e+9	3.37e+9	5.50e+0	1.06e+1	2.80e+0
C16	5.03e+1	6.60e+1	1.04e+1	5.65e+1	2.71e+9	3.65e+9	5.03e+1	1.64e+9	3.71e+9	1.26e+1	2.28e+1	6.82e+0
C17	7.99e+10	2.89e+11	1.29e+11	3.82e+10	3.82e+10	2.33e−5	3.82e+10	3.82e+10	2.33e−5	8.79e+10	2.75e+11	1.34e+11
C18	5.74e+6	5.98e+11	2.26e+12	3.35e+16	2.11e+19	2.90e+19	2.86e+13	1.03e+19	2.16e+19	3.13e+1	1.69e+7	6.51e+7
C19	1.77e+11	1.78e+11	2.34e+8	1.78e+11	1.78e+11	1.56e+8	1.77e+11	1.78e+11	1.81e+8	1.76e+11	1.77e+11	3.78e+8
C20	5.48e−1	1.83e+0	4.86e−1	8.71e−1	1.98e+0	4.23e−1	8.17e−1	1.72e+0	4.17e−1	5.86e−1	1.15e+0	2.51e−1
C21	2.40e+1	1.63e+6	7.08e+6	3.56e+9	6.16e+10	4.01e+10	2.17e+9	4.63e+10	4.63e+10	3.99e+0	9.13e+0	8.03e+0
C22	1.22e+5	1.09e+8	1.51e+8	3.95e+9	6.19e+10	4.57e+10	9.30e+7	3.65e+10	3.08e+10	9.50e+0	3.38e+4	8.24e+4
C23	3.60e+0	5.25e+5	1.24e+6	4.36e+9	9.42e+10	8.44e+10	1.65e+9	7.94e+10	8.32e+10	2.73e+0	3.25e+0	2.52e−1
C24	1.18e+1	1.67e+1	2.43e+0	5.76e+8	3.24e+10	2.53e+10	9.72e+8	3.84e+10	4.03e+10	8.64e+0	1.17e+1	2.26e+0
C25	4.40e+1	7.04e+1	1.08e+1	4.53e+8	4.13e+10	3.46e+10	4.57e+7	3.19e+10	3.51e+10	1.88e+1	3.80e+1	1.26e+1

Table 7 (continued)

Function	HLOA			JSOA			BWOA			WHO		
	Best	Ave	Std	Best	Ave	Std	Best	Ave	Std	Best	Ave	Std
C26	1.21e+5	2.04e+5	2.28e+5	7.62e+9	7.21e+10	3.92e+10	3.40e+8	2.78e+10	2.23e+10	1.21e+5	1.21e+5	4.08e−2
C27	1.67e+7	1.76e+14	3.33e+14	2.98e+17	1.89e+21	3.17e+21	1.54e+18	2.21e+21	3.95e+21	9.80e+1	3.04e+14	9.02e+14
C28	1.78e+11	1.78e+11	1.50e+8	1.78e+11	1.78e+11	1.54e+8	1.77e+11	1.78e+11	1.96e+8	1.77e+11	1.78e+11	2.41e+8

Table 8 IEEE CEC 2017 Benchmarks "Constrained Real-Parameter Optimization" results for Dimension 30, from the best ranked algorithms

Function	HLOA			JSOA			BWOA			WHO		
	Best	Ave	Std	Best	Ave	Std	Best	Ave	Std	Best	Ave	Std
C01	3.72e+3	6.69e+3	1.75e+3	1.18e+4	2.69e+4	1.19e+4	1.41e+4	2.85e+4	1.03e+4	2.27e+3	6.03e+3	3.18e+3
C02	3.17e+3	5.74e+3	1.73e+3	1.22e+4	2.72e+4	1.04e+4	1.43e+4	5.06e+4	4.59e+4	1.21e+3	4.50e+3	1.81e+3
C03	5.44e+4	2.37e+5	1.10e+5	5.52e+4	2.54e+5	1.22e+5	8.97e+4	2.17e+5	1.10e+5	2.92e+4	6.22e+4	2.73e+4
C04	3.23e+2	3.95e+2	3.58e+1	3.86e+2	4.28e+2	2.36e+1	3.73e+2	4.31e+2	3.05e+1	1.48e+2	2.22e+2	4.94e+1
C05	3.26e+4	4.85e+5	1.14e+6	2.67e+5	2.10e+6	5.12e+6	9.99e+4	9.44e+6	2.58e+7	1.14e+2	2.16e+4	1.14e+5
C06	1.75e+3	2.73e+4	3.74e+4	2.11e+3	1.16e+5	1.34e+5	2.45e+3	7.87e+4	9.28e+4	3.02e+3	8.70e+3	3.60e+3
C07	-7.52e+1	6.85e+8	6.36e+8	8.47e+8	3.81e+9	1.49e+9	1.96e+9	4.42e+9	1.21e+9	-3.11e+2	2.86e+7	7.00e+7
C08	3.44e+7	9.76e+7	4.17e+7	1.20e+8	1.07e+9	8.94e+8	6.21e+8	6.86e+9	8.43e+9	7.91e+7	2.24e+9	3.69e+9
C09	1.55e+6	7.20e+8	1.69e+9	8.73e+9	1.20e+11	8.65e+10	8.11e+8	4.02e+10	5.34e+10	3.06e+0	1.05e+6	5.73e+6
C10	2.35e+9	8.71e+10	7.74e+10	3.27e+12	6.31e+12	3.34e+12	2.92e+12	2.17e+13	1.21e+13	2.39e+9	6.02e+10	7.11e+10
C11	1.47e+7	1.96e+8	1.44e+8	1.42e+9	2.91e+9	7.20e+8	1.00e+9	2.36e+9	8.47e+8	2.01e+6	1.81e+8	2.96e+8
C12	2.78e+6	4.83e+7	6.62e+7	9.08e+10	2.16e+11	6.04e+10	9.00e+10	2.10e+11	5.66e+10	5.29e+4	4.50e+7	1.03e+8
C13	3.84e+8	2.71e+9	3.01e+9	1.05e+11	2.15e+11	5.43e+10	9.15e+10	2.19e+11	5.87e+10	1.88e+7	2.91e+8	7.16e+8
C14	8.75e+6	1.37e+8	1.32e+8	1.06e+11	3.83e+11	1.14e+11	1.90e+11	4.24e+11	1.04e+11	2.40e+5	3.21e+7	5.75e+7
C15	1.81e+1	2.30e+1	3.84e+0	4.63e+10	1.33e+11	4.38e+10	1.34e+10	1.24e+11	5.00e+10	1.49e+1	2.57e+1	6.99e+0
C16	1.95e+2	2.26e+2	1.52e+1	4.76e+10	1.35e+11	4.23e+10	6.17e+10	1.40e+11	4.34e+10	1.07e+2	1.56e+2	2.03e+1
C17	2.41e+12	5.62e+12	1.71e+12	3.54e+11	3.54e+11	0.00e+0	3.54e+11	3.54e+11	0.00e+0	2.28e+12	5.76e+12	1.60e+12
C18	2.05e+13	1.59e+16	4.11e+16	5.42e+20	1.62e+21	6.13e+20	5.65e+20	1.46e+21	5.59e+20	3.31e+12	1.76e+16	6.51e+16
C19	1.85e+12	1.85e+12	8.56e+8	1.85e+12	1.85e+12	5.41e+8	1.85e+12	1.85e+12	7.97e+8	1.84e+12	1.84e+12	1.87e+9
C20	6.37e+0	8.49e+0	9.15e−1	7.11e+0	9.44e+0	8.31e−1	7.26e+0	8.83e+0	8.06e−1	5.81e+0	7.22e+0	6.22e−1
C21	1.97e+8	3.89e+9	3.61e+9	1.84e+12	4.84e+12	1.59e+12	1.99e+12	3.69e+12	1.29e+12	1.07e+8	4.57e+9	6.01e+9
C22	2.81e+9	1.59e+10	9.78e+9	1.77e+12	4.45e+12	1.57e+12	9.45e+11	4.03e+12	1.95e+12	3.36e+8	9.56e+9	9.97e+9
C23	3.49e+8	7.73e+9	5.94e+9	2.16e+12	8.54e+12	3.37e+12	2.78e+12	6.70e+12	2.64e+12	1.89e+8	4.01e+9	5.20e+9
C24	1.81e+1	8.73e+7	3.38e+8	1.44e+12	3.72e+12	1.21e+12	1.21e+12	3.80e+12	1.38e+12	1.81e+1	1.91e+8	8.86e+8
C25	1.95e+2	1.13e+8	4.24e+8	4.73e+11	4.04e+12	1.79e+12	1.30e+12	3.23e+12	1.31e+12	1.76e+2	2.23e+9	8.59e+9

Table 8 (continued)

Function	HLOA			JSOA			BWOA			WHO		
	Best	Ave	Std	Best	Ave	Std	Best	Ave	Std	Best	Ave	Std
C26	1.15e+8	3.26e+9	2.24e+9	1.14e+12	3.95e+12	1.75e+12	1.76e+12	4.11e+12	1.58e+12	8.23e+6	3.64e+9	5.13e+9
C27	6.24e+16	2.01e+19	3.14e+19	1.50e+23	1.88e+24	1.47e+24	6.83e+22	9.30e+23	8.05e+23	5.38e+15	4.86e+19	1.29e+20
C28	1.85e+12	1.85e+12	7.62e+8	1.85e+12	1.85e+12	6.30e+8	1.85e+12	1.85e+12	7.19e+8	1.85e+12	1.85e+12	8.13e+8

Table 9 IEEE CEC 2017 Benchmarks "Constrained Real-Parameter Optimization" results for Dimension 50, from the best ranked algorithms

Function	HLOA			JSOA			BWOA			WHO		
	Best	Ave	Std	Best	Ave	Std	Best	Ave	Std	Best	Ave	Std
C01	1.40e+4	2.09e+4	3.73e+3	3.90e+4	1.10e+5	4.31e+4	3.64e+4	1.14e+5	6.50e+4	1.41e+4	2.63e+4	8.64e+3
C02	1.23e+4	2.61e+4	3.04e+4	4.39e+4	1.53e+5	8.01e+4	4.02e+4	1.27e+5	8.43e+4	9.65e+3	1.77e+4	4.40e+3
C03	1.77e+5	9.63e+5	5.38e+5	2.45e+5	9.23e+5	6.32e+5	1.69e+5	6.87e+5	4.39e+5	7.11e+4	1.58e+5	5.95e+4
C04	6.61e+2	7.28e+2	4.51e+1	7.39e+2	7.81e+2	2.56e+1	7.09e+2	7.85e+2	3.76e+1	3.44e+2	5.33e+2	9.98e+1
C05	2.65e+5	6.17e+6	1.98e+7	4.61e+5	4.54e+7	7.29e+7	3.27e+5	5.36e+7	8.84e+7	3.74e+3	2.18e+5	5.12e+5
C06	2.57e+3	2.65e+4	4.24e+4	6.73e+3	1.57e+5	1.88e+5	3.20e+3	1.12e+5	1.28e+5	5.89e+3	1.46e+4	4.98e+3
C07	1.11e+9	4.43e+9	1.79e+9	2.45e+9	1.15e+10	5.72e+9	9.45e+9	1.71e+10	3.77e+9	-2.28e+2	9.22e+8	7.92e+8
C08	2.20e+8	7.06e+8	2.98e+8	8.94e+8	6.45e+9	7.02e+9	1.74e+9	3.14e+10	3.68e+10	5.71e+8	5.77e+10	7.21e+10
C09	2.61e+8	7.34e+10	1.18e+11	2.28e+11	9.82e+11	3.79e+11	1.45e+11	8.18e+11	4.61e+11	7.83e+2	1.29e+7	4.93e+7
C10	8.61e+11	2.45e+12	1.09e+12	2.00e+13	7.84e+13	5.55e+13	1.64e+13	8.19e+13	5.33e+13	7.12e+11	3.27e+12	2.49e+12
C11	3.50e+8	1.72e+9	8.56e+8	6.23e+9	9.23e+9	1.42e+9	4.67e+9	7.96e+9	1.68e+9	7.67e+7	2.89e+9	4.87e+9
C12	4.30e+8	1.67e+9	1.07e+9	5.71e+11	8.04e+11	9.41e+10	5.11e+11	7.70e+11	1.10e+11	2.73e+8	5.91e+9	6.48e+9
C13	4.70e+9	3.77e+10	3.81e+10	4.83e+11	8.56e+11	1.37e+11	4.52e+11	7.88e+11	1.47e+11	2.65e+9	1.46e+10	1.12e+10
C14	9.97e+8	4.73e+9	4.28e+9	8.43e+11	1.57e+12	2.51e+11	9.22e+11	1.53e+12	2.62e+11	5.33e+8	1.90e+10	2.13e+10
C15	2.12e+1	2.58e+1	4.57e+0	3.08e+11	5.45e+11	1.19e+11	2.72e+11	5.16e+11	1.09e+11	2.12e+1	2.37e+8	8.65e+8
C16	3.39e+2	3.88e+2	2.29e+1	3.17e+11	5.44e+11	9.80e+10	3.34e+11	5.33e+11	9.96e+10	2.40e+2	4.57e+8	2.50e+9
C17	8.83e+12	2.02e+13	3.86e+12	1.04e+12	1.04e+12	7.45e−4	1.04e+12	1.04e+12	7.45e−4	1.21e+13	1.94e+13	4.24e+12
C18	1.70e+16	1.83e+18	1.91e+18	3.96e+21	7.29e+21	1.43e+21	3.60e+21	6.47e+21	1.61e+21	3.91e+17	4.77e+19	7.98e+19
C19	5.28e+12	5.28e+12	2.20e+9	5.28e+12	5.28e+12	9.79e+8	5.28e+12	5.28e+12	1.28e+9	5.26e+12	5.27e+12	4.34e+9
C20	1.40e+1	1.66e+1	1.37e+0	1.61e+1	1.78e+1	8.23e−1	1.50e+1	1.73e+1	1.08e+0	1.29e+1	1.45e+1	9.36e−1
C21	5.04e+9	6.52e+10	4.37e+10	6.93e+12	1.04e+13	1.75e+12	5.03e+12	9.95e+12	1.88e+12	9.92e+9	1.58e+11	1.31e+11
C22	2.59e+10	1.82e+11	1.42e+11	5.31e+12	1.08e+13	1.94e+12	6.11e+12	9.88e+12	1.75e+12	1.75e+10	3.65e+11	6.20e+11
C23	2.04e+10	1.05e+11	6.55e+10	1.26e+13	2.04e+13	4.39e+12	1.27e+13	2.06e+13	3.42e+12	4.62e+10	3.50e+11	3.20e+11
C24	1.81e+1	8.70e+9	1.70e+10	4.46e+12	9.09e+12	1.86e+12	4.93e+12	8.89e+12	2.24e+12	2.75e+1	7.44e+10	1.05e+11
C25	3.77e+2	7.08e+9	1.26e+10	5.98e+12	9.49e+12	1.71e+12	5.36e+12	8.83e+12	2.02e+12	4.96e+8	8.49e+10	1.20e+11

Table 9 (continued)

Function	HLOA			JSOA			BWOA			WHO		
	Best	Ave	Std	Best	Ave	Std	Best	Ave	Std	Best	Ave	Std
C26	6.33e+9	4.62e+10	3.65e+10	5.91e+12	9.97e+12	2.03e+12	5.93e+12	1.01e+13	1.96e+12	9.95e+9	1.60e+11	1.53e+11
C27	2.63e+19	5.81e+20	5.24e+20	7.36e+23	3.46e+24	1.57e+24	1.30e+24	3.53e+24	1.57e+24	5.14e+18	4.43e+21	8.06e+21
C28	5.28e+12	5.28e+12	1.69e+9	5.28e+12	5.28e+12	1.07e+9	5.28e+12	5.28e+12	9.14e+8	5.28e+12	5.28e+12	1.75e+9

Table 10 IEEE CEC 2017 Benchmarks "Constrained Real-Parameter Optimization" results for Dimension 100, from the best ranked algorithms

Function	HLOA			JSOA			BWOA			WHO		
	Best	Ave	Std	Best	Ave	Std	Best	Ave	Std	Best	Ave	Std
C01	6.61e+4	1.04e+5	1.60e+4	1.93e+5	4.70e+5	1.49e+5	2.08e+5	4.13e+5	1.60e+5	6.03e+4	1.29e+5	4.16e+4
C02	6.58e+4	1.38e+5	7.54e+4	2.12e+5	5.57e+5	1.69e+5	1.96e+5	5.16e+5	2.16e+5	5.52e+4	1.06e+5	4.06e+4
C03	7.89e+5	1.85e+6	8.11e+5	6.25e+5	2.03e+6	9.76e+5	4.19e+5	2.11e+6	1.04e+6	2.32e+5	5.86e+5	2.05e+5
C04	1.45e+3	1.60e+3	6.44e+1	1.56e+3	1.65e+3	4.91e+1	1.62e+3	1.69e+3	4.14e+1	1.05e+3	1.35e+3	2.08e+2
C05	1.28e+6	3.63e+6	1.12e+7	1.27e+6	7.04e+6	1.94e+7	1.14e+6	2.38e+7	4.91e+7	1.85e+5	2.25e+6	2.29e+6
C06	4.67e+3	4.08e+4	4.67e+4	9.12e+3	3.65e+5	2.35e+5	2.40e+4	3.23e+5	2.88e+5	8.15e+3	2.24e+4	7.67e+3
C07	2.58e+10	4.54e+10	8.84e+9	2.20e+10	3.89e+10	1.76e+10	6.88e+10	9.78e+10	1.11e+10	6.51e+9	2.30e+10	9.30e+9
C08	6.52e+9	1.35e+10	4.33e+9	1.63e+10	7.68e+10	6.90e+10	4.76e+10	3.52e+11	3.43e+11	3.44e+10	1.77e+12	1.85e+12
C09	3.41e+11	1.49e+12	8.02e+11	2.66e+12	4.91e+12	1.13e+12	1.66e+12	4.70e+12	1.22e+12	1.05e+8	9.62e+9	2.19e+10
C10	3.03e+13	4.85e+13	1.27e+13	1.27e+14	5.33e+14	5.85e+14	1.43e+14	5.94e+14	4.02e+14	4.39e+13	9.76e+13	3.81e+13
C11	8.92e+9	2.21e+10	6.07e+9	3.67e+10	4.55e+10	3.95e+9	2.67e+10	4.23e+10	5.26e+9	5.56e+9	1.77e+11	5.01e+11
C12	5.89e+10	1.55e+11	5.12e+10	4.86e+12	5.73e+12	3.66e+11	4.37e+12	5.59e+12	5.33e+11	2.11e+11	9.13e+11	4.67e+11
C13	1.17e+11	6.00e+11	3.10e+11	5.21e+12	5.95e+12	3.13e+11	5.07e+12	5.95e+12	4.08e+11	3.64e+11	9.67e+11	7.79e+11
C14	1.20e+11	3.52e+11	1.30e+11	9.59e+12	1.13e+13	7.21e+11	8.25e+12	1.13e+13	9.15e+11	3.50e+11	1.57e+12	8.26e+11
C15	2.43e+1	2.31e+10	4.93e+10	3.35e+12	4.24e+12	4.15e+11	3.42e+12	4.27e+12	3.89e+11	2.45e+10	4.56e+11	4.14e+11
C16	7.23e+2	9.18e+9	2.08e+10	3.46e+12	4.37e+12	3.33e+11	3.07e+12	4.20e+12	4.43e+11	1.45e+10	3.82e+11	3.03e+11
C17	8.19e+13	1.12e+14	1.25e+13	6.47e+12	6.47e+12	4.97e−3	6.47e+12	6.47e+12	4.97e−3	7.32e+13	1.05e+14	1.44e+13
C18	1.48e+20	1.09e+21	1.06e+21	9.07e+22	1.13e+23	9.26e+21	7.68e+22	1.07e+23	1.33e+22	1.46e+21	3.04e+22	4.68e+22
C19	2.16e+13	2.16e+13	5.19e+9	2.16e+13	2.16e+13	2.71e+9	2.16e+13	2.16e+13	2.09e+9	2.15e+13	2.15e+13	1.54e+10
C20	3.40e+1	3.80e+1	1.87e+0	3.59e+1	3.96e+1	1.66e+0	3.56e+1	3.92e+1	1.50e+0	3.31e+1	3.51e+1	1.01e+0
C21	8.33e+11	2.65e+12	7.64e+11	5.08e+13	6.53e+13	6.33e+12	4.35e+13	6.16e+13	7.05e+12	2.77e+12	1.00e+13	4.51e+12
C22	1.71e+12	3.86e+12	1.35e+12	4.48e+13	6.36e+13	8.99e+12	4.82e+13	6.49e+13	6.47e+12	3.71e+12	1.11e+13	1.05e+13
C23	1.60e+12	5.50e+12	1.58e+12	9.85e+13	1.29e+14	1.27e+13	7.72e+13	1.23e+14	1.52e+13	5.15e+12	2.08e+13	1.53e+13
C24	8.69e+11	2.04e+12	8.04e+11	3.94e+13	5.91e+13	7.27e+12	3.48e+13	5.58e+13	8.28e+12	2.27e+12	9.30e+12	7.58e+12
C25	7.96e+11	1.90e+12	8.51e+11	4.17e+13	5.79e+13	6.56e+12	4.60e+13	5.98e+13	5.55e+12	2.57e+12	8.76e+12	4.06e+12

Table 10 (continued)

Function	HLOA			JSOA			BWOA			WHO		
	Best	Ave	Std	Best	Ave	Std	Best	Ave	Std	Best	Ave	Std
C26	1.19e+12	2.73e+12	1.13e+12	4.67e+13	6.31e+13	6.59e+12	4.55e+13	6.12e+13	6.98e+12	3.49e+12	9.78e+12	5.82e+12
C27	3.99e+22	1.25e+23	6.64e+22	1.66e+25	3.05e+25	5.20e+24	9.92e+24	2.57e+25	7.40e+24	8.53e+22	1.33e+24	1.36e+24
C28	2.16e+13	2.16e+13	2.68e+9	2.16e+13	2.16e+13	2.10e+9	2.16e+13	2.16e+13	2.21e+9	2.16e+13	2.16e+13	2.52e+9

Table 11 Statistical results of Wilcoxon signed-rank test for IEEE CEC 2017 benchmark functions at Dimension 10, with a significance level of %5

HLOA vs JSOA		HLOA vs BWOA		HLOA vs WHO	
(+/=/-)	p-value	(+/=/-)	p-value	(+/=/-)	p-value
25/0/3	**2.25E-4**	23/0/5	**5.85E-4**	2/0/26	**4.16E-4**

The bold numbers in the table indicate a significant difference between the two related Algorithms where HLOA was outstanding

Table 12 Friedman test for IEEE CEC 2017 benchmark functions at Dimension 10

	HLOA	JSOA	BWOA	WHO
Mean of ranks	2.21	3.59	3.05	1.14
Overall ranks	**2**	**4**	**3**	**1**

The bold number in a table indicates the order of the ranked algorithms by the Freidman test

Table 13 Statistical results of Wilcoxon signed-rank test for IEEE CEC 2017 benchmark functions at Dimension 30, with a significance level of %5

HLOA vs JSOA		HLOA vs BWOA		HLOA vs WHO	
(+/=/-)	*p*-value	(+/=/-)	*p*-value	(+/=/-)	*p*-value
27/0/1	**4.60E-05**	24/0/4	**2.94E-04**	9/0/19	3.74E-01

The bold numbers in the table indicate a significant difference between the two related Algorithms where HLOA was outstanding

Widow Optimization Algorithm (BWOA), Dingo Optimization Algorithm (DOA), Coot Bird Algorithm (COOT), Crystal Structure Algorithm (CSA), Enhanced Jaya Algorithm (EJAYA), Rat Swarm Optimizer (RSO), Smell Agent Optimization (SAO) and, Tunicate Swarm Algorithm (TSA). Meanwhile, there are no significant differences between HLOA versus the Jumping Spider Optimization Algorithm (JSOA) and Wild Horse Optimizer (WHO). Moreover, in the Friedman test analysis, the HLOA algorithm is ranked first, whereas the JSOA, WHO, and BWOA are ranked second, third, and fourth, respectively. Based on this analysis, in the rest of the paper, these algorithms are only used in IEEE CEC 2017 "Constrained Real-Parameter Optimization", IEEE CEC-06 2019 "100-Digit Challenge", and real-world applications.

On the other hand, the findings obtained by computational analysis of HLOA on benchmark functions from IEEE CEC 2017 "Constrained Real-Parameter Optimization" problems for dimensions 10, 30, 50, and 100 are shown in Tables 7, 8, 9, and 10. Say tables display the best, mean, and standard deviation computed. To examine the disparities among the algorithms, a Wilcoxon signed-rank test was used with a significance level of 5%. The ranking between the algorithms HLOA, BWOA, JSOA, and WHO was determined using the Friedman test.

Table 11 summarizes the Wilcoxon rank-sum test for 10-dimensional problems and indicates that HLOA outperformed all the algorithms. Nevertheless, in Table 12 "Friedman test", it is ranked in second place.

Table 14 Friedman test for IEEE CEC 2017 benchmark functions at Dimension 30

	HLOA	JSOA	BWOA	WHO
Mean of ranks	1.86	3.45	3.27	1.43
Overall ranks	**2**	**4**	**3**	**1**

The bold number in a table indicates the order of the ranked algorithms by the Freidman test

Table 15 Statistical results of Wilcoxon signed-rank test for IEEE CEC 2017 benchmark functions at Dimension 50, with a significance level of %5

HLOA vs JSOA		HLOA vs BWOA		HLOA vs WHO	
(+/=/-)	*p*-value	(+/=/-)	*p*-value	(+/=/-)	*p*-value
26/0/2	**6.10E-5**	26/0/2	**6.10E-5**	16/0/12	6.51E-02

The bold numbers in the table indicate a significant difference between the two related Algorithms where HLOA was outstanding

For 30-dimensional problems, the Wilcoxon rank-sum test in Table 13 shows that HLOA outperformed the JSOA and BWOA algorithms. Meanwhile, there are no significant differences with WHO. Whereas, in Table 14 "Friedman test" ranks HLOA in second place.

According to the results presented in Table 15, it can be observed that in the case of 50-dimensional problems, the HLOA algorithm demonstrated superior performance compared to the JSOA and BWOA algorithms, as indicated by the Wilcoxon rank-sum test. In contrast, there are no substantial disparities with the WHO. In comparison, the Friedman test assigns the highest rank to HLOA. See Table 16.

In the context of 100-dimensional problems, the Wilcoxon rank-sum test in Table 17 shows that HLOA outperformed all algorithms. Meanwhile, the Friedman test has determined that HLOA holds the highest rank, as seen in Table 18.

Additionally, the computational results of HLOA on benchmark functions from CEC-06 2019 “The 100-Digit Challenge” problems are shown in Table 19, displaying the best, mean, and standard deviation values. Furthermore, Fig. 12 summarizes the convergence graphs of all functions versus the best-ranked algorithms. To analyze the significant differences between the results, Wilcoxon Signed-rank test with a significance level of %5 was carried out. Table 20 summarizes the result of this test and indicates that HLOA outperformed Black Widow Optimization Algorithm (BWOA). Meanwhile, there are no significant differences between HLOA with the Jumping Spider Optimization Algorithm (JSOA) and Wild Horse Optimizer (WHO).

Table 16 Friedman test for IEEE CEC 2017 benchmark functions at Dimension 50

	HLOA	JSOA	BWOA	WHO
Mean of ranks	1.57	3.52	3.20	1.71
Overall ranks	**1**	**4**	**3**	**2**

The bold number in a table indicates the order of the ranked algorithms by the Freidman test

Table 17 Statistical results of Wilcoxon signed-rank test for IEEE CEC 2017 benchmark functions at Dimension 100, with a significance level of %5

HLOA vs JSOA		HLOA vs BWOA		HLOA vs WHO	
(+/=/-)	p-value	(+/=/-)	p-value	(+/=/-)	p-value
26/0/2	**1.19E-04**	26/0/2	**9.90E-05**	17/0/11	**9.43E-03**

The bold numbers in the table indicate a significant difference between the two related Algorithms where HLOA was outstanding

Table 18 Friedman test for IEEE CEC 2017 benchmark functions at Dimension 100

	HLOA	JSOA	BWOA	WHO
Mean of ranks	1.54	3.48	3.16	1.82
Overall ranks	**1**	**4**	**3**	**2**

The bold number in a table indicates the order of the ranked algorithms by the Freidman test

5 Real-world applications

In this section, the capabilities of the HLOA were tested by solving five optimization problems, which are three Real-World Single Objective Bound Constrained Numerical Optimization problems taken from the CEC 2020 special session (Kumar et al. 2020), the Multiple Gravity Assist (MGA) problems provided by the European Space Agency (ESA) [89] and the Optimal Power Flow Problem. For all engineering problems solved, HLOA was compared against the three best-ranked algorithms calculated from the Friedman test, see Table 6.

5.1 Constraint handling

The Penalization of Constraints method was used for constraint handling. The mathematical formulation of this method is described in Eq. 20 and taken from Peraza-Vázquez et al. (2021).

$$F(\vec{x}) = \begin{cases} f(\vec{x}), & if\ MCV(\vec{x}) \leq 0 \\ f_{\max} + MCV(\vec{x}), & otherwise. \end{cases} \tag{20}$$

Where $f(\vec{x})$ is the fitness function value of a feasible solution (a solution that does not violate constraints), whereas f_{max} is the fitness function value of the worst solution in the population, and $MCV(\vec{x})$ is the Mean Constraint Violation (Peraza-Vázquez et al. 2021) represented in Eq. 21.

$$MCV(x^{\rightarrow}) = \frac{\sum_{i=1}^{p} G_i(x^{\rightarrow}) + \sum_{j=1}^{m} H_j(x^{\rightarrow})}{p+m} \tag{21}$$

Table 19 IEEE CEC-C06 2019 Benchmarks ‘‘The 100-Digit Challenge:’’ results

Algorithms												
Function	HLOA			BWOA			JSOA			WHO		
	Best	Ave	Std	Best	Ave	Std	Best	Ave	Std	Best	Ave	Std
CEC-1	-4.441E-16	-4.441E-16	0.000E+00	4.238E+04	1.704E+05	2.671E+05	-4.441E-16	-4.441E-16	0.000E+00	2.593E-10	1.720E-08	4.305E-08
CEC-2	-2.000E+02	-2.000E+02	0.000E+00	1.735E+01	1.787E+01	4.941E-01	-2.000E+02	-2.000E+02	0.000E+00	-2.000E+02	-2.000E+02	0.000E+00
CEC-3	-1.864E+02	-1.864E+02	8.672E-14	1.270E+01	1.270E+01	1.218E-03	-1.864E+02	-1.864E+02	8.672E-14	-1.864E+02	-1.864E+02	8.672E-14
CEC-4	-4.590E+00	-4.502E+00	2.687E-01	2.377E+03	8.875E+03	5.894E+03	-4.590E+00	-4.561E+00	1.608E-01	-4.590E+00	-4.561E+00	1.608E-01
CEC-5	-1.077E+00	-1.077E+00	2.220E-16	1.764E+00	3.122E+00	8.127E-01	-1.077E+00	-1.077E+00	1.797E-16	-1.077E+00	-1.077E+00	0.000E+00
CEC-6	0.000E+00	0.000E+00	0.000E+00	8.312E+00	1.120E+01	1.216E+00	0.000E+00	0.000E+00	0.000E+00	0.000E+00	0.000E+00	0.000E+00
CEC-7	-2.835E+13	-1.755E+13	1.196E+13	4.019E+02	9.562E+02	3.151E+02	-2.835E+13	-2.592E+13	7.524E+12	-4.755E+11	-7.761E+10	1.036E+11
CEC-8	1.000E+00	1.000E+00	0.000E+00	5.289E+00	6.361E+00	4.656E-01	1.000E+00	1.000E+00	0.000E+00	1.000E+00	1.000E+00	0.000E+00
CEC-9	1.553E-21	7.621E-02	2.325E-01	2.285E+02	1.207E+03	8.101E+02	2.301E-20	3.273E-17	1.072E-16	0.000E+00	9.244E-34	5.063E-33
CEC-10	-1.068E+02	-1.035E+02	7.374E+00	2.021E+01	2.049E+01	1.340E-01	-1.068E+02	-1.022E+02	8.369E+00	-1.068E+02	-1.061E+02	3.552E+00

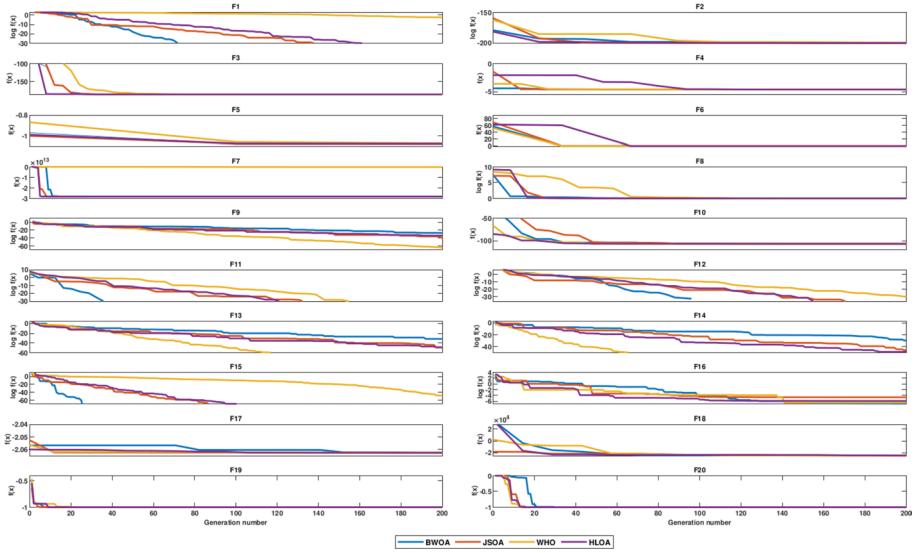

Fig. 9 Convergence curves of the best-ranked algorithms by Friendam test. From F1 to F20, functions shown in Appendix A

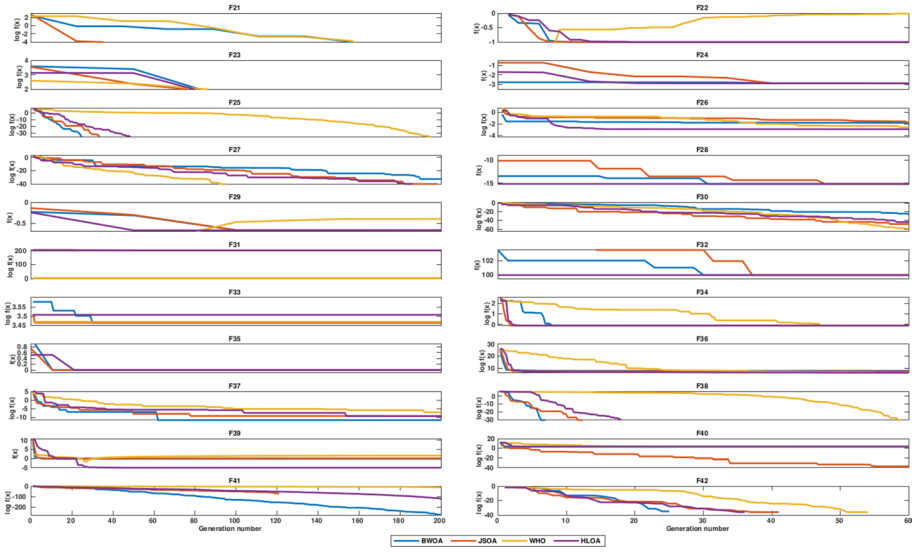

Fig. 10 Convergence curves of the best-ranked algorithms by Friendam test. From F21 to F42, functions shown in Appendix A

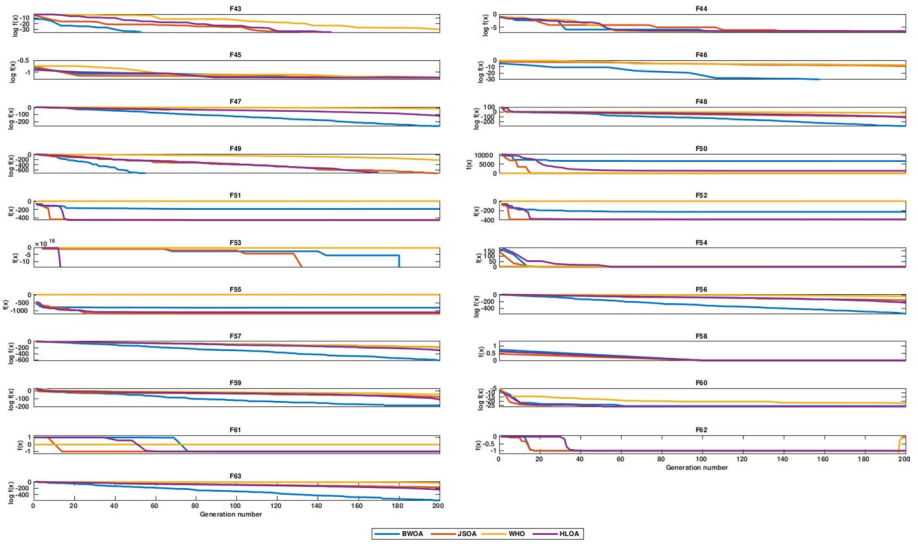

Fig. 11 Convergence curves of the best-ranked algorithms by Friendam test. From F43 to F63, functions shown in Appendix A

Table 20 Statistical results of Wilcoxon signed-rank test for CEC 2019, with a significance level of %5

HLOA vs JSOA		HLOA vs BWOA		HLOA vs WHO	
(+/=/-)	*p*-value	(+/=/-)	*p*-value	(+/=/-)	*p*-value
1/6/3	0.465	10/0/0	**0.005**	2/5/3	0.686

The bold numbers in the table indicate a significant difference between the two related Algorithms where HLOA was outstanding

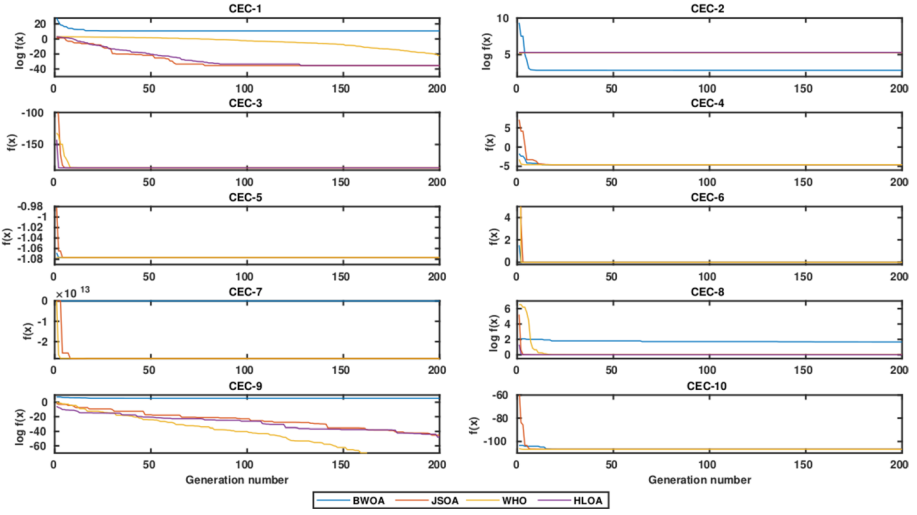

Fig. 12 Convergence Curves of CEC 2019 functions

Table 21 Comparison Results of the Process Flow Sheeting problem

Algorithms	Optimal values for variables			
	x_1	x_2	x_3	f_{min}
HLOA	0.94194	−2.1	1	1.076554818
JSOA	0.94194	−2.1	1	1.076554818
BWOA	0.94194	−2.1	1	1.076554818
WHO	0.94194	−2.1	1	1.076554818

Here, the $MCV(\vec{x})$ is the mean sum of the inequalities $(G_i(\vec{x}))$ and the equalities $(_{H_j(\vec{x})})$ constraints, depicted by Eq. 22 and 23, respectively. Notice that the inequality $_{g_i(\vec{x})}$ and equality $h_j(\vec{x})$ constraints only have a value, the punishment if the constraint is violated.

$$G_i(\vec{x}) = \begin{cases} 0, & if \;\; g_i(\vec{x}) \leq 0 \\ g_i(\vec{x}), & otherwise. \end{cases} \tag{22}$$

$$H_j(\vec{x}) = \begin{cases} 0, & if \; |h_j(\vec{x})| - \delta \leq 0 \\ |h_j(\vec{x})|, & otherwise \end{cases} \tag{23}$$

5.2 Process flow sheeting problem

This non-convex constrained optimization problem has three decision variables with three inequality constraints (Kumar et al. 2020) as described in Eq. 24. The best-known feasible objective function value is $f(\vec{x}) = 1.0765430833$.

$$\begin{aligned} &Minimize && f(\vec{x}) = -0.7x_3 + 5(0.5 - x_1)^2 + 0.8 \\ &Subject\ \text{to} && g_1(\vec{x}) = -e^{(x_1 - 0.2)} - x_2 \leq 0 \\ & && g_2(\vec{x}) = x_2 + 1.1x_3 \leq -1.0 \\ & && g_3(\vec{x}) = x_1 - x_3 \leq 0.2 \\ &with\ \text{bounds}: && 0.2 \leq x_1 \leq 1, -2.22554 \leq x_2 \leq 1, x_3 \in \{0, 1\} \end{aligned} \tag{24}$$

In Table 21, the comparison results show that HLOA, JSOA, BWOA, and WHO reported feasible and competitive solutions, as seen in the convergence graph in Fig. 13. The HLOA difference with the best-known feasible objective function value for all algorithms is 1.17347E-05.

5.3 Process synthesis problem

This problem has seven decision variables and nine inequality constraints with non-linearities in real and binary variables (Kumar et al. 2020). The mathematical representation is shown in Eq. 25. The best-known feasible objective function value is $f(\vec{x}) = 2.9248305537$.

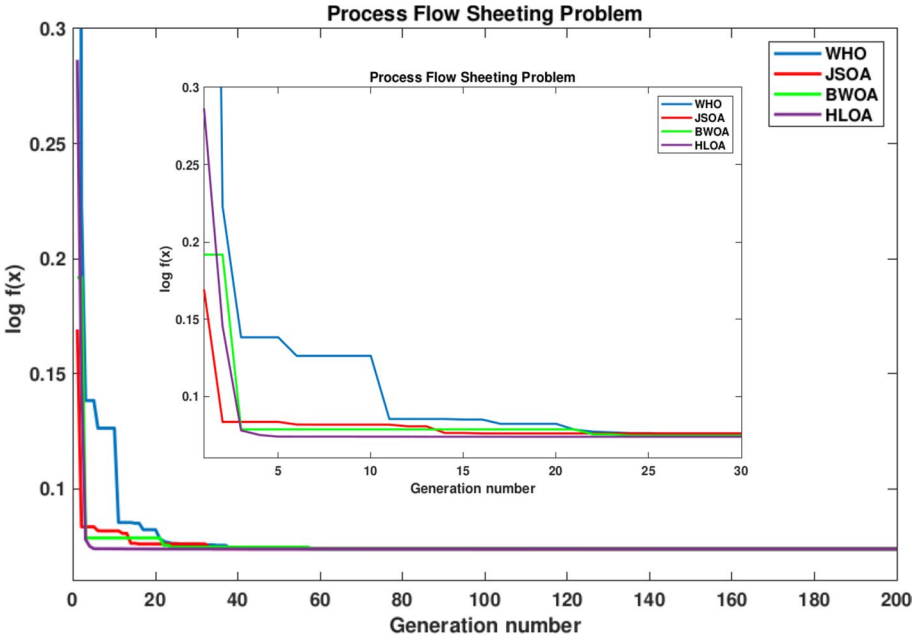

Fig. 13 Convergence graph of the Process Flow Sheeting Problem

$$
\begin{aligned}
\textit{Minimize} \quad & f(\vec{x}) = (1-x_1)^2 + (2-x_2)^2 + (3-x_3)^2 + (1-x_4)^2 + \\
& (1-x_5)^2 + (1-x_6)^2 - \ln(1+x_7) \\
\textit{Subject to} \quad & g_1(\vec{x}) = x_1 + x_2 + x_3 + x_4 + x_5 + x_6 \leq 5 \\
& g_2(\vec{x}) = {x_1}^2 + {x_2}^2 + {x_3}^2 + {x_6}^2 \leq 5.5 \\
& g_3(\vec{x}) = x_1 + x_4 \leq 1.2 \\
& g_4(\vec{x}) = x_2 + x_5 \leq 1.8 \\
& g_5(\vec{x}) = x_3 + x_6 \leq 2.5 \\
& g_6(\vec{x}) = x_1 + x_7 \leq 1.2 \\
& g_7(\vec{x}) = x_2^2 + x_5^2 \leq 1.64 \\
& g_8(\vec{x}) = x_3^2 + x_6^2 \leq 4.25 \\
& g_9(\vec{x}) = x_3^2 + x_5^2 \leq 4.64 \\
\textit{with} \ \text{bounds} \quad & 0 \leq x_1, x_2, x_3 \leq 1, \\
& x_4, x_5, x_6, x_7 \in \{0, 1\}
\end{aligned}
\tag{25}
$$

In Table 22, the comparison results show that all algorithms reported feasible and competitive solutions, as seen in the convergence graph in Fig. 14. Note that the HLOA and BWOA have the most competitive values, whilst HLOA difference to the best-know feasible objective function value is 1.11E-04.

Table 22 Comparison results of the Process Synthesis problem

Optimal values for variables	Algorithms			
	HLOA	JSOA	BWOA	WHO
x_1	0.19849	0.19468	0.19754	0.19551
x_2	1.2806	1.2806	1.2805	1.2806
x_3	1.9546	1.955	1.9548	1.9549
x_4	1	1	1	1
x_5	0	0	0	0
x_6	0	0	0	0
x_7	1	1	1	1
f_{min}	2.92494158706362	2.92495120667677	2.92487042815638	2.92496872672763

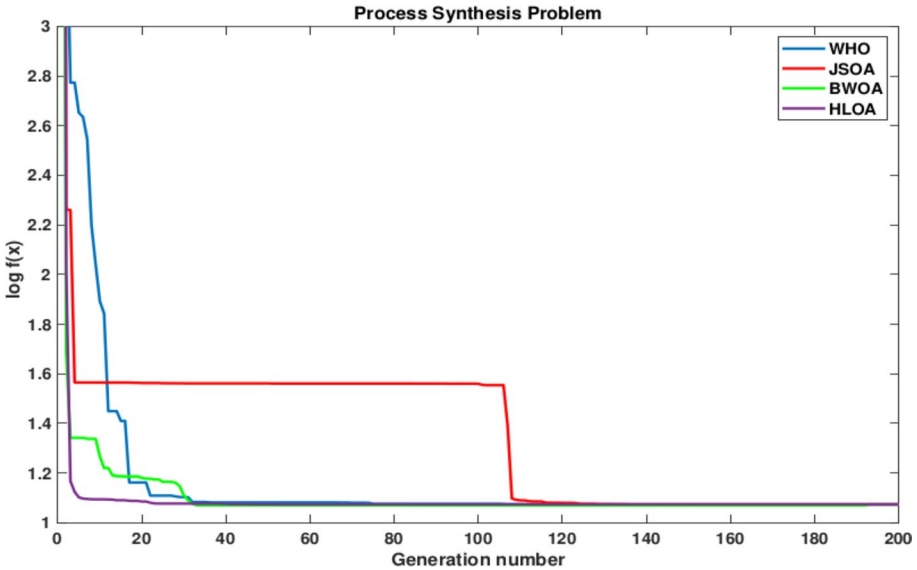

Fig. 14 Convergence graph of the Process Synthesis Problem

5.4 Optimal design of an industrial refrigeration system

This problem stated in Eq. 26, have fourteen decision variables and fifteen inequality constraints formulated and a non-linear inequality-constrained optimization problem (Kumar et al. 2020). Where the best-known feasible objective function value is $f(\vec{x}) =$ 3.22130008E-02.

$$
\begin{aligned}
& f(\vec{x}) = 63098.88x_2x_4x_{12} + 5441.5x_2^2x_{12} + 115055.5x_2^{1.664}x_6 + 6172.27x_2^2x_6 \\
& +63098.88x_1x_3x_{11} + 5441.5x_1^2x_{11} + 115055.5x_1^{1.664}x_5 + 6172.27x_1^2x_5 + \\
\textit{Minimize} \quad & 140.53x_1x_{11} + 281.29x_3x_{11} + 70.26x_1^2 + 281.29x_3^2 + \\
& 14437x_8^{1.8812}x_{12}^{0.3424}x_{10}x_{14}^{-1}x_1^2x_7x_9^{-1} + \\
& 20470.2x_7^{2.893}x_{11}^{0.316}x_1^2 \\
\textit{Subject to} \quad & g_1(\vec{x}) = 1.524x_7^{-1} \leq 1 \\
& g_2(\vec{x}) = 1.524x_8^{-1} \leq 1 \\
& g_3(\vec{x}) = 0.07789x_1 - 2x_7^{-1}x_9 \leq 1 \\
& g_4(\vec{x}) = 7.05305x_9^{-1}x_1^2x_{10}x_8^{-1}x_2^{-1}x_{14}^{-1} \leq 1 \\
& g_5(\vec{x}) = 0.0833x_{13}^{-1}x_{14} \leq 1 \\
& g_6(\vec{x}) = 47.136x_2^{0.333}x_{10}^{-1}x_{12} - 1.333x_8x_{13}^{2.1195} + 62.08x_{13}^{2.1195}x_{12}^{-1}x_8^{0.2}x_{10}^{-1} \leq 1 \\
& g_7(\vec{x}) = 0.04771x_{10}x_8^{1.8812}x_{12}^{0.3424} \leq 1 \\
& g_8(\vec{x}) = 0.0488x_9x_7^{1.893}x_{11}^{0.316} \leq 1 \\
& g_9(\vec{x}) = 0.0099x_1x_3^{-1} \leq 1 \\
& g_{10}(\vec{x}) = 0.0193x_2x_4^{-1} \leq 1 \\
& g_{11}(\vec{x}) = 0.0298x_1x_5^{-1} \leq 1 \\
& g_{12}(\vec{x}) = 0.056x_2x_6^{-1} \leq 1 \\
& g_{13}(\vec{x}) = 2x_9^{-1} \leq 1 \\
& g_{14}(\vec{x}) = 2x_{10}^{-1} \leq 1 \\
& g_1(\vec{x}) = x_{12}x_{11}^{-1} \leq 1 \\
\textit{with} \text{ bounds} \quad & 0.001 \leq x_i \leq 5, i = 1, 2, .., 14
\end{aligned}
\tag{26}
$$

In Table 23, the comparison results show that HLOA and JSOA algorithms reported feasible solutions, whereas BWOA and WHO results are infeasible, as seen in the convergence graph, see Fig. 15. Note that the HLOA algorithm is ranked as the first-best obtained solution, and the difference with the best-known feasible objective function value is improved by -9.93E-04.

5.5 Multiple gravity assist (MGA) optimization problem: cassini spacecraft trajectory design

The Multiple Gravity Assist (MGA) problem is a straightforward benchmark for evaluating global optimization techniques in Space Mission Design-related challenges. The mathematical representation is a finite-dimension global optimization problem with nonlinear constraints. For an interplanetary probe powered by a chemical propulsion engine to travel from the Earth to another planet or asteroid, the best potential trajectory must be found. The MGA mathematical approach can be found in Zuo et al. (2016); Wagner and Wie (2015). Where the European Space Agency (ESA) raises an MGA issue with the Cassini spacecraft trajectory design problem [89]. The objective of this mission is to reach Saturn and get captured by its gravity into an orbit having pericenter radius r_p set to 108950 km, and eccentricity fixed to 0.98. The lower and upper variable bounds are shown in Table 24.

Table 23 Comparison results of the Optimal Design of an Industrial Refrigeration System

Optimal values for variables	Algorithms			
	HLOA	JSOA	BWOA	WHO
x_1	0.001	0.001	0.001	0.001
x_2	0.001	0.0010003	0.001	0.001
x_3	0.001	0.001	0.001	0.001
x_4	0.001	0.001	0.001	0.001
x_5	0.001	0.001	0.001	0.0010002
x_6	0.001	0.001	0.001	0.001
x_7	1.5284	1.58	1.5239	1.5082
x_8	1.524	1.5241	1.3249	1.524
x_9	4.8055	4.9599	2.895	4.9999
x_{10}	2.0036	2.1421	2.0499	2.0189
x_{11}	0.001	0.001	0.0074473	0.015076
x_{12}	0.001	0.001	0.001	0.015076
x_{13}	0.0072995	0.007508	0.0074762	0.025947
x_{14}	0.087629	0.089784	0.079109	0.025947
f_{min}	0.033206223934	0.034988	0.052832403932352*	0.044098911284881*

* The solution does not satisfy one or more constraints

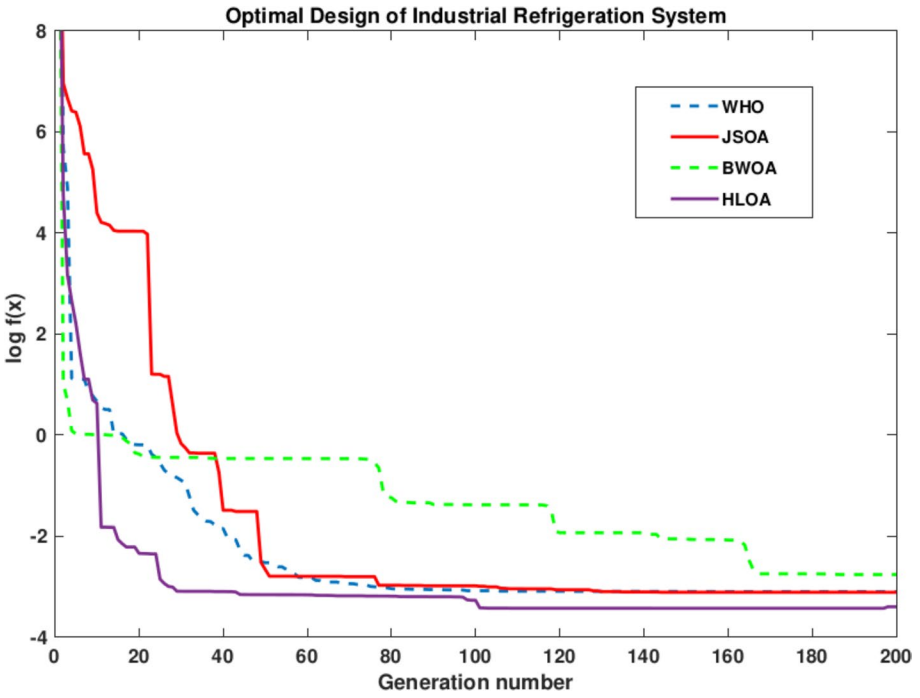

Fig. 15 Convergence graph of the Optimal Design of an Industrial Refrigeration System. The dotted lines represent an infeasible solution shown by an algorithm

Table 24 Lower and Upper Bounds of variables

State	Variable	Lower Bounds	Upper Bounds	Units
x(1)	t_0	-1000	0	*MJD*2000*
x(2)	T_1	30	400	days
x(3)	T_2	100	470	days
x(4)	T_3	30	400	days
x(5)	T_4	400	2000	days
x(6)	T_5	1000	6000	days

* Modified Julian Date 2000

Table 25 Constraints on the various fly-by pericenters

Fy-by pericenters	km
rp_1	6351.8
rp_2	6351.8
rp_3	6778.1
rp_4	671492

The Constraints of the various fly-by pericenters are shown in Table 25. The planetary fly-by sequence and more details can be found in [89]. The best-known feasible objective function value is $f(\vec{x}) = 4.9307$.

The comparison results in Table 26 show that HLOA, JSOA, BWOA, and WHO reported feasible solutions. The HLOA and WHO showed competitive results, whereas BWOA was outstanding, as seen in the convergence graph in Fig. 16. The HLOA difference with the best-known feasible objective function value is 4.26E-01.

5.6 Optimal power flow

The optimal power flow (OPF) is a non-linear optimization problem that combines an optimization function with the power flow problem to calculate the operating conditions of a power system network subjected to practical and physical constraints (Nucci et al. 2021; Huneault and Galiana 1991), OPF mathematical formulation can be described as follows:

$$\begin{aligned} &\text{Minimize } J(x,u), \\ &\text{Subjected to } g(x,u)=0, \\ &\text{and } h(x,u)\leq 0 \end{aligned} \tag{27}$$

Where $J(x, u)$ is the objective function, $g(x, u)$ is the set of equality constraints, while $h(x, u)$ are the inequality constraints. The set of control variables u, defined in Eq. 28, is P_G, active power generation at the PV buses; V_G, voltage magnitude; Q_C, shunt Volt-Amperes Reactive (VAR) compensator; T transformer tap settings. Subindices NG, NC, and NT are the number of generators, the number of regulating transformers, and the VAR compensators, respectively.

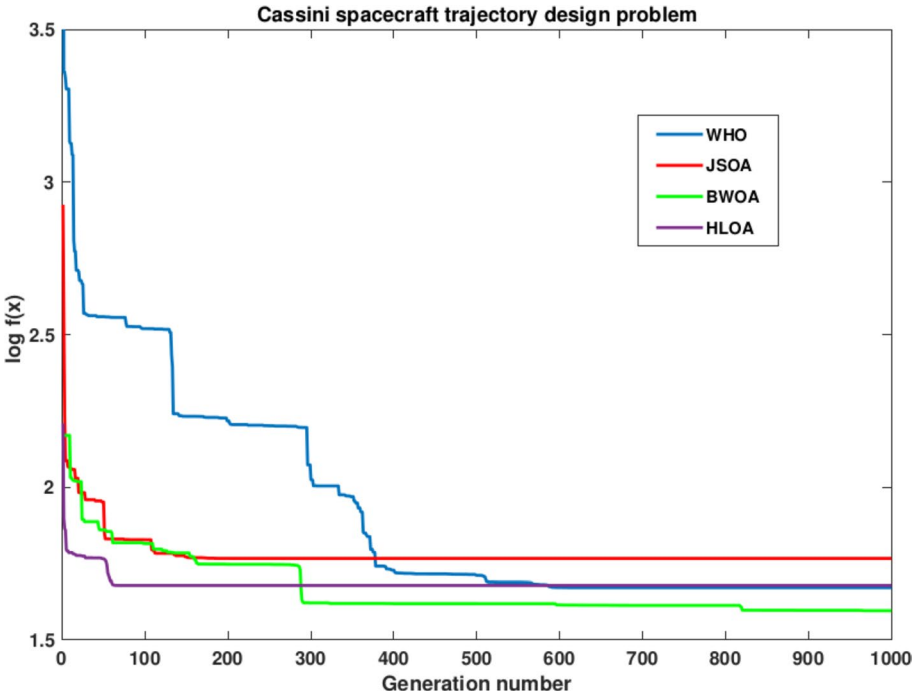

Fig. 16 MGA Optimization: Cassini Spacecraft Trajectory Design Problem

$$u^T = \left[P_{G_2} \cdots P_{G_{NG}}, V_{G_1} \cdots V_{G_{NG}}, Q_{C_1} \cdots Q_{C_{NC}}, T_1 \cdots T_{NT}\right] \tag{28}$$

The set of state variables x^T, stated in Eq. 29, are:

P_{G1}: Active power generation at slack bus
V_L: Voltage at PQ buses
Q_G: Generators reactive power output
S_l: Line flow, transmission line loadings

$$x^T = \left[P_{G_1}, V_{L_1} \cdots V_{L_{NL}}, Q_{G_1} \cdots Q_{G_{NC}}, S_{l_1} \cdots S_{l_{nl}}\right] \tag{29}$$

Where subindices NL and nl are the numbers of load buses and transmission lines, respectively.

The real and reactive power equality constraints taken from the power flow equations are defined in Eq. 30 and 31.

$$P_{Gi} - P_{Di} - V_i \sum_{j=1}^{NB} V_j \left[G_{ij} \cos(\theta_{ij}) + B_{ij} \sin(\theta_{ij})\right] = 0 \tag{30}$$

$$Q_{Gi} - Q_{Di} - V_i \sum_{j=1}^{NB} V_j \left[G_{ij} \sin(\theta_{ij}) + B_{ij} \cos(\theta_{ij})\right] = 0 \tag{31}$$

Table 26 Comparison results for the Cassini Spacecracft Trajectory Design

Optimal values for variables	Algorithms			
	HLOA	JSOA	BWOA	WHO
x_1	−767.4051	−803.93006	−789.577110052954	−766.16821
x_2	173.92445	161.05094	158.658439545012	170.39407
x_3	414.38194	449.38348	449.385957886722	416.44468
x_4	52.698608	60.027747	54.3533764089	52.857507
x_5	1041.7422	795.06518	1028.07660808395	1040.5838
x_6	4696.4909	3837.03	4557.84620923363	4575.138
f_{min}	5.3580	5.7519	4.93248908962165	5.3302

Table 27 Generator, transformer and shunt var compensator inequality constraints

	Min	Max	Initial		Min	Max	Initial
P_{G1}	50	200	99.23	T_{11}	0.9	1.1	1.078
P_{G2}	20	80	80	T_{12}	0.9	1.1	1.069
P_{G5}	15	50	50	T_{15}	0.9	1.1	1.032
P_{G8}	10	35	20	T_{36}	0.9	1.1	1.068
P_{G11}	10	30	20	QC_{10}	0	5	0
P_{G13}	12	40	20	QC_{12}	0	5	0
V_{G1}	0.95	1.1	1.05	QC_{15}	0	5	0
V_{G2}	0.95	1.1	1.04	QC_{17}	0	5	0
V_{G5}	0.95	1.1	1.01	QC_{20}	0	5	0
V_{G8}	0.95	1.1	1.01	QC_{21}	0	5	0
V_{G11}	0.95	1.1	1.05	QC_{23}	0	5	0
V_{G13}	0.95	1.1	1.05	QC_{24}	0	5	0
				QC_{29}	0	5	0

Where P_G and Q_G are the active and reactive power generation, whereas P_D and Q_D are the active and reactive load demand, NB is the number of buses, G_{ij} and B_{ij} are the conductance and susceptance between bus i and j of the admittance matrix $Y_{ij} = G_{ij} + jB_{ij}$. The inequality constraints of the OPF formulation [?], summarized in Table 27, are defined in Eq. 32 to 35. Where Eq. 32 represent the generator constraints; Eq. 33 represent the transformer constraints; Eq. 34 define the shunt VAR compensator constraints; and Eq. 35 represent the security constraints.

$$\begin{aligned} V_{G_i}^{min} \le V_{G_i} \le V_{G_i}^{max}, i = 1, \cdots, NG \\ P_{G_i}^{min} \le P_{G_i} \le P_{G_i}^{max}, i = 1, \cdots, NG \\ Q_{G_i}^{min} \le Q_{G_i} \le Q_{G_i}^{max}, i = 1, \cdots, NG \end{aligned} \tag{32}$$

$$T_i^{min} \le T_i \le T_i^{max}, i = 1, \cdots, NT \tag{33}$$

$$Q_{Ci}^{min} \leq Q_{GCi} \leq Q_{Ci}^{max}, i = 1, \cdots, NG \tag{34}$$

$$\begin{aligned} V_{L_i}^{min} \leq V_{L_i} \leq V_{L_i}^{max}, i = 1, \cdots, NL \\ S_{l_i} \leq S_{l_i}^{max}, i = 1, \cdots, nl \end{aligned} \tag{35}$$

The Black Widow Optimization (BWOA), Jumping Spider Optimization (JSOA), and Wild Horse Optimizer (WHO) algorithms previously ranked by the Friedman test, see Table 6, are contrasted against the Horned Lizard optimization algorithm (HLOA) to solve the Optimal Power Flow problem for the IEEE-30 bus test system. The IEEE test system, depicted in Fig. 17, consists of six generators placed at nodes 1, 2, 5, 8, 11, and

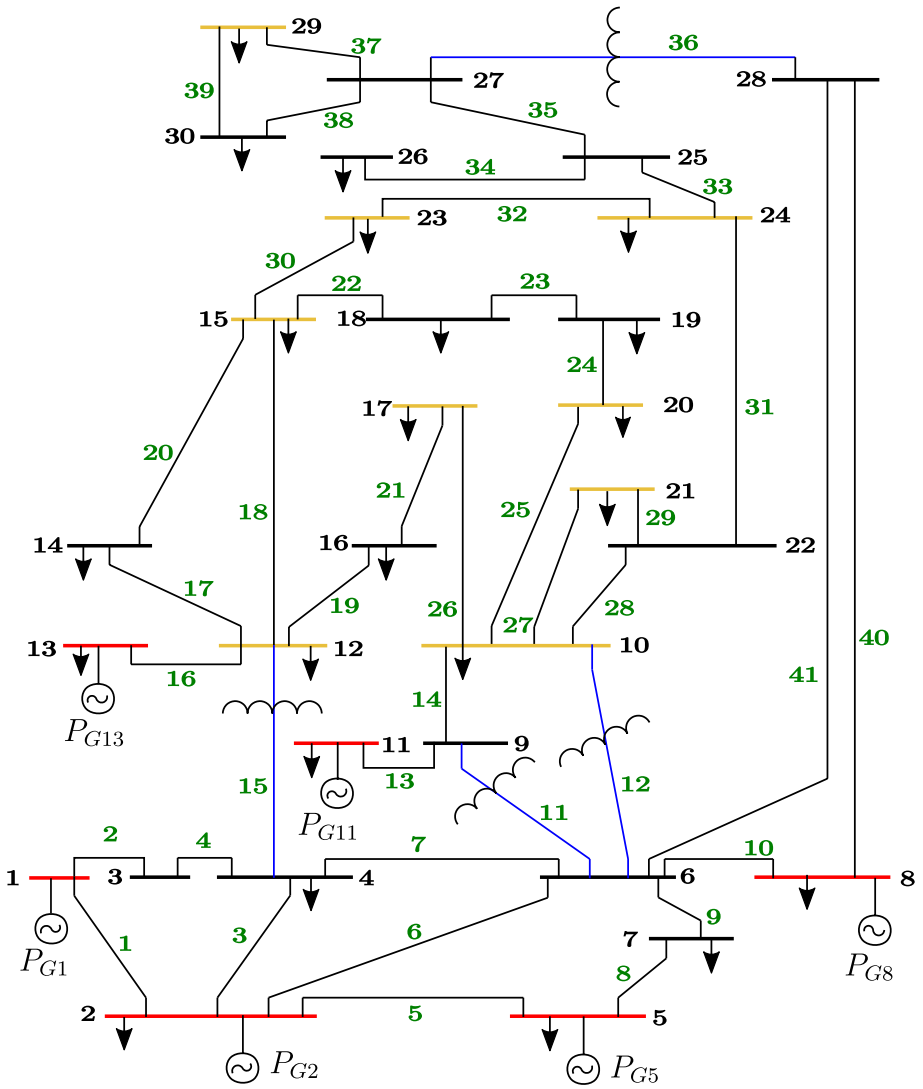

Fig. 17 IEEE 30-bus system (Nusair and Alasali 2020)

13, highlighted in red color, four transformers located in lines 11, 12, 15, and 36, highlighted in blue color and nine reactive compensators at nodes 17, 20, 21, 23, 24 and 29 highlighted in yellow. Line and node numbering is depicted in green and black color, respectively. Three cases of studies are conducted, the minimization of generation fuel cost and the minimization of active and reactive power transmission losses. In the first case, the objective function represents the total fuel of the six generator units, and it is defined as follows:

$$J = \sum_{i=1}^{NG} f_i(\$/h) \tag{36}$$

Where f_i is a quadratic function as described in Ela et al. (2010).

The objective function for the minimization of active power transmission losses is defined in Eq. 37, whilst the reactive power minimization function is stated in Eq. 38 (Fig. 17).

$$J = \sum_{i=1}^{NB} P_i = \sum_{i=1}^{NB} P_{Gi} - \sum_{i=1}^{NB} P_{Di} \tag{37}$$

$$J = \sum_{i=1}^{NB} Q_i = \sum_{i=1}^{NB} P_{Qi} - \sum_{i=1}^{NB} Q_{Di} \tag{38}$$

From the convergence graph analysis, it is confirmed that HLOA outperforms BWOA, WHO, and JSOA algorithms for the first and third case of study, see Fig. 18 and 20 respectively. However, for the second case of study, minimization of active power transmission losses, the HLOA algorithm achieves very competitive results as illustrated in Fig. 19. All tests were run for a population size of 30 and 500 iterations. Table 28 summarizes the algorithms' minimum obtained values for each case of study.

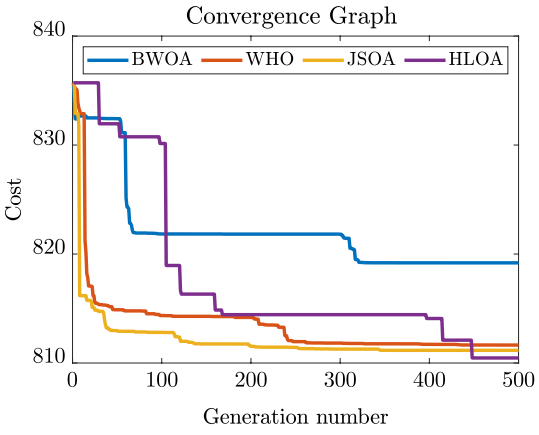

Fig. 18 First study case, Minimization of fuel cost

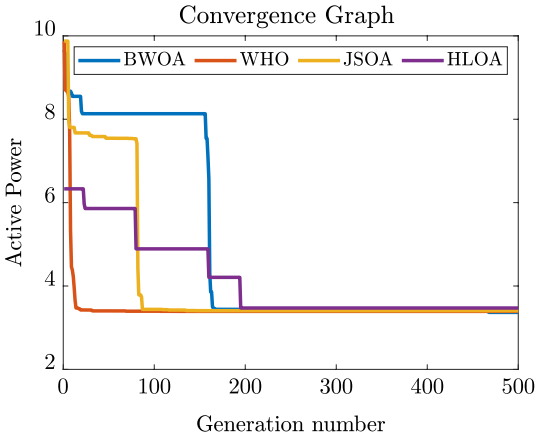

Fig. 19 Second study case, minimization of active power transmission losses

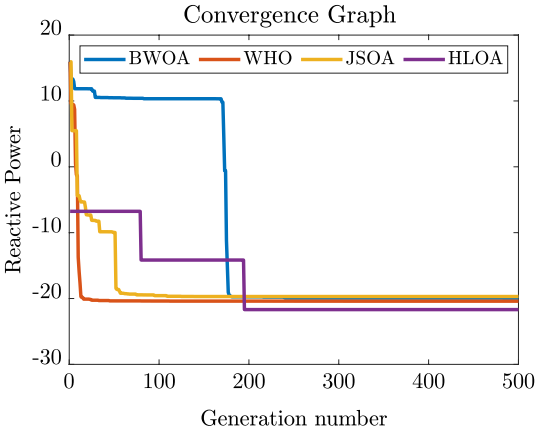

Fig. 20 Third study case, minimization of reactive power transmission losses

Table 28 Obtained results

Minimization studies	BWOA	WHO	JSOA	HLOA
Fuel cost	819.191	811.648	811.165	810.464
Active Power	3.367	3.391	3.408	3.471
Reactive Power	−19.943	−20.404	−19.698	−21.682

6 Conclusion

This paper presents a novel metaheuristic optimization algorithm inspired by the horned lizard's defense behavior, named the Horned Lizard Optimization Algorithm (HLOA). The defense behavior included the following four methods: crypsis (the ability of an organism to conceal itself by having a color, pattern, and shape that allows it to blend into the surrounding environment), skin darkening or lightening, bloodstream shooting, and move-to-escape. Furthermore, the rapid skin color change is influenced

by the α-melanophore stimulating hormone (*alpha*-MHS) rate, is also modeled. These models progressively refine the search vectors by evolving them (recombining vectors) at each iteration. They provide a suitable balance between exploration and exploitation in the solution search space. The algorithm's performance was evaluated on Sixty-three well-known testbench functions, twenty-eight functions for 10-dimensional, 30-dimensional, 50-dimensional, and 100-dimensional from IEEE CEC-2027 "Constrained Real-Parameter Optimization", and ten functions from IEEE CEC06-2019 "100-Digit Challenge". Furthermore, five real-world optimization problems, the Multiple Gravity Assist Optimization Problem, the Optimal Power Flow problem, and the rest of the problems are taken from CEC2020. Moreover, the HLOA performance is compared to ten of the most recent algorithms published in the scientific literature. The statistical results show that the HLOA algorithm outperforms BWOA, DOA, COOT, CSA, EJAYA, RSO, SAO, and TSA. At the same time, it has competitive results with JSOA and WHO algorithms.

The following are the findings and conclusions of this study:

- The algorithm has no parameters to configure in modeling the Horned Lizard defense tactics. The only parameters of the algorithm are those common to all bio-inspired, that is, the size of the population and the number of iterations.
- The Wilcoxon rank-sum test demonstrates that, in many situations, HLOA is significantly superior to alternative bio-inspired algorithms. The HLOA also ranks highest compared to other algorithms by the Friedman statistics test.
- For 10-dimensional problems, the Wilcoxon rank-sum test shows that HLOA outperformed all the algorithms. Nevertheless, it is ranked in second place by the Friedman test. Furthermore, the Wilcoxon rank-sum demonstrates that HLOA outperforms JSOA and BWOA algorithms for 30-dimensional problems. Meanwhile, there are no significant differences with WHO. In addition, HLOA ranks second in Friedman's test. In the case of 50-dimensional problems, the HLOA algorithm demonstrated superior performance compared to the JSOA and BWOA algorithms, as indicated by the Wilcoxon rank-sum test. In contrast, there are no substantial disparities with the WHO. In comparison, the Friedman test assigns the highest rank to HLOA. Finally, in the context of 100-dimensional problems, the Wilcoxon rank-sum test shows that HLOA outperformed all algorithms. Meanwhile, the Friedman test has determined that HLOA holds the highest rank. This n-dimensional analysis shows that the HLOA algorithm performs better for dimensions 50 and 100.
- HLOA shows competitive results on the Process Flow Sheeting Problem, Process Synthesis Problem, and Multiple Gravity Assist Optimization Problem. While showing the best performance on the Optimal Design of an Industrial Refrigeration System
- In the optimal power flow problem, HLOA better minimizes fuel cost and reactive power than BWOA, WHO, and JSOA algorithms.
- HLOA can solve real-world problems with unknown search spaces with outstanding results.

On the other hand, currently under development for future work is an improved version of the HLOA algorithm to solve for multi-objective and many-objective optimization. Moreover, efforts are focused on hyper-parameter optimization of convolutional neural networks for medical applications.

Appendix A Additional Tables

Additional tables are shown in this section (See Tables 29, 30, 31, 32 and 33).

Table 29 Color palette in its hexadecimal, decimal, and normalized form

#	Color name	Hexadecimal number	Decimal number	Normalized number
1	White	#FFFFFF	16777215	0
2	Yellow	#FFFF00	16776960	0.00001519920000000
3	Orange	#FF6600	16737792	0.00157159600000000
4	light coral	#FF8080	16744576	0.00194543600000000
5	vivid orange	#FF9900	16750848	0.00234979400000000
6	Fuchsia	#FF00FF	16711935	0.00355333640000000
7	Red	#FF0000	16711680	0.00390619100000000
8	pale cyan	#CCFFFF	13434879	0.19921876199999999
9	lavender blue	#CCCCFF	13421823	0.19999696000000000
10	Silver	#C0C0C0	12632256	0.24705882400000001
11	Pale blue	#9999FF	12632256	0.39999392000000000
12	vivid purple	#993399	10040217	0.40155639700000001
13	dark Rose	#993366	10040166	0.40155943599999999
14	Gray	#808080	8421504	0.49803921600000001
15	olive green	#808000	8421376	0.49804684500000002
16	purple	#800080	8388736	0.49999234100000001
17	Brown	#800000	8388608	0.49999999699999997
18	Dark orange	#664221	6701601	0.60055342899999997
19	Hot Pink	#660066	6684774	0.60155639699999996
20	Dark gray	#333333	3355443	0.80000000000000000
21	Pale yellow	#FFFFCC	16777164	0.90000044700000004
22	aqua	#00FFFF	65535	0.99609380900000000
23	Green lime	#00FF00	65280	0.99610900899999999
24	Sky Blue	#00CCFF	52479	0.99687200799999998
25	bluish green	#008080	32896	0.99803924499999996
26	green	#008000	32768	0.99804687500000000
27	vivid blue	#0066CC	26316	0.99843144399999995
28	Navy blue	#0000FF	255	0.99998480099999998
29	Navy	#000080	128	0.99999237100000005
30	Black	#000000	0	1

Table 30 Description of the Testbench Functions. From F1 to F21

ID	Function	Dim	Interval	f_{min}
F1	$f(\mathbf{x}) = -a.exp(-b\sqrt{\frac{1}{n}\sum_{i=1}^{n} x_i^2}) - exp(\frac{1}{d}\sum_{i=1}^{n}\cos(c \cdot x_i)) + a + exp(1)$	30	$[-32, 32]$	0
F2	$f(x, y) = -200e\left(-0.2\sqrt{x^2 + y^2}\right)$	2	$[-32, 32]$	-200
F3	$f(x, y) = -200e\left(-0.2\sqrt{x^2 + y^2}\right) + 5e(\cos(3x) + \sin(3y))$	2	$[-32, 32]$	-195.629028238419
F4	$f(\mathbf{x}) = \sum_{i=1}^{d-1}(e^{-0.2}\sqrt{x_i^2+x_{i+1}^2} + 3\left(\cos(2x_i) + \sin(2x_{i+1})\right))$	2	$[-35, 35]$	-4.590101633799122
F5	$f(x, y) = \cos(x)\sin(x) - \frac{x}{x^2+1}$	2	$x \in [-1, 1]$ $y \in [-1, 2]$	-2.02181
F6	$f(\mathbf{x}) = \sum_{i=1}^{n} \quad x_i \sin(x_i + 0.1x_i)$	30	$[0, 10]$	0
F7	$f(\mathbf{x}) = \prod_{i=1}^{n} \sin\left(x_i\right) \cdot \sqrt{x_i}$	30	$[0, 10]$	$2.808n$
F8	$f(x, y) = \quad x^2 + y^2 + xy \quad + \quad \sin(x) \quad + \quad \cos(y)$	2	$[-500, 500]$	1
F9	$f(x, y) = (1.5 - x + xy)^2 + (2.25 - x + xy^2)^2 + (2.625 - x + xy^3)^2$	2	$[-4.5, 4.5]$	0
F10	$f(x, y) = \sin(x)e(1 - \cos(y))^2) + \cos(y)e((1 - \sin(x))^2) + (x - y)^2$	2	$[-6.28, 6.28]$	-106.764537
F11	$f(\mathbf{x}) = x_1^2 + 2x_2^2 - 0.3\cos\left(3\pi x_1\right) - 0.4\cos\left(4\pi x_2\right) + 0.7$	2	$[-100, 100]$	0
F12	$f(\mathbf{x}) = x_1^2 + 2x_2^2 - 0.3\cos\left(3\pi x_1\right)\left[\cos\left(4\pi x_2\right)\right] + 0.3$	2	$[-100, 100]$	0
F13	$f(x, y) = (x + 2y - 7)^2 + (2x + y - 5)^2$	2	$[-10, 10]$	0
F14	$f(x, y) = (x + 10)^2 + (y + 10)^2 + e^{-x^2-y^2}$	2	$[-20, 0]$	$e{-}200$
F15	$f(\mathbf{x}) = \sum_{i=1}^{n-1}\left(x_i^2\right)^{\left(x_{i+1}^2+1\right)} + \left(x_{i+1}^2\right)^{\left(x_i^2+1\right)}$	30	$[-1, 4]$	0
F16	$f(\mathbf{x}) = 100\sqrt{\lvert x_2 - 0.01x_1^2\rvert} + 0.01 \quad x_1 + 10$	2	$x_1 \in [-15, 5]$ $x_2 \in [-5, 3]$	0
F17	$f(x, y) = -0.0001(\quad \sin(x)\sin(y)\exp(\quad 100 - \frac{\sqrt{x^2+y^2}}{\pi} \quad) \quad + 1\ )^{0.1}$	2	$[-10, 10]$	-2.06261218
F18	$f(x, y) = 10^5x^2 + y^2 - (x^2 + y^2)^2 + 10^{-5}(x^2 + y^2)^4$	2	$[-20, 20]$	-24771.09375
F19	$f(x, y) = -\frac{1+\cos(12\sqrt{x^2+y^2})}{(0.5(x^2+y^2)+2)}$	2	$[-5.2, 5.2]$	-1

Table 30 (continued)

ID	Function	Dim	Interval	f_{min}
F20	$f(x,y) = -\cos(x)\cos(y)exp(-(x-\pi)^2-(y-\pi)^2)$	2	$[-100, 100]$	-1
F21	$f(x,y) = x^2 + y^2 + 25(\sin^2(x) + sin^2(y))$	2	$[-5, 5]$	0

Table 31 Description of the Testbench Functions. From F22 to F42

ID	Function	Dim	Interval	f_{min}
F22	$f(\mathbf{x}) = -exp(-0.5\sum_{i=1}^{n} x_i^2)$	30	$[-1, 1]$	-1
F23	$f(\mathbf{x}) = [1 + (x_1 + x_2 + 1)^2(19 - 14x_1 + 3x_1^2 - 14x_2 + 6x_1x_2 + 3x_2^2)][30 + (2x_1 - 3x_2)^2(18 - 32x_1 + 12x_1^2 + 48x_2 - 36x_1x_2 + 27x_2^2)]$	2	$[-2, 2]$	3
F24	$f(\mathbf{x}) = \frac{sin(10\pi x)}{2x} + (x-1)^4$	1	$[-0.5, 2.5]$	-0.8690
F25	$f(\mathbf{x}) = 1 + \sum_{i=1}^{n} \frac{x_i^2}{4000} - \prod_{i=1}^{n} cos(\frac{x_i}{\sqrt{i}})$	30	$[-600, 600]$	0
F26	$f(\mathbf{x}) = \left[\left(\lvert x\rvert^2 - d\right)^2\right]^{\alpha} + \frac{1}{d}\left(\frac{1}{2}\lvert x\rvert^2 + \sum_{i=1}^{d} x_i\right) + \frac{1}{2}$	10	$[-2, 2]$	0
F27	$f(x, y) = (x^2 + y - 11)^2 + (x + y^2 - 7)^2$	2	$[-6, 6]$	0
F28	$f(x, y) = -\lvert \sin(x)\cos(y)exp(\lvert 1 - \frac{\sqrt{x^2+y^2}}{\pi}\rvert)\rvert$	2	$[-10, 10]$	-19.208
F29	$f(x, y) = -\frac{\sin^2(x-y)\sin^2(x+y)}{\sqrt{x^2+y^2}}$	2	$[0, 10]$	0.673667521146855
F30	$f(x, y) = 100(y - x^3)^2 + (1 - x)^2$	2	$[0, 10]$	0
F31	$f(x, y) = \sin^2(3\pi x) + (x-1)^2(1 + \sin^2(3\pi y)) + (y-1)^2(1 + \sin^2(2\pi y))$	2	$[-10, 10]$	0
F32	$f(x, y) = 0.26(x^2 + y^2) - 0.48xy$	2	$[-10, 10]$	0
F33	$f(x, y) = \sin(x + y) + (x - y)^2 - 1.5x + 2.5y + 1$	2	$x \in [-1.5, 4]$ $y \in [3, 4]$	-1.9133
F34	$f(\mathbf{x}) = 1 + \sum_{i=1}^{n} sin^2(x_i) - 0.1e^{(\sum_{i=1}^{n} x_i^2)}$	30	$[-10, 10]$	0
F35	$f(\mathbf{x}) = \sum_{i=1}^{n} \lvert x_i\rvert^{i+1}$	30	$[-1, 0]$	0
F36	$f(\mathbf{x}) = \sum_{i=1}^{n} (x^2 - i)^2$	30	$[-500, 500]$	0
F37	$f(\mathbf{x}) = \sum_{i=1}^{n} ix_i^4 + \text{random}[0, 1)$	30	$[-1.28, 1.28]$	0
F38	$f(x, y) = 10n + \sum_{i=1}^{n} (x_i^2 - 10cos(2\pi x_i))$	30	$[-5.12, 5.12]$	0
F39	$f(\mathbf{x}) = x_1 + \beta\left(\sum_{i=2}^{n} x_i^2\right)^{\alpha}$	30	$[-5, 5]$	$-\gamma$
F40	$f(x, y) = \sum_{i=1}^{n} [b(x_{i+1} - x_i^2)^2 + (a - x_i)^2]$	30	$[-5, 5]$	0
F41	$f(\mathbf{x}) = 1 - cos(2\pi\sqrt{\sum_{i=1}^{D} x_i^2}) + 0.1\sqrt{\sum_{i=1}^{D} x_i^2}$	30	$[-100, 100]$	0
F42	$f(x, y) = 0.5 + \frac{\sin^2(x^2+y^2)^2 - 0.5}{1+0.001(x^2+y^2)^2}$	2	$[-100, 100]$	0

Table 32 Description of the Testbench Functions. From F43 to F63

ID	Function	Dim	Interval	f_{min}
F43	$f(x,y) = 0.5 + \frac{\sin^2(x^2-y^2)-0.5}{(1+0.001(x^2+y^2))^2}$	2	$[-100, 100]$	0
F44	$f(x,y) = 0.5 + \frac{\sin(\cos(\lvert x^2-y^2\rvert))-0.5}{(1+0.001(x^2+y^2))^2}$	2	$[-100, 100]$	0.00156685
F45	$f(x,y) = 0.5 + \frac{\cos(\sin(\lvert x^2-y^2\rvert))-0.5}{(1+0.001(x^2+y^2))^2}$	2	$[-100, 100]$	0.292579
F46	$f(\mathbf{x}) = \sum_{i=1}^{d} \lvert x_i\rvert$	30	$[-100, 100]$	0
F47	$f(\mathbf{x}) = max_{i\epsilon\lvert 1,d\rvert}\lvert x_i\rvert$	30	$[-100, 100]$	0
F48	$f(\mathbf{x}) = \sum_{i=1}^{d} \lvert x_i\rvert + \prod_{i=1}^{d} \lvert x_i\rvert$	30	$[-100, 100]$	0
F49	$f(\mathbf{x}) = \sum_{i=1}^{d} x_i^{10}$	30	$[-10, 10]$	0
F50	$f(\mathbf{x}) = 418.9829d - \sum_{i=1}^{n} x_i \sin(\sqrt{\lvert x_i\rvert})$	30	$[-500, 500]$	0
F51	$f(\mathbf{x}) \sum_{i=1}^{d} \sum_{j=1}^{5} j \sin((j+1)x_i + j)$	30	$[-10, 10]$	−29.6733337
F52	$f(\mathbf{x}) = \sum_{i=1}^{d} \sum_{j=1}^{5} j \cos((j+1)x_i + j)$	30	$[-10, 10]$	−25.740858
F53	$f(\mathbf{x}) = \prod_{i=1}^{d} \left(\sum_{j=1}^{5} \cos((j+1)x_i + j)\right)$	30	$[-10, 10]$	−186.7309
F54	$f(\mathbf{x}) = \sum_{i=1}^{d} x_i^2$	30	$[-5.12, 5.12]$	0
F55	$f(\mathbf{x}) \frac{1}{2} \sum_{i=1}^{d} (x_i^4 - 16x_i^2 + 5x_i)$	30	$[-5, 5]$	−39.16599
F56	$f(\mathbf{x}) = \sum_{i=1}^{d} ix_i^2$	30	$[-10, 10]$	0
F57	$f(x,y) = 2x^2 - 1.05x^4 + \frac{x^6}{6} + xy + y^2$	2	$[-5, 5]$	0
F58	$f(x,y,z) = \frac{4}{3}(x^2 + y^2 - xy)^{0.75} + z$	3	$[0, 2]$	0
F59	$f(\mathbf{x}) = \begin{bmatrix} e^{-\sum_{i=1}^{n} \left(\frac{x_i}{\beta}\right)^{2m}} & -2e^{-\sum_{i=1}^{n} (x_i - c)^2} \end{bmatrix} \cdot \prod_{i=1}^{n} \cos^2(x_i)$	30	$[-5, 5]$	0
F60	$f(\mathbf{x}) = (\sum_{i=1}^{n} \lvert x_i\rvert) exp(-\sum_{i=1}^{n} sin(x_i^2))$	30	$[-2\pi, 2\pi]$	0
F61	$f(x) = \exp\left(-\sum_{i=1}^{n} \left(\frac{xi}{\beta}\right)^2\right) - 2\exp\left(-\sum_{i=1}^{n} xi^2\right) \prod_{i=1}^{n} \cos^2(xi)$	30	$[-2\pi, 2\pi]$	−1
F62	$f(x) = \left(\sum_{i=1}^{n} \sin^2(x_i) - e^{-\sum_{i=1}^{n} x_i^2}\right) e^{-\sum_{i=1}^{n} \sin^2 \sqrt{\lvert x_i\rvert}}$	30	$[-10, 10]$	−1
F63	$f(\mathbf{x}) = \sum_{i=1}^{n} x_i^2 + (\sum_{i=1}^{n} 0.5ix_i)^2 + (\sum_{i=1}^{n} 0.5ix_i)^4$	30	$[-5, 10]$	0

Table 33 CEC 2017 Constrained Real-Parameter Optimization.

Problem/search range	Type of objective	Number of constraints	
		E	I
C01	Non Separable	0	1
$[-100, 100]^D$			Separable
CO2	Non Separable	0	1
$[-100, 100]^D$	Rotated		Non Separable, Rotated
C03	Non Separable	1	1
$[-100, 100]^D$		Separable	Separable
C04	Separable	0	2
$[-10, 10]^D$			Separable
C05	Non Separable	0	2
$[-10, 10]^D$			Non Separable,Rotated
C06	Separable	6	0
$[-20, 20]^D$			Separable
C07	Separable	2	0
$[-50, 50]^D$		Separable	
C08	Separable	2	0
$[-100, 100]^D$		Non Separable	
C09	Separable	2	0
$[-10, 10]^D$		Non Separable	
C10	Separable	2	0
$[-100, 100]^D$		Non Separable	
C11	Separable	1	1
$[-100, 100]^D$		Non Separable	Non Separable
C12	Separable	0	2
$[-100, 100]^D$			Separable
C13	Non Separable	0	3
$[-100, 100]^D$			Separable
C14	Non Separable	1	1
$[-100, 100]^D$		Separable	Separable
C15	Separable	1	1
$[-100, 100]^D$			
C16	Separable	1	1
$[-100, 100]^D$		Non Separable	Separable
C17	Non Separable	1	1
$[-100, 100]^D$		Non Separable	Separable
C18	Separable	1	2
$[-100, 100]^D$			Non Separable
C19	Separable	0	2
$[-50, 50]^D$			Non Separable

Table 33 (continued)

Problem/search range	Type of objective	Number of constraints	
		E	I
C20	Non Separable	0	2
$[-100, 100]^D$			
C21	Rotated	0	2
$[-100, 100]^D$			Rotated
C22	Rotated	0	3
$[-100, 100]^D$			Rotated
C23	Rotated	1	1
$[-100, 100]^D$		Rotated	Rotated
C24	Rotated	1	1
$[-100, 100]^D$		Rotated	Rotated
C25	Rotated	1	1
$[-100, 100]^D$		Rotated	Rotated
C26	Rotated	1	1
$[-100, 100]^D$		Rotated	Rotated
C27	Rotated	1	2
$[-100, 100]^D$		Rotated	Rotated
C28	Rotated	0	2
$[-50, 50]^D$			Rotated

Details of 28 test problems. D is the number of decision variables, I is the number of inequality constraints, and E is the number of equality constraints

Acknowledgements This project was supported by Instituto Politécnico Nacional (IPN) through grant SIP−no. 20221568 and SIP−no. 20231424. Also, by CONAHCyT (Mexican Council of Humanities, Science, and Technology) through grant no. CF-2023-I-342

Author Contributions Conceptualization, H.P.-V.; methodology, H.P.-V.; software, H.P.-V.; validation, N.S., M.M-T. and A.B.M.-C.; formal analysis, M.M-T. and A.P.-D.; investigation, N.S. and A.B.M.-C.; resources, H.P.-V.; data curation, M.M-T. and N.S.; writing-original draft preparation, H.P.-V.; writing-review and editing, H.P.-V., A.P.-D. and M-M-T.; visualization, N.S. and A.B.M.-C.; supervision, H.P.-V. and A.P.-D.; project administration, H.P.-V.; funding acquisition, H.P.-V. and A.B.M-C.

Funding This project was supported by Instituto Politécnico Nacional (IPN) through grant SIP−no. 20221568 and SIP−no. 20231424. Also, by CONAHCyT (Mexican Council of Humanities, Science, and Technology) through grant no. CF-2023-I-342

Code availability The source code used to support the findings of this study has been deposited in the MathWorks repository at ((link provided if the manuscript is accepted)).

Declarations

Conflict of interest The authors declare that they have no conflict of interest.

Consent to participate All authors accept their participation and collaboration

Consent for publication All authors have read and agreed to the published version of the manuscript.

References

Abdel-Basset M, Mohamed R, Azeem SAA, Jameel M, Abouhawwash M (2023) Kepler optimization algorithm: a new metaheuristic algorithm inspired by Kepler's laws of planetary motion. Knowl-Based Syst 268:110454. https://doi.org/10.1016/J.KNOSYS.2023.110454

Abdelhamid AA, Towfek SK, Khodadadi N, Alhussan AA, Khafaga DS, Eid MM, Ibrahim A (2023) Waterwheel plant algorithm: a novel metaheuristic optimization method. Processes 11:1502. https://doi.org/10.3390/PR11051502

Abdollahzadeh B, Gharehchopogh FS, Khodadadi N, Mirjalili S (2022) Mountain gazelle optimizer: a new nature-inspired metaheuristic algorithm for global optimization problems. Adv Eng Softw 174:103282. https://doi.org/10.1016/J.ADVENGSOFT.2022.103282

Abedinpourshotorban H, Shamsuddin SM, Beheshti Z, Jawawi DNA (2016) Electromagnetic field optimization: a physics-inspired metaheuristic optimization algorithm. Swarm Evol Comput 26:8–22. https://doi.org/10.1016/J.SWEVO.2015.07.002

Abualigah L, Diabat A, Mirjalili S, Elaziz MA, Gandomi AH (2021) The arithmetic optimization algorithm. Comput Methods Appl Mech Eng 376:113609. https://doi.org/10.1016/J.CMA.2020.113609

Ahmad MF, Isa NAM, Lim WH, Ang KM (2022) Differential evolution: a recent review based on state-of-the-art works. Alex Eng J 61:3831–3872. https://doi.org/10.1016/J.AEJ.2021.09.013

Ahmadi-Javid A (2011) Anarchic society optimization: A human-inspired method. 2011 IEEE Congress of Evolutionary Computation, CEC 2011, 2586–2592. https://doi.org/10.1109/CEC.2011.5949940

Ahrari A, Essam D (2022) An introduction to evolutionary and memetic algorithms for parameter optimization. Adapt Learn Optim 26:37–63. https://doi.org/10.1007/978-3-030-88315-7_3/COVER

Alatas B (2010) Chaotic harmony search algorithms. Appl Math Comput 216:2687–2699. https://doi.org/10.1016/J.AMC.2010.03.114

Almazán-Covarrubias JH, Peraza-Vázquez H, Peña-Delgado AF, García-Vite PM (2022) An improved dingo optimization algorithm applied to she-pwm modulation strategy. Appl Sci 12:992. https://doi.org/10.3390/APP12030992

Ashrafi SM, Dariane AB (2011) A novel and effective algorithm for numerical optimization: Melody search (ms). Proceedings of the 2011 11th international conference on hybrid intelligent systems, HIS 2011, pp 109–114. https://doi.org/10.1109/HIS.2011.6122089

Atashpaz-Gargari E, Lucas C (2007) Imperialist competitive algorithm: An algorithm for optimization inspired by imperialistic competition. 2007 IEEE Congress on Evolutionary Computation, CEC 2007, pp 4661–4667. https://doi.org/10.1109/CEC.2007.4425083

Beyer H-G, Beyer H-G, Schwefel H-P (2002) Evolution strategies - a comprehensive introduction. Nat Comput 1(1):3–52. https://doi.org/10.1023/A:1015059928466

Burtt E (1981) The adaptiveness of animal colors. Bioscience 31:723–729. https://doi.org/10.2307/1308778

Cassini spacecraft trajectory design problem. European Space Agency

Cooper WE, Sherbrooke WC (2010) Plesiomorphic escape decisions in cryptic horned lizards (phrynosoma) having highly derived antipredatory defenses. Ethology 116:920–928. https://doi.org/10.1111/J.1439-0310.2010.01805.X

Dehghani M, Samet H (2020) Momentum search algorithm: a new meta-heuristic optimization algorithm inspired by momentum conservation law. SN Appl Sci 2:1–15. https://doi.org/10.1007/S42452-020-03511-6/TABLES/7

Dehghani M, Trojovský P (2021) Teamwork optimization algorithm: a new optimization approach for function minimization/maximization. Sensors 21:4567. https://doi.org/10.3390/S21134567

Dehghani M, Trojovská E, Zuščák T (2022) A new human-inspired metaheuristic algorithm for solving optimization problems based on mimicking sewing training. Sci Rep 12:1–24. https://doi.org/10.1038/s41598-022-22458-9

Dhiman G, Garg M, Nagar A, Kumar V, Dehghani M (2021) A novel algorithm for global optimization: rat swarm optimizer. J Ambient Intell Humaniz Comput 12:8457–8482. https://doi.org/10.1007/s12652-020-02580-0

Duan X, Hou P (2021) Research on teaching quality evaluation model of physical education based on simulated annealing algorithm. Mobile Inf Syst. https://doi.org/10.1155/2021/4407512

Ela AAAE, Abido MA, Spea SR (2010) Optimal power flow using differential evolution algorithm. Electric Power Syst Res 80:878–885. https://doi.org/10.1016/J.EPSR.2009.12.018

El-Kenawy ESM, Abdelhamid AA, Ibrahim A, Mirjalili S, Khodadad N, Duailij MAA, Alhussan AA, Khafaga DS (2022) Al-biruni earth radius (ber) metaheuristic search optimization algorithm. Comput Syst Sci Eng 45:1917–1934

Fadakar E, Ebrahimi M (2016) A new metaheuristic football game inspired algorithm. In: 1st conference on swarm intelligence and evolutionary computation, CSIEC 2016 - Proceedings, pp 6–11. https://doi.org/10.1109/CSIEC.2016.7482120

Grigg JW, Buckley LB (2013) Conservatism of lizard thermal tolerances and body temperatures across evolutionary history and geography. Biol Lett. https://doi.org/10.1098/RSBL.2012.1056

Hansen P, Mladenovićі N (2018) Variable neighborhood search. Handbook Heuristics 1–2:759–787. https://doi.org/10.1007/978-3-319-07124-4_19/TABLES/4

Harifi S, Mohammadzadeh J, Khalilian M, Ebrahimnejad S (2021) Giza pyramids construction: an ancient-inspired metaheuristic algorithm for optimization. Evol Intel 14:1743–1761. https://doi.org/10.1007/S12065-020-00451-3/METRICS

Holland JH (2006) Genetic algorithms and the optimal allocation of trials. SIAM J Comput 2:88–105. https://doi.org/10.1137/0202009

Huneault M, Galiana FD (1991) A survey of the optimal power flow literature. IEEE Trans Power Syst 6:762–770. https://doi.org/10.1109/59.76723

Ikram RMA, Dehrashid AA, Zhang B, Chen Z, Le BN, Moayedi H (2023) A novel swarm intelligence: cuckoo optimization algorithm (coa) and sailfish optimizer (sfo) in landslide susceptibility assessment. Stochastic Environ Res Risk Assess 37:1717–1743. https://doi.org/10.1007/S00477-022-02361-5

Irizarry R (2004) Lares: an artificial chemical process approach for optimization. Evol Comput 12:435–459. https://doi.org/10.1162/1063656043138897

Ismail K, Elshaer A, Abdelaleem BH, Elruby AY, Khodadadi N, Harati E, Caso FD, Nanni A (2023) Optimizing truss structures using composite materials under natural frequency constraints with a new hybrid algorithm based on cuckoo search and stochastic paint optimizer (csspo). Buildings 13:1551. https://doi.org/10.3390/BUILDINGS13061551

Joyce T, Herrmann JM (2017) A review of no free lunch theorems, and their implications for metaheuristic optimisation. Stud Comput Intell 744:27–51. https://doi.org/10.1007/978-3-319-67669-2_2

Karami H, Sanjari MJ, Gharehpetian GB (2014) Hyper-spherical search (hss) algorithm: a novel meta-heuristic algorithm to optimize nonlinear functions. Neural Comput Appl 25:1455–1465. https://doi.org/10.1007/S00521-014-1636-7/FIGURES/22

Kaur S, Awasthi LK, Sangal AL, Dhiman G (2020) Tunicate swarm algorithm: a new bio-inspired based metaheuristic paradigm for global optimization. Eng Appl Artif Intell 90:103541. https://doi.org/10.1016/j.engappai.2020.103541

Kaveh A, Bakhshpoori T (2019) Cyclical parthenogenesis algorithm. Outlines, MATLAB Codes and Examples, Metaheuristics, pp 167–177

Kaveh A, Dadras A (2017) A novel meta-heuristic optimization algorithm: thermal exchange optimization. Adv Eng Softw 110:69–84. https://doi.org/10.1016/J.ADVENGSOFT.2017.03.014

Kaveh A, Talatahari S, Khodadadi N (2022) Stochastic paint optimizer: theory and application in civil engineering. Eng Comput 38:1921–1952. https://doi.org/10.1007/S00366-020-01179-5/FIGURES/25

Kennedy J, Eberhart R (1995) Particle swarm optimization. Proc ICNN'95 - Int Conf Neural Netw 4:1942–1948. https://doi.org/10.1109/ICNN.1995.488968

Khan MS, Ul Hassan CHA, Sadiq HA, Ali I, Rauf A, Javaid N (2018) A new meta-heuristic optimization algorithm inspired from strawberry plant for demand side management in smart grid. Lecture Notes Data Eng Commun Technol 8:143–154. https://doi.org/10.1007/978-3-319-65636-6_13

Kim JH (2016) Harmony search algorithm: a unique music-inspired algorithm. Procedia Eng 154:1401–1405. https://doi.org/10.1016/J.PROENG.2016.07.510

Kim C, Lee B (2023) Torcwa: Gpu-accelerated fourier modal method and gradient-based optimization for metasurface design. Comput Phys Commun 282:108552. https://doi.org/10.1016/J.CPC.2022.108552

Kumar A, Wu G, Ali MZ, Mallipeddi R, Suganthan PN, Das S (2020) A test-suite of non-convex constrained optimization problems from the real-world and some baseline results. Swarm Evolut Comput. https://doi.org/10.1016/j.swevo.2020.100693

Labbi Y, Attous DB, Gabbar HA, Mahdad B, Zidan A (2016) A new rooted tree optimization algorithm for economic dispatch with valve-point effect. Int J Electr Power Energy Syst 79:298–311. https://doi.org/10.1016/J.IJEPES.2016.01.028

Lam AYS, Li VOK (2012) Chemical reaction optimization: A tutorial. Memetic Comput 4:3–17. https://doi.org/10.1007/S12293-012-0075-1/METRICS

Lara-Reséndiz RA, Arenas-Moreno DM, Beltrán-Sánchez E, Gramajo W, Verdugo-Molina J, Sherbrooke WC (2015) Cruz, FRM-DL: selected body temperature of nine species of mexican horned lizards (phrynosoma). Revista Mexicana de Biodiversidad 86:275–278. https://doi.org/10.7550/RMB.48028

Leaché AD, McGuire JA (2006) Phylogenetic relationships of horned lizards (phrynosoma) based on nuclear and mitochondrial data: evidence for a misleading mitochondrial gene tree. Mol Phylogenet Evol 39:628–644. https://doi.org/10.1016/J.YMPEV.2005.12.016

Liu Y, Liu J, Ma L, Tian L (2017) Artificial root foraging optimizer algorithm with hybrid strategies. Saudi J Biol Sci 24:268–275. https://doi.org/10.1016/J.SJBS.2016.09.013

Ma B, Hu Y, Lu P, Liu Y (2023) Running city game optimizer: a game-based metaheuristic optimization algorithm for global optimization. J Comput Des Eng 10:65–107. https://doi.org/10.1093/JCDE/QWAC131

Maheri A, Jalili S, Hosseinzadeh Y, Khani R, Miryahyavi M (2021) A comprehensive survey on cultural algorithms. Swarm Evol Comput 62:100846. https://doi.org/10.1016/J.SWEVO.2021.100846

Middendorf G (2001) Blood-squirting variability in horned lizards (phrynosoma). Copeia. https://doi.org/10.1643/0045-8511(2001)001[1114:BSVIHL]2.0.CO;2

Mirjalili S (2016) Sca: a sine cosine algorithm for solving optimization problems. Knowl-Based Syst 96:120–133. https://doi.org/10.1016/J.KNOSYS.2015.12.022

Mittal H, Tripathi A, Pandey AC, Pal R (2021) Gravitational search algorithm: a comprehensive analysis of recent variants. Multimed Tools Appl 80:7581–7608. https://doi.org/10.1007/S11042-020-09831-4/TABLES/8

Moghdani R, Salimifard K (2018) Volleyball premier league algorithm. Appl Soft Comput 64:161–185. https://doi.org/10.1016/J.ASOC.2017.11.043

Mora-Gutiérrez RA, Ramírez-Rodríguez J, Rincón-García EA (2014) An optimization algorithm inspired by musical composition. Artif Intell Rev 41:301–315. https://doi.org/10.1007/S10462-011-9309-8/METRICS

Naruei I, Keynia F (2021) A new optimization method based on coot bird natural life model. Expert Syst Appl 183:115352. https://doi.org/10.1016/j.eswa.2021.115352

Naruei I, Keynia F (2021) Wild horse optimizer: a new meta-heuristic algorithm for solving engineering optimization problems. Eng Comput. https://doi.org/10.1007/s00366-021-01438-z

Niall KK (2017) Erwin schrödinger's color theory: Translated with modern commentary. Erwin Schrödinger's Color Theory: Translated with Modern Commentary, pp 1–193. https://doi.org/10.1007/978-3-319-64621-3/COVER

Nucci CA, Borghetti A, Napolitano F, Tossani F (2021) Basics of power systems analysis. Springer Handbooks, pp 273–366. https://doi.org/10.1007/978-981-32-9938-2_5/FIGURES/85

Nusair K, Alasali F (2020) Optimal power flow management system for a power network with stochastic renewable energy resources using golden ratio optimization method. Energies 13:3671. https://doi.org/10.3390/en13143671

Pan JS, Zhang SQ, Chu SC, Yang HM, Yan B (2023) Willow catkin optimization algorithm applied in the tdoa-fdoa joint location problem. Entropy 25:171. https://doi.org/10.3390/E25010171

Patil S, Suparna HS, Bharanidharan N, Dharani N (2022) Puzzle optimization algorithm based weighted feature selection for identification of rice leaf disease through thermal images. Proceedings - 2nd international conference on smart technologies, communication and robotics 2022, STCR 2022. https://doi.org/10.1109/STCR55312.2022.10009526

Peña-Delgado AF, Peraza-Vázquez H, Almazán-Covarrubias JH, Cruz NT, García-Vite PM, Morales-Cepeda AB, Ramirez-Arredondo JM (2020) A novel bio-inspired algorithm applied to selective harmonic elimination in a three-phase eleven-level inverter. Math Problems Eng. https://doi.org/10.1155/2020/8856040

Peraza-Vázquez H, Peña-Delgado A, Ranjan P, Barde C, Choubey A, Morales-Cepeda AB (2021) A bio-inspired method for mathematical optimization inspired by arachnida salticidade. Mathematics 10:102. https://doi.org/10.3390/math10010102

Peraza-Vázquez H, Peña-Delgado AF, Echavarría-Castillo G, Morales-Cepeda AB, Velasco-Álvarez J, Ruiz-Perez F (2021) A bio-inspired method for engineering design optimization inspired by dingoes hunting strategies. Math Probl Eng 2021:1–19. https://doi.org/10.1155/2021/9107547

Pisinger D, Ropke S (2010) Large neighborhood search, pp 399–419. https://doi.org/10.1007/978-1-4419-1665-5_13

Pratha SJ, Asanambigai V, Mugunthan SR (2023) Hybrid mutualism mechanism-inspired butterfly and flower pollination optimization algorithm for lifetime improving energy-efficient cluster head selection in wsns. Wireless Pers Commun 128:1567–1601. https://doi.org/10.1007/S11277-022-10010-X/FIGURES/14

Ray T, Liew KM (2003) Society and civilization: an optimization algorithm based on the simulation of social behavior. IEEE Trans Evol Comput 7:386–396. https://doi.org/10.1109/TEVC.2003.814902

Ruxton GD, Sherratt TN, Speed MP (2004) Avoiding attack: the evolutionary ecology of crypsis, warning signals and mimicry. Avoiding Attack. https://doi.org/10.1093/ACPROF:OSO/9780198528609.001.0001

Sadollah A, Eskandar H, Lee HM, Yoo DG, Kim JH (2016) Water cycle algorithm: a detailed standard code. SoftwareX 5:37–43. https://doi.org/10.1016/J.SOFTX.2016.03.001

Salawudeen AT, Mu'azu MB, Sha'aban YA, Adedokun AE (2021) A novel smell agent optimization (sao): an extensive cec study and engineering application. Knowl-Based Syst 232:107486. https://doi.org/10.1016/j.knosys.2021.107486

Salimi H (2015) Stochastic fractal search: a powerful metaheuristic algorithm. Knowl-Based Syst 75:1–18. https://doi.org/10.1016/J.KNOSYS.2014.07.025

Sherbrooke WC, Sherbrooke WC (1988) Integumental biology of horned lizards (phrynosoma)

Sherbrooke WC (1997) Physiological (rapid) change of color in horned lizards. Amphibia-Reptilia 18:155–175. https://doi.org/10.1163/156853897X00044

Stevens M, Merilaita S (2011) Animal camouflage: Function and mechanisms. Animal camouflage: mechanisms and function, pp 1–16

Talatahari S, Azizi M, Tolouei M, Talatahari B, Sareh P (2021) Crystal structure algorithm (crystal): a metaheuristic optimization method. IEEE Access 9:71244–71261. https://doi.org/10.1109/ACCESS.2021.3079161

Tan WH, Mohamad-Saleh J (2023) A hybrid whale optimization algorithm based on equilibrium concept. Alex Eng J 68:763–786. https://doi.org/10.1016/J.AEJ.2022.12.019

Trojovska E, Dehghani M, Trojovsky P (2022) Fennec fox optimization: a new nature-inspired optimization algorithm. IEEE Access 10:84417–84443. https://doi.org/10.1109/ACCESS.2022.3197745

Uymaz SA, Tezel G, Yel E (2015) Artificial algae algorithm (aaa) for nonlinear global optimization. Appl Soft Comput 31:153–171. https://doi.org/10.1016/J.ASOC.2015.03.003

Wagner S, Wie B (2015) Hybrid algorithm for multiple gravity-assist and impulsive delta-v maneuvers. J Guid Control Dyn 38:2096–2107. https://doi.org/10.2514/1.G000874

Wang L, Cao Q, Zhang Z, Mirjalili S, Zhao W (2022) Artificial rabbits optimization: a new bio-inspired meta-heuristic algorithm for solving engineering optimization problems. Eng Appl Artif Intell 114:105082. https://doi.org/10.1016/J.ENGAPPAI.2022.105082

Westland S, Ripamonti C, Cheung V (2012) Computational colour science using matlab

Xing B, Gao W-J (2014) Invasive weed optimization algorithm. Intell Syst Ref Library 62:177–181. https://doi.org/10.1007/978-3-319-03404-1_13/COVER

Xu H, Lu Y, Guo Q (2022) Application of improved butterfly optimization algorithm combined with black widow optimization in feature selection of network intrusion detection. Electronics 11:3531. https://doi.org/10.3390/ELECTRONICS11213531

Yu C, Lahrichi N, Matta A (2023) Optimal budget allocation policy for tabu search in stochastic simulation optimization. Comput Oper Res 150:106046. https://doi.org/10.1016/J.COR.2022.106046

Yuan Y, Wang S, Lv L, Song X (2020) An adaptive resistance and stamina strategy-based dragonfly algorithm for solving engineering optimization problems. Eng Comput (Swansea, Wales) 38:2228–2251. https://doi.org/10.1108/EC-08-2019-0362/FULL/PDF

Yuan Y, Lv L, Wang S, Song X (2020) Multidisciplinary co-design optimization of structural and control parameters for bucket wheel reclaimer. Front Mech Eng 15:406–416. https://doi.org/10.1007/S11465-019-0578-2/METRICS

Yuan Y, Ren J, Wang S, Wang Z, Mu X, Zhao W (2022) Alpine skiing optimization: a new bio-inspired optimization algorithm. Adv Eng Softw 170:103158. https://doi.org/10.1016/J.ADVENGSOFT.2022.103158

Yuan Y, Mu X, Shao X, Ren J, Zhao Y, Wang Z (2022) Optimization of an auto drum fashioned brake using the elite opposition-based learning and chaotic k-best gravitational search strategy based grey wolf optimizer algorithm. Appl Soft Comput 123:108947. https://doi.org/10.1016/J.ASOC.2022.108947

Yuan Y, Shen Q, Wang S, Ren J, Yang D, Yang Q, Fan J, Mu X (2023) Coronavirus mask protection algorithm: a new bio-inspired optimization algorithm and its applications. J Bionic Eng 20:1747–1765. https://doi.org/10.1007/S42235-023-00359-5/TABLES/13

Yuan Y, Shen Q, Xi W, Wang S, Ren J, Yu J, Yang Q (2023) Multidisciplinary design optimization of dynamic positioning system for semi-submersible platform. Ocean Eng 285:115426. https://doi.org/10.1016/J.OCEANENG.2023.115426

Yuan Y, Yang Q, Ren J, Fan J, Shen Q, Wang X, Zhao Y (2023) Learning-imitation strategy-assisted alpine skiing optimization for the boom of offshore drilling platform. Ocean Eng 278:114317. https://doi.org/10.1016/J.OCEANENG.2023.114317

Zhang Y, Chi A, Mirjalili S (2021) Enhanced jaya algorithm: a simple but efficient optimization method for constrained engineering design problems. Knowl-Based Syst 233:107555. https://doi.org/10.1016/j.knosys.2021.107555

Zhao Z, Cui Z, Zeng J, Yue X (2011) Artificial plant optimization algorithm for constrained optimization problems. Proceedings - 2011 2nd International conference on innovations in bio-inspired computing and applications, IBICA 2011, pp 120–123. https://doi.org/10.1109/IBICA.2011.34

Zuo M, Dai G, Peng L, Wang M, Xiong J (2016) Multiple gravity assist spacecraft trajectories design based on bfs and ep de algorithm. Int J Aerosp Eng 2016:1–13. https://doi.org/10.1155/2016/3416046

Authors and Affiliations

Hernán Peraza-Vázquez[1] · Adrián Peña-Delgado[2] · Marco Merino-Treviño[1,3] · Ana Beatriz Morales-Cepeda[3] · Neha Sinha[4]

✉ Hernán Peraza-Vázquez
hperaza@ipn.mx

✉ Adrián Peña-Delgado
apea@utaltamira.edu.mx

✉ Marco Merino-Treviño
mmerino@ipn.mx

Ana Beatriz Morales-Cepeda
ana.mc@cdmadero.tecnm.mx

Neha Sinha
neha.cse.2203005@iiitbh.ac.in

[1] Instituto Politécnico Nacional, CICATA Altamira, km.14.5 Carretera Tampico -Puerto Industrial Altamira, 89120 Mexico City, Tamaulipas, Mexico

[2] Universidad Tecnológica de Altamira, Boulevard de los Ríos Km. 3 + 100, Puerto Industrial Altamira, 89601 Mexico City, Tamaulipas, Mexico

[3] TecNM/Instituto Tecnológico de Ciudad Madero, Juventino Rosas y Jesús Urueta s/n, Col. Los Mangos, 89318 Ciudad Madero, Tamaulipas, Mexico

[4] Department of Computer Science and Engineering, Indian Institute of Information Technology Bhagalpur, Bhagalpur, Bihar 813210, India